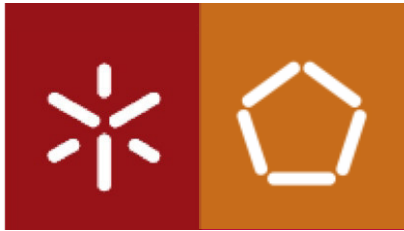**Universidade do Minho**
Instituto de Engenharia

Alexandre Felipe Leitão

Development of Vascular Grafts of
Bacterial Cellulose

2014

Universidade do Minho
Instituto de Engenharia

Alexandre Felipe Leitão

Development of Vascular Grafts of
Bacterial Cellulose

Dissertação de Doutoramento em
Engenharia Biomédica

Trabalho realizado sob a orientação do
Orientador: Professor Doutor Francisco Miguel Portela Gama
Co-Orientador: Doutor Fernando Octávio de Queirós Dourado

2014

DECLARAÇÃO

Nome: Alexandre Felipe Leitão

Endereço electrónico: alxleitao@gmail.com

Título da tese: Development of Vascular Grafts of Bacterial Cellulose

Orientador: Professor Doutor Francisco Miguel Portela Gama

Co-Orientador: Doutor Fernando Octávio de Queirós Dourado

Ano de conclusão: 2014

Designação do Doutoramento: Engenharia Biomédica

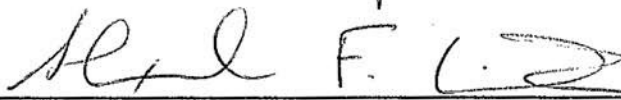Universidade do Minho, ___/___/_____

Assinatura: _____

STATEMENT OF INTEGRITY

I hereby declare having conducted my thesis with integrity. I confirm that I have not used plagiarism or any form of falsification of results in the process of the thesis elaboration.

I further declare that I have fully acknowledged the Code of Ethical Conduct of the University of Minho.

University of Minho, _October 10th 2014_

Full name: _Alexandre Felipe Leitão_

Signature: _Alex F. L._

Palavras não chegam para descrever aquilo que nesta página deveria constar. Vocês são a força motriz que me faz ser quem sou e estar onde estou hoje.

Mãe e Pai obrigado.

Meu querido Avô e amigo obrigado.

André, obrigado.

Sara, a minha outra metade, obrigado.

A vós dedico esta tese.

Agradecimentos

A todos aqueles que tiveram presentes e ajudaram-me a concretizar este trabalho agradeço-vos. Em particular:

Prof. Miguel Gama, sem si certamente não estaríamos aqui. Agradeço a orientação nos trabalhos, a disponibilidade nas dúvidas e a confiança nas incertezas.

Prof. Augusto Faustino, agradeço a disponibilidade e prestabilidade nos fins de manhã ao microscópio mas mais do que isso a amizade que do meu lado, se gerou.

Dr. Miguel Faria, Dra. Ivone Silva e Dr. Luís Loureiro agradeço-vos todo o apoio numa parte tão importante e extensa deste doutoramento. Sem vós o trabalho não se teria realizado nem os resultados conseguidos.

Todos os colegas que me ajudaram, acompanharam e conviveram comigo em Braga, no Porto, em San Sebastian e Aachen, a vossa ajuda foi fundamental para o trabalho e o meu conhecimento. Agradeço os bons momentos, o vosso tempo, amizade e paciência.

Às irmãs e irmãos com que ri e partilhei inúmeros bons momentos: Paula Pereira, Sílvia Pedrosa, Dina Silva, Thalita Calado, Renata Pertile, João Pedro Silva e Raniere Fagundes. Vocês foram, são e serão minha família hoje e sempre.

Sara Oliveira agradeço-te teres surgido na minha vida. Até tu apareceres eu não sabia o que era estar completo.

Summary

Bypass surgery is a vascular surgeon's fundamental tool in the treatment of some arterial and venous diseases, many of which are caused by atherosclerosis. The procedure uses a vascular graft to replace, bypass or maintain function of damaged, occluded or diseased blood vessels. The most common approach is to use a native vessel, such as the saphenous vein, from the patient as the bypass conduit. Alternatively, when an autologous vessel is not available due to progression of the disease or prior surgeries, synthetic alternatives are used. However, the current synthetic alternatives have been plagued with little success in small caliber vessels (<6mm).

Bacterial cellulose (BC) has been presented as an alternative material for the production of a vascular graft. It presents good mechanical characteristics allied with non-thrombogenicity, hemo- and biocompatibility. Several methods have been suggested in the literature that allow the production of tubular BC grafts. The work developed and presented in this thesis had two aims: further development and performance enhancement of a current production method and also, the development of a new and effective method for graft production.

A current, and common, method of graft production takes advantage of the way in which the *Gluconacetobacter* bacteria produces BC at air-culture medium interfaces. By providing an oxygen permeable tubular scaffold it is possible to produce tubular BC constructs. However, the tubular BC constructs produced in this method were found to be lacking in mechanical strength. Towards enhancing their performance a nanocomposite of BC and poly(vinyl alcohol) (PVA) was developed.

Blood contacting materials have necessarily to be able to perform well in regards to their hemocompatibility and thrombogenicity and, as such, the BC/PVA nanocomposite was so tested, as well as BC. The standard characterization of the whole blood clotting time, plasma recalcification and hemolysis index were all determined. In addition, as a more in depth analysis, complement system and Factor XII activation along with a detailed characterization of platelet adhesion and activation was also assessed. Results suggested that both BC and BC/PVA induced

low levels of Factor XII and platelet activation and this is possibly the main cause for the good hemocompatibility presented by of both materials. The presence of PVA in the nanocomposite did not hinder the hemocompatibility of BC, in some cases adding to the performance of the material.

Along with the, aforementioned, necessary characterization of the BC/PVA nanocomposite, the mechanical and morphological characteristics of the material were also tested and shown to be significantly different in terms of fiber structure and organization upon drying. The performance of the nanocomposite regarding mechanical characteristics was expected to outperform those of BC. However, the tensile tests performed suggested otherwise. A more detailed morphological analysis of BC/PVA showed that, once dried, the fiber structure changed dramatically; presenting two very distinct, dense and porous, regions. These structural characteristics were found to be associated with a heterogeneous distribution of PVA throughout the nanocomposite which affected the mechanical performance and permeability of the dried nanocomposite.

Finally, through the course of several developmental stages of the graft, an alternative method of production that allied both technical facility and low cost was discovered. This method was able of outperforming the previous iteration of the BC grafts and was, later, shown to be a viable and cost effective method of graft production. The grafts produced by this novel method allowed for mechanically strong and yet compliant grafts to be produced, as was demonstrated by the mechanical characterization performed, in a reproducible way. Continued characterization showed a luminal topography similar to that of a native vessel, far exceeding ePTFE and Dacron in this regard. Additionally, an important mechanical characteristic; and frequent cause of graft failure, compliance was also determined and shown to be comparable on the luminal surface when compared to native arteries and again outperforming the current industry standards. The grafts were later shown to perform well *in vivo* in pigs. Surgical implantation was performed in a femoro-femoral arterial bypass bridge to study the *in vivo* viability of the graft. Results demonstrated patency after 1 month of implantation with the presence of an endothelial cell population on the luminal surface of the graft.

Resumo

Cirurgia de bypass é uma ferramenta fundamental no tratamento de algumas doenças arteriais e venosas, muitas destas doenças causadas por aterosclerose. Este procedimento utiliza uma prótese vascular para substituir, formar uma ponte ou manter o funcionamento de um vaso danificado, obstruído ou doente. O processo mais comum utiliza um vaso nativo, como a veia safena, como a prótese vascular. Quando um vaso autólogo não estiver disponível, devido à progressão natural da doença ou cirurgias anteriores, utilizam-se alternativas sintéticas. Contudo, as actuais alternativas sintéticas têm obtido pouco sucesso em vasos de pequeno calibre (<6mm).

Celulose bacteriana (BC) apresenta-se como uma alternativa para a produção de próteses vasculares. Apresenta boas características mecânicas aliadas a não-trombogenicidade, hemo- e biocompatibilidade. Vários métodos de produção de vasos de celulose bacteriana têm sido propostos na literatura. O trabalho desenvolvido e apresentado nesta tese teve dois objectivos: continuar o desenvolvimento e melhorar o desempenho dos actuais métodos de produção, bem como, o desenvolvimento de uma nova e eficaz maneira de produzir próteses.

O actual e mais comum, método de produção aproveita a forma como as bactérias do género *Gluconacetobacter* produzem BC nos interfaces ar-meio de cultura. Utilizando um suporte tubular permeável a oxigénio é possível produzir estruturas tubulares de celulose. Contudo, as estruturas tubulares produzidas por estes métodos demonstraram fracas propriedades mecânicas. Com o objectivo de melhorar o desempenho mecânico desenvolveu-se um nanocompósito de BC e poli(vinil álcool) (PVA).

Materiais que contactam com sangue têm que ser capazes de ter um bom desempenho em termos de hemocompatibilidade e trombogenicidade e como tal, o nanocompósito de BC/PVA, bem como a BC, foram testadas. Foi feita a caracterização do tempo de coagulação de sangue total, recalcificação do plasma e índice de hemólise. Para além destes, foi analisada a activação do sistema de complemento e Factor XII bem como uma caracterização detalhada da adesão e

activação de plaquetas. Os resultados sugerem que a BC e o BC/PVA, induzem baixos níveis de activação do Factor XII e plaquetas, o que poderá ser a principal razão pela boa hemocompatibilidade apresentada pelos materiais. A presença de PVA no nanocompósito não afecta a hemocompatibilidade da BC, em alguns casos até melhorando o seu desempenho.

Para além desta caracterização do BC/PVA, o nanocompósito foi caracterizado a nível mecânico e morfológico e os resultados mostraram diferenças significativas em termos de estrutura e organização das fibras após secagem. Esperava-se que o desempenho do nanocompósito, em termos de características mecânicas, seria superior à BC, no entanto isto não se veio a verificar. Uma análise morfológica mais detalhada do BC/PVA mostrou que, após secagem, a estrutura das fibras sofre alterações profundas; apresentando duas regiões distintas, uma densa e outra porosa. Estas distintas regiões devem-se à distribuição heterogénea do PVA no nanocompósito, por seu turno, afecta o desempenho mecânico e permeabilidade do nanocompósito seco.

Por fim, a longo do curso de várias fases de desenvolvimento das próteses, foi descoberto um método alternativo de produção que aliava facilidade técnica e baixo custo. Este método mostrou ser capaz de produzir próteses melhores que todas as versões anteriores e, mais tarde, mostrou ser um método de produção viável e de baixo-custo. As próteses produzidas por este método novo permitem obter forças mecânicas superiores sem perder a complacência do material, como foi demonstrado pela caracterização mecânica, de forma reprodutível. A continuada caracterização das próteses mostrou uma topografia luminal semelhante ao dos vasos nativos, superando o ePTFE e o Dacron. Adicionalmente, uma importante característica mecânica, e frequente causa de falha das próteses, a complacência foi também determinada e mostrou ser comparável à complacência da superfície luminal de artérias nativas, tendo portanto um melhor desempenho que as próteses industriais actuais. As próteses mostraram, mais tarde, ter também um bom desempenho *in vivo* em porcos. As próteses foram implantadas numa ponte femoral de forma a estudar a viabilidade in vivo. Os resultados obtidos demonstraram patência ao fim de 1 mês de implantação com a presença de células endoteliais na superfície luminal da prótese.

Publications

This thesis is based off of the following publications:

Chapter 1

Leitão, AF; Silva, I; Faria, M; Gama, M; *Polymers in Vascular Grafts* in *Encyclopedia of Biomedical Polymers and Polymeric Biomaterials*; Taylor & Francis; 2014 (in Press) (DOI: 10.1081/e-ebpp-120050697)

Chapter 2

Leitão, A.F.; Gupta, S.; Silva, J.P.; Reviakine, I.; Gama, M.; *Hemocompatibility study of a bacterial cellulose/polyvinyl alcohol nanocomposite*; Colloids and Surfaces B: Biointerphases; Vol. 111, C:493-502; 2013 (DOI: 10.1016/j.colsurfb.2013.06.031)

Chapter 3

Leitão A.F.; Silva, J.P.; Dourado, F.; Gama, M.; *Production and Characterization of a New Bacterial Cellulose/Poly(Vinyl Alcohol) Nanocomposite*; Materials; Volume 6, pp 1956-1966; 2013 (DOI:10.3390/ma6051956)

Chapter 4

Leitão A.F.; Faustino, A.M.R.; Faria, M.A.; Moreira, R.; Mela, P.; Silva, I.; Loureiro, L.; Gama, M.; *A Novel Small-Caliber Bacterial Cellulose Vascular Prosthesis: Production, Characterization and Preliminary In vivo Testing*; Biomaterials (submitted)

Annex A

Alexandre F. Leitão and Miguel Gama; *TUBULAR BACTERIAL CELLULOSE GRAFTS FOR VASCULAR APPLICATIONS AND METHOD OF PRODUCTION*; Provisionary Patent Number: 107904; Date of Priority: 23-09-2014

Table of Contents

Chapter 1

Chapter 4

Chapter 5

Annex A

List of Abbreviations

A5	Fluorescent-annexin 5
AHA	American Heart Association
ASTM	American Society for Testing and Materials
ATCC	American Type Culture Collection
AVG	Arteriovenous grafts
BC	Bacterial Cellulose
BC/PVA	Bacterial Cellulose/Poly(Vinyl Alcohol)
BCIP	5-Bromo-4-Chloro-3-Indolyl Phosphate
BSA	Bovine Serum Albumin
C	Compliance
CAT	Computer Assisted Tomography
CI	Critical Ischemia
CLSM	Confocal Laser Scanning Microscopy
CVD	Cardiovascular Disease
CVF	Cobra Venom Factor
D	Diffusion Coefficient
DAB	Diaminobenzidine
dBC	dried Bacterial Cellulose
dBC/PVA	dried Bacterial Cellulose/Poly(Vinyl Alcohol)
D_{Diast}	Diastolic Diameter
D_{Syst}	Systolic Diameter
ePTFE	expanded Polytetrafluoroethylene
EU	Endotoxin Units
FXII	Factor XII
HEPES	4-(2-hydroxyethyl)-1-piperazineethanesulfonic acid buffer
HIA	Human Iliac Artery
HSV	Human Saphenous Vein
IC	Intermittent Claudication

IMA	Internal Mammary Artery
IND	Inter-nodal Distance
L	Membrane Thickness
LPS	Lipopolysaccharide
LSV	Long Saphenous Vein
MRI	Magnetic Resonance Imaging
ndBC	never-dried Bacterial Cellulose
ndBC/PVA	never-dried Bacterial Cellulose/Poly(Vinyl Alcohol)
NO	Nitric Oxide
PAD	Peripheral Arterial Disease
PBS	Phosphate Buffer Saline
PCL	Polycaprolactone
P_{Diast}	Diastolic Pressure
PEG	Polyethylene Glycol
PET	Poly(ethylene terephthalate)
PFA	Porcine Femoral Artery
PLA	Polylactic Acid
Plt	Platelet
PMA	Phorbol 12-myristate 13-acetate
PPP	Platelet Poor Plasma
PRP	Platelet Rich Plasma
PS	Phosphatidylserine
P_{Syst}	Systolic Pressure
PTFE	Polytetrafluoroethylene
PU	Polyurethane
PVA	Poly(Vinyl Alcohol) or Polyvinyl Alcohol
RGD	Arg-Gly-Asp
SEM	Scanning Electron Microscopy
SMC	Smooth Muscle Cell
SMCs	Smooth Muscle Cells
TEBV	Tissue Engineered Blood Vessel

TRAP	Thrombin Receptor-Activating Peptide
WHO	World Health Organization

List of Figures

Chapter 3

Chapter 4

Annex A

Figure A-4 - Endotoxin (LPS) concentration in EU/ml (Endotoxin Units/ml) as determined over 3, 24 hour, washes in 5% SDS and water (negative control).

Figure A-5 Representative photographs and Haematoxylin and Eosin histopathological microscopy images of in vivo tests. (A) Femoral-femoral artery BC graft placement, (B) Doppler Sonography screenshot showing blood flow through the BC graft after one month of implantation, (C) 100x magnification of the luminal surface of the graft with cell adhesion on the surface of the graft along and some cell infiltration, (D) 200x External surface of BC graft showing formation of neo-vessels (arrow), (E) External surface of the BC grafts showing a smooth transition from surrounding tissues into the BC graft with cell infiltration, (F) 200x magnification of a cell population in a transitional region from adventitia into the BC grafts.

List of Tables

Chapter 2

Chapter 3

Chapter 4

Annex A

Bacterial Cellulose (BC). Suture retention strength for the BC graft and untreated BC are not statistically different (p>0.05; n=4)

Table A-3 - Compliance (presented as value x10-2 %/mmHg) with standard deviation (SD) as collected from the literature for Internal Mammary Artery (IMA), Human Saphenous Vein (HSV), Human Iliac Artery (HIA), Tissue Engineered Blood Vessel (TEBV), Polyurethane (PU), Polyethylene terephthalate (PET), expanded Polytetrafluoroethylene (ePTFE), Bacterial Cellulose/Chitosan blend (BC/Chi) and measurements for the compliance of the BC grafts as measured externally and internally (n=5).

Aims and Thesis Outline

Cellulose is the most common naturally occurring polymer on the planet. Bacterial cellulose (BC) is identical to plant cellulose but is excreted pure by bacteria of the *Gluconacetobacter* genus. It is a linear chain of glucose monomers linked by β (1→4) polysaccharide bonds that forms a hydrogel that has been widely studied for potential biomedical applications among which are vascular grafts. The aim of this thesis is precisely to address one of those potential applications: BC and BC/PVA as potential vascular bypass grafts.

Chapter 1 starts by presenting the reasoning behind the need for a vascular graft and the requirements a functional graft must meet. It goes on to present a review on some of the current polymers being studied for their potential application with a short state of the art for each.

The initial approach of the work presented here was to use a method described in the literature for graft production and develop it in order to produce a viable graft solution. The method adopted for this was the development of a BC/PVA nanocomposite material. The theory was that BC and PVA would produce an interpenetrated network of fibers. The resulting nanocomposite would take on properties of both polymers.

Any blood contacting material, especially in the case of a vascular graft, must be well characterized in regards to hemocompatibility and thrombogenicity. The work pertaining to this characterization resided in Chapter 2. Three common hemocompatibility indicators were assessed along with a more in depth analysis that allowed a greater assessment of the mechanics behind the good hemocompatibility and non-thrombogenicity of both BC and BC/PVA.

In Chapter 3 further characterization of the nanocomposite is presented; now on a mechanical and morphological level. The nanocomposite would necessarily need to perform well on a mechanical level in order to be viable. As such mechanical characterization was a necessary requirement. However, during the course of the study presented in this chapter, dramatic changes to the fibrilar structure of the

dried nanocomposite were revealed. The chapter focuses closely on those morphological changes and their significance to the performance of BC/PVA

Through several different modifications performed to the production methods of the graft and formulations of the nanocomposite a novel method for production was found, studied and developed. The methodology allowed the production of a graft that outperformed all previous iterations in mechanical strength and compliance while retaining the hemocompatibility qualities of BC. The small differences found between the behaviors of BC/PVA and BC did not seem to justify the continued use of PVA and so, PVA was abandoned, at least for now, in favor of a more cost-efficient and logistically simpler methodology.

This production method is described in Chapter 4 along with a mechanical and morphological characterization, of special note the study of the mechanical compliance. Furthermore, in chapter 4, the performance of the graft in a live animal model was also studied and is also presented The novel methodology outlined in this chapter proved effective and reproducible having ultimately led to an application for a provisionary patent (included as Annex A).

In the final Chapter (5) a general conclusion of the work is presented and future perspectives, in regards to the further development of the graft, are outlined.

Chapter 1

Polymers in Vascular Grafts

Cardiovascular disease (CVD) is one of the major leading causes of death in today's world. Among the most common is atherosclerosis, a thickening of the arterial wall to the buildup of plaque. When the disease causes complications, due to occlusion of the vessel or arterial wall lesions that ultimately lead to thrombosis, usually a bypass is required to redirect blood flow around the occluded vessel. The preferred vessels for the bypass procedure are autografts, veins and arteries culled from the patient. When these vessels are not available, due to the natural progression of the disease or prior procedures, synthetic alternatives must be used. These alternatives are created from polymeric materials that can substitute the autografts completely and remain in the patients for years and decades or serve as a temporary substitute that will allow tissue-engineering. In this chapter we intend to show some of the polymers that are currently being studied, and two in particular that have been in use for over 50 years; that can one day serve the purpose of substituting the autografts completely and provide a better future for patients worldwide.

Introduction

Cardiovascular disease (CVD) is a broad term encompassing several different diseases among which atherosclerosis and hypertension are the most common. The causes, prevention, and/or treatment of all forms of CVD remain active fields of biomedical research, with hundreds of scientific studies being published on a weekly basis. The ongoing research in the various fields that are related to this topic all have one single objective: improving the quality of life of patients worldwide via prevention of the disease and by finding better courses of treatment.

The leading cause of death associated with vascular disease is atherosclerosis, a syndrome that affects arterial blood vessels. Atherosclerosis is defined as a chronic inflammatory response in the walls of arteries, closely associated with high cholesterol levels in the blood, and can remain asymptomatic for decades. Eventually the blood flow through the affected arteries can be cut off completely and blood flow must be reestablished around the occluded vessel. In these extreme cases the most common procedures performed are bypass surgeries.

Since the 1950s, when autologous vessels are not available to perform the bypass procedure, synthetic alternatives have to be used. The current, most common synthetic alternatives, are known simply as Dacron and expanded polytetrafluoroethylene (ePTFE). They have been used countless times in life saving procedures. While they perform well, as long as certain conditions are met, they are not perfect and do not provide a definitive solution.

Much research has focused on improving the current grafts and/or discovering new better grafts and material combinations. Research has focused on polymeric materials; either non-degradable polymers that remain *in vivo* for undetermined periods of time or biodegradable polymers that serve as tissue-engineering scaffolds, ultimately allowing for native tissue to form a new blood vessel. Our objective in this entry is to outline the need for the prosthetics, the standardized methodologies to assess their viability, an unbiased review of the current state of research being performed on several polymers with the objective of developing new synthetic vascular grafts and finally what we consider to be the future perspectives of the research performed in this ongoing field.

CVD: the need for vascular grafts

The World Health Organization (WHO) estimates that 17.3 million people died in 2008 of cardiovascular disease (CVD), of which 80% occurred in low- and middle-income countries. The American Heart Association (AHA) estimates that, from 1999 to 2009, the relative rate of death attributable to CVD declined by 32.7%. Yet, it is still responsible for 1 of every 3 deaths in the United States (one every 40 seconds) [1]. On the basis of CVD is atherosclerosis, a complex disease involving the heart and blood vessels and is responsible for several disorders such as stroke, myocardial infarction and peripheral arterial disease (PAD).

Atherosclerosis was described for the first time in 1904 by Marchand to define arterial stiffening in association with fatty degeneration. Atherosclerosis is a systemic disease affecting large and medium-sized arteries. Accumulation of lipids in both smooth muscle cells (SMCs) and macrophages leads to inflammatory response and arterial thickening, which plays a major role in atherogenesis [2].

Atherosclerotic plaques remain asymptomatic, below critical stenosis (>70%), due to compensatory vessel enlargement and to the development of collateral circulation in response to chronic hypoxia. Chronic injury leads to endothelium dysfunction, increased oxidative stress and reduction in bioactivity or synthesis of endothelium-derived nitric oxide (NO), which results in a reduced vascular tone and ischemia [3-5]. The atherosclerotic plaque may become unstable, ulcerate and rupture with subsequent distal embolization or vessel occlusion due to exposure of the highly thrombogenic sub-intimal surface. The exposure of the sub-intimal surface promotes platelet adherence and activation – atherothrombosis [6] – leading to the acute clinical presentations or worsening of a chronic controlled disease, followed by a high morbidity and mortality. Despite significant improvement in medical and surgical management of CVD, atherosclerosis still remains a serious life-threatening disease [2].

Cardiovascular risk factors play a major role in atherosclerosis pathogenesis. They may be hereditary or acquired, related to behavioral or environmental factors. The INTERHEART study, spearheaded by Dr. Yusuf and colleagues over 52 countries, found that 90% of myocardial infarction risk factors were abnormal lipids, smoking, hypertension, diabetes, abdominal obesity, psychosocial factors, irregular diet and an

absence of a planned exercise program [7]. We now have overwhelming evidence that risk factor control is highly cost-effective and significantly reduces CVD morbidity and mortality.

Clinical manifestations of CVD manifest mainly as cerebral vascular disease, coronary heart disease and PAD, and can cause severe disability with great limitations in patient habits and decreased quality of life or even death. PAD is a chronic disease with prevalence in several epidemiologic studies in the range of 3-10%, increasing to 15-20% in people over 70 years of age [5]. Initially asymptomatic, it can become progressively symptomatic presenting with pain in the calves due to exercise – intermittent claudication (IC) – and, when severe, evolves to critical ischemia (CI) with a high risk of limb loss. Patients with CI have high amputation rates: 25% will be amputated at time of diagnosis and another 30% over the following year [8]. In association with PAD, these patients have other co-morbidities as a consequence of diffuse atherosclerosis involvement with the heart, cerebral-vascular and kidney disease. In PAD´s treatment we have to recognize the disease, quantify the extent of local and systemic disease, identify and control risk factors, and establish a comprehensive treatment program [8].

In vascular surgery, surgical bypass is fundamental in the treatment of arterial and some venous diseases (Figure 1-1A). Vascular grafts are used to replace, bypass or maintain function of damaged, occluded or diseased blood vessels of small, medium and large diameter. The chosen conduit and its success depend on several factors such as availability, size, ease of handling and technical facility, thrombogenicity, resistance to infection and dilation, durability, long-term patency and price.

Depending on the target vessel different options of autografts can be considered. In coronary surgery the best conduits are internal mammary artery, radial artery and long saphenous veins (LSV). Visceral arteries are also best substituted by LSV or by the iliac vessels, hypogastric and more uncommonly by the external iliac artery [9]. In PAD surgery the most common autograft in use is the long saphenous vein (using either the reversed or "in situ" techniques) and diameters of 3mm are required for good long term results [10]. Short saphenous vein or arm veins can be an alternative when no LSV is available. Autologous vein grafts remain the conduit of choice for infrainguinal revascularization, and long-term results are quite good when a good run-off is present [10]. Infrainguinal vein graft failure still occurs in 20- 50% of cases, and remains a major

problem for vascular surgeons and patients. Recovery of the thrombosed vein graft has a very low patency. Furthermore, replacement of a failed bypass graft with a new one requires that the surgeon finds an alternative graft for limb salvage. Thus, the results of repeat bypass surgery, after failed previous bypass, are inferior to those of primary bypass surgery. It is therefore imperative to maintain the patency of infrainguinal bypass grafts [11]. Autogenous arterial or venous conduits are not always available, due to venous insufficiency or inadequate LSV diameter/length, previous harvest of vein for cardiac surgery or previous varicose vein surgery. These factors raise the need for alternative grafts. At present, these include autologous or non-autologous biological grafts (obtained using different methods for harvesting and preservation), tissue engineering (using either synthetic- or biological-based scaffolds for cell seeding), endovascular methodologies [12], gene therapy [13] and non-degradable synthetic grafts.

For large vessel replacement, graft size match, resistance to infection and durability are of great importance. Aorto-iliac reconstructions have blood flow properties that allow long patency due to minimal tissue ingrowth and endothelial repopulation [9]. Infra-renal aortic graft diameters range from 16 to 22 mm and, Poly(ethylene terephthalate) (PET) or ePTFE prosthesis—single tube or bifurcated—are the most commonly used (Figure 1-1B and 1C). The size of the graft should be as close as possible to that of the native artery that is replaced. Ten-year primary patency is 89.2% for aorto-iliac bypass and 78% for aorto-bifemoral bypass [14]. The replacement of an aortic infected graft can be made with prosthetic grafts, arterial homografts or deep veins of the lower limb. The latter present a high grade of morbidity and increased operative time. Alternatively, arterial homografts are a solution with good early results but a high grade of late degeneration. A study comparing cryo-preserved arterial homograft with silver-coated Dacron grafts for the treatment of infected aortic grafts demonstrated comparable effectiveness with respect to early mortality and midterm survival. Graft-inherent complications, aneurismal homograft degeneration, and reinfection of the silver-coated grafts, have also been observed [15].

In peripheral lower limb bypass there are two types of arteries to be replaced: femoral and popliteal arteries, with a medium size (6-8mm), and distal popliteal, tibial, peroneal
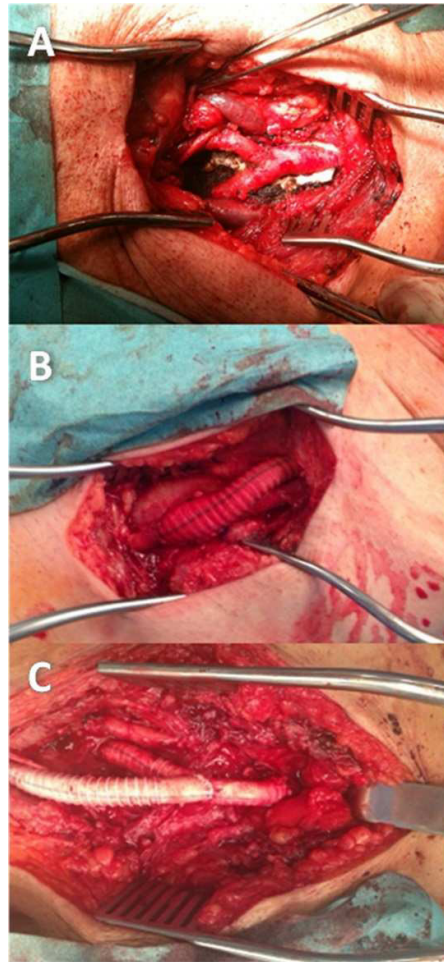
Figure 1-1 - Photographs of the surgical application of the three most common bypass grafts. A) a vein graft, B) Dacron graft and C) and ePTFE graft.

and foot arteries with small size arteries (<6mm) [9]. With the expanding use and indications for endovascular surgery, the number of vessels needing replacement is decreasing, with a lower rate of preoperative morbidity. Treatment of the common femoral artery has limitations due to increased rate of infection in groin surgeries. Bypasses at and from common femoral artery should, when possible, be performed with an autologous graft.

In small size arteries (< 6mm), intimal hyperplasia at the proximal or distal anastomosis site is of paramount importance. In these grafts, thromboresistance of the inner lining, shear stress and behavior of the conduits are important aspects in the choice of the graft. In these cases, autologous grafts are again the best choice.

Femoro-popliteal bypass may be made with a synthetic graft when the distal anastomosis is above the knee and the patient has no ulcer that can increase the risk of graft infection. In the case of bellow knee bypass, LSV is the preferred choice. A meta-analysis of femoral-popliteal bypass grafts for lower extremity arterial insufficiency refers that primary graft patency was 57.4% for above-knee ePTFE, 77.2% for above-knee vein, and 64.8% for below-knee vein at 5 years; there was a significant difference between above-knee grafts at 3, 4 and 5 years [14]. Another study reported a similar patency, to the aforementioned study, for infragenicular bypasses with ePTFE for limb salvage in above-knee (27%) and below-knee (25%) over 5 years [16].

When LSV is unavailable, alternative techniques have been applied to increase patency, such as the use of a cryopreserved allografts, composed synthetic-LSV graft, vein cuffs and ePTFE cuffs at the distal anastomosis in order to reduce the risk of intimal hyperplasia [10]. These technical maneuvers and the use of numerous pharmacological adjuvants, included at the time of production or implantation, are of paramount importance to increase artificial vascular grafts patency. In carotid surgery Dacron patches are used routinely in most centers for carotid endarterectomy and carotid bypasses are used in the treatment of aneurismal disease of the carotid artery. Autogenous LSV, again, is the first choice for carotid bypass, although high rate of restenosis has been described [17]. Alternative, PTFE prosthesis can be used due to the high flow and short length, with long term graft patency of 95-97% [18].

Arteriovenous grafts (AVG), used to connect an artery to a vein, are commonly used in hemodialysis patients. In these patients it is need a high flow graft that is also durable, resistant to infection and to continuous trauma (due to multiple puncture, two to three times a week) to guarantee an efficient hemodialysis for the patient. Autogenous veins are the conduct of choice, with an emerging of new techniques to recover the arm veins, and only in extreme cases, prosthetic grafts are considered.

Vascular Graft Requirements

As described above, by far, the preferred grafts are autogenous, i.e., the donor and the patient are the same individual and this vastly decreases the risk of rejection. However,

the progression of the disease in these patients many times limits the availability of viable vessels. When this occurs two alternatives are available: biological (which can be allografts or xenografts) or synthetic grafts (which consist of polymers that can be either synthetic or biological).

The biological alternative to the autogenous vessels are allografts and xenografts. Theoretically, biografts meet all the conditions for the best vascular graft. They promise "off-the-shelf" availability, a wide variety of sizes, excellent handling characteristics, and patency rates similar to those of autogenous vessels [9]. Disappointingly, clinical applications of these grafts have not met the high expectancy awaited. This is in large part due to the lack of long-term patency associated with tissue degeneration.

Therefore a large amount of study has gone into assessing and discovering a synthetic alternative graft vessel. A viable synthetic vascular graft should combine fundamental characteristics that are inherent to autografts: biocompatibility, namely hemocompatibility, and mechanical compliance. Hemocompatibility is linked with the blood-material interaction, the mechanisms of which are still not completely understood. However, it is well established that the material should provide a minimal risk of hemolysis, clotting and thrombosis, along with a minimal risk of infection or triggering of the immune response.

Biocompatibility, particularly in the case of a tissue engineering approach, ultimately refers to the ability of the biomaterial to stimulate cell adhesion, invasion and proliferation. The grafts should allow for the migration of cells from the surrounding tissues in order to, at least, produce an endothelium on the luminal surface of the graft. In tissue engineered approaches, where cell-seeding might be adopted, this will allows for gradual cell migration, proliferation and production of an extra-cellular matrix while at the same time the material is slowly degraded. This approach allows the synthetic graft to be completely substituted by newly formed native tissue, thus reducing the risk of long-term deterioration and improve the overall long-term patency.

Finally, and of no less importance, is the matching of mechanical properties. The grafts should provide mechanical characteristics similar to those of the native vessels, especially in terms of compliance, in order to allow for a consistent and uninterrupted blood flow through the graft. This will ultimately avoid problems such as intimal hyperplasia, which is closely associated with mismatch of mechanical properties [19, 20].

Methods for Analysis and Testing

Over the years several assays and tests have been suggested in order to determine the viability of synthetic grafts before advancing to any clinical assays. The main guidelines for hemocompatibility testing are laid out in ISO 10993-4. Essentially, the ISO lays out that it is necessary to perform assays for immunology (complement system), hematology, platelets, thrombosis and coagulation.

Complement activation- is the most relevant test for determining the immune response to a blood contacting material. It can be performed *in vitro* by exposing isolated complement proteins to the material surface and determining the decrease in total CH50 levels, a classical approach, alternatively the determination of C3- and C5-convertase cleavage products formed over time. The amount of cleaved products can be easily determined by semi-quantitative Western blot and compared with baseline levels in order to determine activation of the complement system. Currently there are no clearly determined acceptable levels and data is generally presented as comparisons with other materials. The *American Society for Testing and Materials* (ASTM) F1984-99 and ASTM F2065-00 standards should be considered when assessing this particular parameter.

Hematology– is generally assessed by determination of the hemolytic index and can be determined by the method suggested by the *Standard Practice for Assessment of Hemolytic Properties of Materials* from the ASTM F756-00, 2000. Additionally, leukocyte activation via microscopic analysis or flow cytometry, for determination of L-selectin and CD11b expression, are also indicators of hemolytic activity of a material.

Pro-coagulant Activity– several tests can be explored in order to thoroughly evaluate the potential activation of the coagulation cascade by surface-material interaction, *i.e.*, coagulation triggered by the intrinsic (or contact) activation pathway. The contact activation pathway is a result of direct activation of Factor XII, via conformational change induced by exposure to the material surface. Direct quantification of how much activated Factor XII is produced can be achieved by use of a chromogenic, or fluorogenic, substrate that is broken down by the activated form of Factor XII [21, 22]. Alternatively, indirect assessment of the activation of this pathway can be made by determination of the partial thromboplastin time or plasma recalcification profiles [23, 24].

Thrombogenicity- Platelet-material interactions can lead to both platelet activation and/or adhesion, depending on their state of activation and the presence of ligands [25, 26]. Ultimately, the involvement of activated platelets along with the coagulation cascade results in the formation of a thrombus (Figure 1-2). The clearest *in vitro* measure of the thrombogenicity is the determination of whole blood clotting time through spectrophotometric analysis. Scanning Electron Microscopy, and to a lesser extent light microscopy, are also useful tools in determining platelet adhesion and activation, though the cues here are visual (formation of pseudopodia and platelet aggregates) rather than biochemical. Activation and subsequent adhesion of platelets can also be determined by fluorescence and confocal microscopy. Most assays suggested for determination of thrombogenicity must be tested in dynamic (preferably *in vivo*) conditions. Angiography, intravascular ultrasound, Doppler ultrasound, computer assisted tomography (CAT) and magnetic resonance imaging (MRIs) are useful tools for the determination of the *in vivo* performance in regard to percentage of occlusion and flow reduction. Also it is important to analyze, after *in vivo* placement, the gravimetric analysis of the thrombus mass and histological inspection of the prosthesis and surrounding tissues.
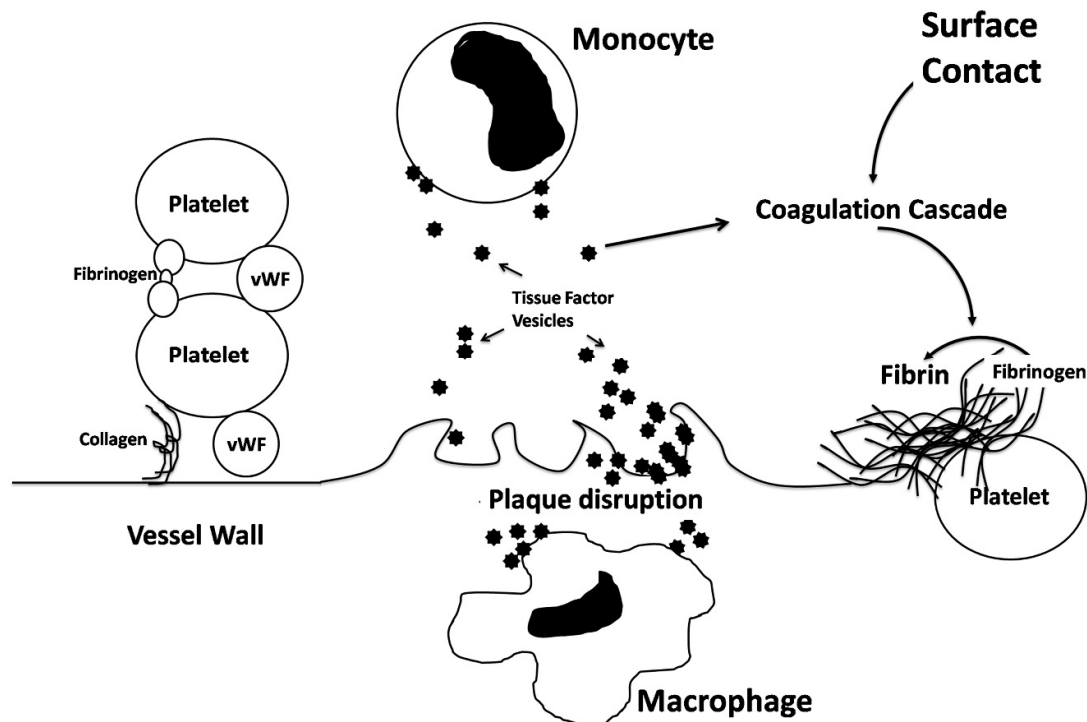
Figure 1-2 - - Schematic representation of activation and amplification pathways of coagulation by activator complexes (generating thrombin for platelet activation and fibrin formation) and thrombus formation on disrupted atherosclerotic plaques.

Platelet activation- It is paramount that platelet activation be minimized in blood contacting materials. The extent of free platelet activation can be easily determined by cytometric analysis. Platelets are exposed to the material surface and the presence of certain activation markers (like CD62P or CD63) determined with the use of fluorescent antibodies. Also, the formation of platelet aggregates due to material activation should be determined by means of an aggregometer. These tests can be performed both *in vitro* and *in vivo*. Other *in vivo* tests that are important for assessment of platelet activation are determination of platelet count, template bleeding time (as a measure of platelet function) or alternatively platelet function analysis with collagen filters. Additionally gamma labeling and platelet lifespan assays are good measures of platelet viability.

Mechanical properties - The mechanical properties of the graft must assure adequate mechanical compliance. As discussed above the mechanical compliance is paramount in order to allow an uninterrupted pulsatile flow through the vessel matching the mechanical characteristics of the surrounding tissue. This parameter can be quantified by setting up a pulsatile flow into a graft and measuring the volume changes caused by the increase in pressure. The best possible graft will match the compliance of the native vessel it is intended to substitute. Assuring mechanical strength and compliance will minimize the risk of mechanical failure of the graft.

In vivo tests - The final assays before potentially moving on to a clinical trial are *in vivo* tests. The *in vivo* tests can produce useful information to build on any of the aforementioned assays and also provide a realistic view of the behavior of the grafts in a complex and dynamic system that simply cannot be reproduced *in vitro*. These assays generally are performed simultaneously with some of the above tests in order to provide a back and forth feedback. Care should be taken into choosing an appropriate animal model. A rat or mouse model is an appropriate one in order to determine the feasibility of the graft over a significant portion of the animal´s life, since their life cycle is short (circa 24 months), rapidly providing insight into feasibility. However, the mechanics and body response of a small animal model are significantly different from those of a larger one and therefore other models such as dog (though today it is rarely used due to ethical and social issues), sheep and pig should also be considered. These larger animals provide many more surgical implantation options and a longer life cycle that can produce results that are more in line with what can be expected in humans. Another important parameter

is precisely the placement of the prosthetic graft. The placement in a high-flow vessel, such as the rat aorta or a sheep's carotid artery, will provide different results from a low-flow vessel, such as the femoral artery of a dog or pig. Nevertheless, translation of *in vivo* results to humans is not always straightforward.

Non-Degradable Polymers

The current standard polymers for synthetic vascular grafts are PET (Dacron) and ePTFE grafts, synthetic non-degradable polymers that offer a conduit for life and limb saving surgeries when autografts are not available. However, as present in the market today, these materials have inherent problems that need to be overcome. One of the broad possibilities that are currently being researched is the development of novel graft that can be readily implanted. The solution may very well be the development of permanent grafts that can out-perform the current options in regards to long-term patency (Figure 1-3). Towards that end the following are the current focus in research in this field.

Poly(ethylene terephthalate)

Poly(ethylene terephthalate) (PET) is a thermoplastic polymer resin of the polyester family. It can exist as both an amorphous and a semi-crystalline polymer depending on processing and thermal history. Since, its introduction in 1939 by DuPont, later patented in 1950 as Dacron®, it has found numerous applications namely as a synthetic fiber (over 60% of its applications). Thermoforming applications make up the bulk of remaining uses found for this polymer with a small percentage being used as an engineering resin often in combination with glass fiber.

It is a relatively inert, hydrophobic and bio-stable polymer that presents a high tensile strength (40-180MPa) and Young's modulus (3-14GPa), values varying widely based on
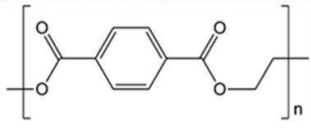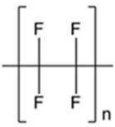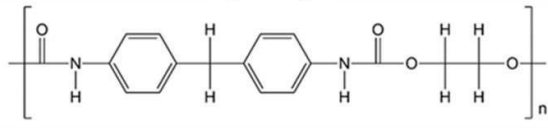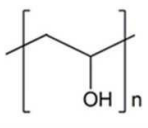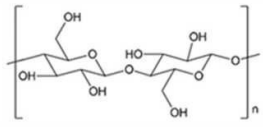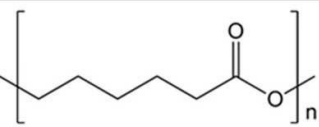
Figure 1-3 - Chemical structure of non-protein polymer monomers. The chemical structure for polyurethane is a representation of one possible polyurethane.

preparation and dimensions [27]. PET has been widely studied for biomedical applications in cardiovascular surgery, as ligaments, joint replacements, implantable sutures and surgical meshes [28-32]. Under the aforementioned name Dacron, it has been used as an aortic vascular graft as far back as 1957 when DeBakey performed a substitution of thoracic and abdominal aorta and of proximal peripheral vessels. To this day, PET is still one of the most commonly used synthetic grafts in large caliber (>8mm) bypass surgery performed above the waist [33] since it is a cheaper alternative to ePTFE. Patency rates for PET have been continuously improved and have been shown to remain patent for up to 8 years after implantation [34]. A prior study actually showed that PET

patency could go up to 25 years, though the follow-up rate was under 20% after 10 years [35].

However, when PET vascular grafts are implanted they trigger the activation of the intrinsic pathway of blood coagulation resulting in surface-induced thrombosis [36]. This is most prevalent when the diameter of PET vascular grafts is smaller than 6mm. There is a considerable reaction between PET and the native artery, as well as with blood, causing a rapid build-up of fibrin at the blood/graft interface [37]. This is due to both the hydrophobic nature of PET, which has been shown to induce protein adhesion [38], and also the low-flow of small caliber vessels. This ultimately results in graft failure and poor clinical results. Hence, the patency of small-diameter PET vascular grafts needs to be improved. The PET vascular grafts are produced by two different methods. Woven, in an over-and-under pattern in the lengthwise and circumferential directions, or the more commonly used knit grafts, by looping the fibers in an interlocking chain, into cylindrical and longitudinally crimped grafts [39]. The crimping of the graft increases flexibility, elasticity, and kink resistance. However, after implantation, these properties are lost as a consequence of tissue ingrowth on average after 7 years [40]. The grafts incorporate a velour finish which increases the surface area. This elevates the number of anchorage points for both fibrin and cells in order to promote tissue integration. The weaving/knitting method of producing the grafts allows them to be shaped and branched so as to fit any needed requirements and mechanical properties can be tailored so as to allow for better compliance with the native arterial wall at the site of anastomosis.

The production method of the grafts has remained essentially the same over the years. The knit PET grafts have been impregnated with gelatin [41], albumin [42] or collagen [43] in order to improve their hemocompatibility. Another approach to ameliorate hemocompatibility is surface modification. The chief methods of surface modification of blood-contacting biomaterials involve coupling bio-agents or increasing hydrophilicity. Heparin has been bonded onto PET grafts showing positive results, namely increasing plasma recalcification times [44] and overall in-patient patency [45]. Silver particles have also been bound to the PET grafts to reduce infection and are currently used in cases where an infected graft has to be substitute [15, 46, 47]. Amination, may also lead to improved patency without any loss of mechanical properties [48, 49]. However, the chemically inert nature of PET impedes significant bonding of functional groups and so

surface modification, such as plasma treatments, have been explored in order to augment the number of *e.g.* heparin-PET bonds.

Expanded polytetrafluoroethylene

Polytetrafluoroethylene (PTFE) was discovered in 1938, patented in 1941 and its commercial name, Teflon, trademarked in 1945 by the DuPont Co. Roy Plunkett. Expanded polytetrafluoroethylene (ePTFE) is a processed version of PTFE. PTFE is heated and rapidly stretched, the end result is that a microporous structure with 70% air is obtained. The process was discovered in 1969 and patented, under the name Gore-Tex, in 1976. PTFE and ePTFE have found numerous applications such as high-performance fabrics, medical implants, filter media, wire and cable insulation, gaskets, lubricants and sealants.

The PTFE molecule is chemically inert and biostable, due to the nature of the carbon-fluorine bond, and has been found to be less prone to biological deterioration than PET [50]. It is also very hydrophobic, due to mitigated London dispersion forces associated with the high electronegativity of fluorine. The electronegativity of the graft surface minimizes its reaction with blood components [51]. Mechanically ePTFE is stiffer than both the native arterial walls and PET. This can be a cause of graft failure due to pseudo-intimal hyperplasia. The Young's modulus for these grafts is around 3-6MPa [52, 53]. Comparatively in native arteries and veins (in a canine model) the Young's modulus is around 600 (circumferentially) and 900kPa (longitudinally), while PET registers 12MPa circumferentially and 0.7 MPa longitudinally.

The ePTFE graft for vascular applications, produced by extrusion, is a non-textile porous tube composed of irregular-shaped solid membranes ("nodes"). Between these solid nodes are fibrous regions and so the overall porosity of the graft is defined by its inter-nodal distance (IND) (available options vary between 30-90µm). The first ePTFE grafts were first introduced experimentally in 1972 and clinically in 1975 in a portal vein replacement [54, 55]. PET and ePTFE are the most widely used synthetic vascular replacements with little difference in performance between them [56].

Despite the aforementioned mechanical compliance issues, ePTFE grafts are commonly used for peripheral vessel bypass, particularly for femoral artery bypass. However, over 30 years since their initial appearance, research has achieved little improvement in regards to patency rates of ePTFE grafts [57]. Over a 5-year time period approximately 50% of implanted grafts have been shown to be blocked [58] and over a 10 year time period a maximum of 28% primary patency (in above-knee femoro-popliteal bypass grafts) [59]. The problem with patency is exacerbated in small caliber grafts. The main cause of graft failure is strongly associated with thrombosis, due to the lack of endothelial cell coverage which leads to protein adhesion that ultimately promotes thrombosis [60-62].

Animal studies have demonstrated rapid endothelization after relatively short periods of time however, this has not transitioned into humans. After 10 years of implantation in human patients, the same grafts that provided a complete endothelization in animals, are almost completely deprived of endothelium [63]. Clinically, when endothelization does occur it is generally limited to 1-2cm from the anastomosis site [64]. This is partially due to low porosity of the standard ePTFE grafts (IND of 30µm). The low porosity does not allow for adequate transanastomic or trans-mural endothelization [33]. Studies have shown that a higher IND (60 or 90µm) promoted a more rapid endothelization in animal models [65, 66]. However, none of these studies have been demonstrated and proven clinically.

In order to resolve the patency issues, a two-stage endothelial cell seeding protocol has shown to greatly enhance clinical patency rates to 90%, up to 52 weeks after implantation, on 3mm diameter coronary grafts [67]. Additionally, surface modification by carbon coating/impregnation [68], heparin coating (with the commercial name Propaten) [69, 70] and growth factor coating, with fibrin glue [71], have been attempted, though the latter seems to have been abandoned in recent years. Both carbon-coating and impregnation have been tested clinically and demonstrated no significant improvement in patency after 36 months [72, 73]. Heparin coating has been tested as a means to improve non-thrombogenicity and has demonstrated that, a luminal coating with immobilized heparin, improves primary patency and reduces intimal hyperplasia development over standard ePTFE grafts up to one year after implantation [74, 75].

Polyurethane

Polyurethanes (PUs) belong to a class of compounds called reaction polymers. They arise from the reaction of an isocyanate with a polyol, via carbamate links. PUs are thermosetting polymers that form a foam that does not melt when heated. They can also be manufactured into a harder thermoplastic form that is used in medical applications.

The thermoplastic PU used in medical settings present a high tensile strength, elasticity and ease of manipulation [76]. These mechanical and physical properties are extremely important in providing good mechanical compliance that ultimately prevents problems such as intimal hyperplasia. Along with its physical/mechanical properties, PU also presents good hemocompatibility, biocompatibility and microbial resistance [77, 78]. Hemocompatibility of PU is, at least, on par with ePTFE [79]. Yet another aspect that has encouraged further study of PU is porosity. Fibrilar PU grafts can be produced by weaving, knitting, electrospinning, or winding [76, 78] while foam PU grafts can be cast and porosity controlled by gas expansion and laser perforation [76]. Results have shown good *in vivo* biocompatibility and accelerated endothelization in small caliber grafts (4mm) associated with the improved porosity. Incorporation of carbon nanotubes have also been explored in order to improve endothelization, *in vitro*, showing promising results [80]. Rapid endothelization (12 weeks after implantation) has been shown critical in preventing hyperplasia and improving patency [81]. Another approach, recently studied, involves a PU graft capable of controlled release of rapamycin, which inhibits the migration and proliferation of smooth muscle cells, thus avoiding intimal hyperplasia [82]. However, pore interconnectivity, a mandatory requirement in order to provide better tissue ingrowth, remains an issue with no clear solution. Blends of PU with collagen/elastin and also polycaprolactone have shown improvements in both mechanical compliance and cell invasion [83, 84].

First-generation PU grafts suffered hydrolytic biodegradation which ultimately led to the abortion of clinical trials [85]. Second generation PU have shown a pressing disadvantage, the material's tendency to oxidize and degrade *in vivo*, creating problems after implantation, which could be overcome by chemically coating the surface with an antioxidant aids in reducing oxidation [86]. Given the good mechanical compliance (a step up as compared to ePTFE), hemocompatibility and potential for controlled porosity

- and despite *in vivo* degradation - several PU grafts are or have been studied. Mitrathane, Pulse-Tec, Vectra and Vascugraft are all brand names for PU grafts. Of these only Vectra is FDA approved however, the only application is for vascular access during hemodialysis which is a short-term application [87]. Continued study is necessary in order to produce small caliber PU graft for clinical applications.

Polyvinyl Alcohol

Polyvinyl Alcohol (PVA) is a nontoxic water-soluble synthetic polymer that forms a hydrogel once polymerized. It has excellent film-forming, emulsifying and adhesive properties. PVA is not prepared by polymerization of the vinyl alcohol monomer but rather partial or complete hydrolysis of poly(vinyl acetate). The removal of the acetate group can be controlled and alters the physical characteristics of the resulting PVA. This polymer presents high tensile strength and its flexibility is dependent on humidity. The water acts as a plasticizer, reducing tensile strength, but increasing elongation and tear strength.

PVA-based materials can be prepared by casting and then cross-linked by irradiation, physical (by thermal cycling) or chemical treatment [88, 89]. The resulting hydrogels can be fine-tuned to present varying mechanical and physical properties, depending on number of hydrogen bonds. The hydrogel is biocompatible and non-irritating to soft tissues and, therefore, it has been of great interest in pharmaceutical and biomedical applications [90-92]. The FDA approved the use of PVA microspheres as an embolization agent and further applications have been found as contact lenses, wound dressings, coating agent for pharmaceuticals and catheters [93, 94].

As a potential vascular graft, PVA has been studied both on its own [95] and composited with other materials [96-98]. Several combinations of PVA with other synthetic and natural polymers, such as gelatin, chitosan, starch and bacterial cellulose, have been proposed and studied. In general, these studies have all presented positive results in regards to hemocompatibility, biocompatibility and mechanical compliance. The intent behind the formulation of these composites is generally to enhance endothelial cell adhesion and proliferation. Gelatin and chitosan are probably the most well studied of

these combinations and have demonstrated good hemocompatibility and endothelization [99-102]. The PVA/bacterial cellulose composite was conceived as a means to enhance the mechanical properties of the PVA hydrogel, while still maintaining elasticity and malleability [96-98]. One of the rare studies demonstrating the *in vivo* performance of PVA based tubular structures was produced by Chaouat and colleagues [95]. In this study, a PVA sheet was either stitched or glued into a tubular shape and showed good patency after 1 week in a rat model. Extensive *in vivo* studies of vascular grafts of this kind are still lacking and so further work is needed to demonstrate its potential.

Bacterial Cellulose

Cellulose is the most abundant organic compound on Earth, a linear polysaccharide with β (1→4)–linked D-glucose monomers. Chemically, bacterial and plant cellulose are identical; however, bacterial cellulose (BC) is obtained pure (free of lignin, pectin or hemicellulose). It is produced, mainly by the *Gluconacetobacter* genus, as a fibrous network hydrogel at air-medium interfaces [103, 104]. The bacteria that produce cellulose are obligatory aerobes and produce the hydrogel as a pellicle [104], which can be exploited to grow into three-dimensional structures given that a three-dimensional oxygen permeable support is provided [105-107].

The BC hydrogel has several beneficial properties for use in the biomedical field, namely: high purity, high water-holding capacity, morphology, tensile strength, malleability, hemocompatibility and biocompatibility [103, 108, 109]. These characteristics have led to BC being long studied for biomedical applications such as wound dressings [110-112], artificial skin [113], tissue engineering scaffold [23, 104, 109, 114], synthetic dura mater [115] and as a vascular graft [107, 108, 116-118].

Several studies addressed the use of BC as a vascular graft and have shown its potential. Dieter Klemm and his group have looked at the *in vivo* behavior of small diameter BC tubes. These studies, carried out over 4weeks, and later over 3 months, in a rat model, showed that a small diameter BC tube can remain patent *in vivo* [108, 118]. These studies also showed that in the course of the 4 weeks the BC grafts were completely covered with connective tissue and, after 3 months, the formation of a neointima. Another study later

demonstrated that, under the registered name BASYC, BC tubes remained patent, in mice, for up to a year. However, *in vitro* studies have shown that, while minimal, BC does slightly trigger coagulation. Indeed, studies by both Andrade *et al* and Fink *et al* [23, 119, 120] showed that BC minimally activates coagulation. However, another study from the same group demonstrate that, comparing to ePTFE, BC has superior hemocompatibility, as assessed by the analysis of the activation of platelets and of the intrinsic pathway of hemostasis [24]. Attempting to improve the BC hemocompatibility, these authors used engineered cell-adhesion peptides (such as RGD), linked to a carbohydrate binding module, allowing the number and proliferation of endothelial cells on BC to be further improved [104].

Surface modification via plasma treatment and addition of aminoalkyl groups has been shown to alter the surface properties of BC. Cell adhesion and proliferation was improved with plasma treatment and addition of aminoalkyl groups demonstrated antimicrobial properties similar to chitosan, these approaches may ultimately prove useful for improving vascular grafts [121, 122].

A drawback to BC is that it is not biodegradable; furthermore, its porosity is insufficient for cell ingrowth to take place. This limits the potential in regards to producing a graft that could, eventually, be substituted integrally by newly formed tissue. Despite this, the potential of BC for *in vitro* and *in vivo* tissue regeneration continues to be explored and shows great promise [107, 109, 116, 117].

Degradable Polymers and Tissue Engineered vessels

A large portion of recent research into the development of novel vascular grafts has been focused on tissue-engineering approaches, by prior cell-seeding or by providing a scaffold that can be colonized *in vivo* by native cells, through migration and adhesion. A permanent vascular graft must offer definitive solutions especially in regards to long-term patency and structural integrity that, at the moment, have yet to be achieved. Therefore, a possible solution has focused on providing a biodegradable scaffold, which temporarily serves as a conduit for blood flow while allowing cells to grow and break-down the grafts, simultaneously producing native tissue and ultimately a new vessel
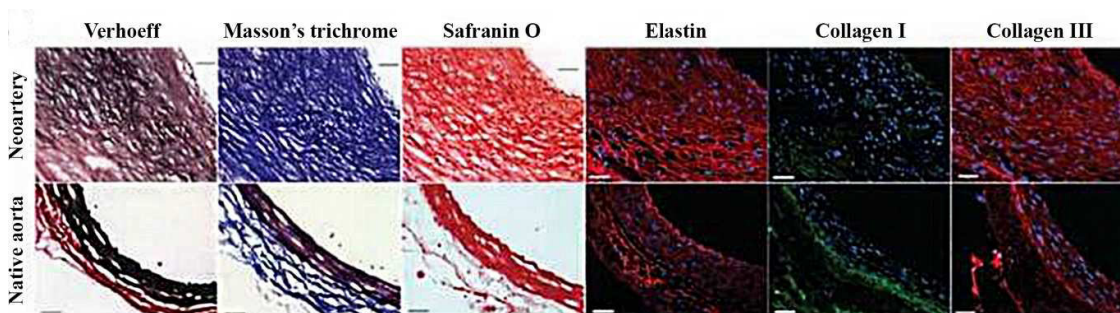
Figure 1-4 - ECM organization and quantification at 90 days. (a) Verhoeff's, Masson's trichrome, and safranin O staining show elastin (black), collagen (blue), and glycosaminoglycansin (red). Immunofluorescent staining shows distribution of elastin (red), collagen I (green), and collagen III (red). Top: day 90 explant, bottom: native aorta. (Adapted by permission from Macmillan Publishers Ltd: Nature Medicine (Wu et al. J Mater Sci Mater Med. 2010, 21(12)3207-3215), copyright 2012)

(Figure 1-4). The following degradable polymers are the current focus of research in attempts to provide a tissue-engineered approach to the vascular graft development field.

Polycaprolactone

Polycaprolactone (PCL) is a hydrophobic synthetic biodegradable polyester that has received a great deal of attention for use as an implantable biomaterial. This is due to its good mechanical properties, good biocompatibility and also, in large part, due to its slow biodegradability. PCL sheets have good mechanical properties but are somewhat limited in terms of compliance, though it is at least comparable to ePTFE and PET. It is however generally accepted that, as it is degraded and substituted by native tissue, compliance should improve over time due to elastogenesis [19].

Under physiological condition, such as in the human body, PCL suffer hydrolysis of its ester linkages. Generally, biodegradable graft approaches are viewed with some reserve. If *in vivo* degradation occurs too rapidly, as compared to overall cell growth, mechanical failure may occur ultimately leading to subsequent aneurysms and ruptures, which in turn can lead to internal bleeding and death. Degradation of PCL occurs at slow enough a pace, taking over 24 months to be completely absorbed, such that mechanical strength is guaranteed during cell invasion [19].

PCL grafts can be easily generated by electrospinning with varying pore sizes and prosthesis thicknesses. This has led to several studies focusing on determining the

feasibility of an electrospun PCL vascular graft over the last 6 years [19, 123-127]. Several studies, performed in rat, both showed rapid and stable endothelization which were responsible for good cell invasion and patency over the course of the studies, as compared to ePTFE [19, 127-129]. However, the poor mechanical compliance and loose cell attachment showed some development of intimal hyperplasia in all the studies [19]. The long term studies also revealed a propensity for calcification of the prosthesis over time (usually in the last months of the assays) although they did not affect the end-term patency of the graft.

In order to improve the mechanical compliance, issues that PCL has exhibited *in vivo*, several studies have focused on either pre-seeding the grafts with vascular endothelium cells [130] or creating nanocomposite grafts, with collagen, elastin and polylactide (Figure 1-5), all showing improved *in vivo* patency [131-133]. Similar approaches involve surface functionalization or the creation of a polymeric system (inclusion of bioactive molecules in the polymer fibers during the electrospinning process) which have also shown promising results, improving endothelial cell adhesion and hemocompatibility [134, 135]. Hybrid approaches of both incorporating other polymers and bioactive molecules have shown positive results [136, 137].

Collagen

Collagen is the most abundant group of proteins found in animals, the most common among which is Collagen I. Once irreversibly hydrolyzed, collagen originates gelatin. It is the main component of the body; making up 25 to 35% of the protein content. As elongated fibrils, collagen can be found in many fibrous tissues of the body, such as tendons, ligaments and skin, and is also abundant in cartilage, bone, gut, inter-vertebral discs and blood vessels [138].

As one of the major body components, it is biocompatible, biodegradable and has the advantage of being easily synthesized. This has led to it being abundantly researched for application in fields such as skin, cartilage, bone and vascular engineering and, additionally, as a drug delivery system [139-141]. The most common method of producing vascular collagen grafts is by electrospinning; however, the chemical nature of
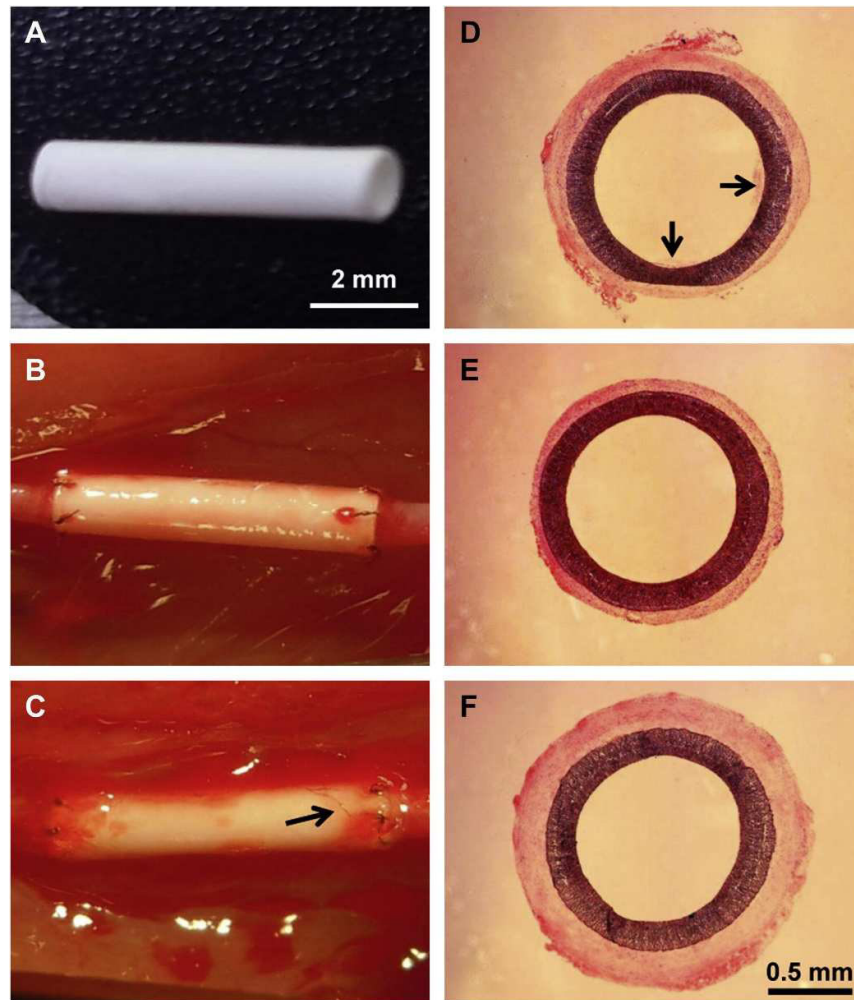
Figure 1-5 - Macroscale characterization of a tissue engineering approach using a polycaprolactone/poly(l-lactic acid) grafts. (A) A graft before implantation. (B) A graft right after implantation. (C) A heparin-SDF-1α-treated graft at 4 weeks after implantation. Arrow indicates microvessels in the wall of the graft. (D–F) H&E staining of an untreated graft (D), a heparin-treated graft (E) and a heparin-SDF-1α-treated graft (F) at 4 weeks after implantation. Arrows in D indicate thrombus formation. (Adapted from Biomaterials, 33(32), Yu et al, The effect of stromal cell-derived factor-1alpha/heparin coating of biodegradable vascular grafts on the recruitment of both endothelial and smooth muscle progenitor cells for accelerated regeneration, 8062-74, Copyright 2012, with permission from Elsevier)

collagen makes it sensible to deterioration during the process. The alternate option is to use a cross-linking agent to create the tubular prosthesis. Glutaraldehyde is used for this purpose, and while increasing strength it often carries the risk of increased toxicity and calcification. Also, without the aided mechanical support provided by seeded cells or other stabilizing polymers, collagen tubes are mechanically weak [142]. On top of all this, it is difficult to precisely control the mechanical behavior of the grafts due to a lack of means to do so. Other than the mechanical compliance issues, and most importantly,

collagen is also well documented as thrombogenic and a pro-coagulant [143-146]. Indeed, while a constituent of the extra cellular matrix, collagen is normally not exposed to circulating blood. Once exposed, it triggers the activation of the Hageman factor and promote clotting and healing of an injured site [146].

Studies have, therefore, mainly focused on combinations of collagen and other polymers [125, 142, 147, 148], bioactive molecules [145] or cell seeding [149]. Cells easily adhere to collagen matrices and so many studies have focused on cell seeding (as mentioned above) with the dual intention of enhancing mechanical compliance and especially hemocompatibility. These approaches have provided a scaffold with adequate characteristics for small diameter vessels. A cell seeded collagen substrate with immobilized heparin demonstrated enhanced hemocompatibility and endothelial cell adhesion [145]. Some studies have researched the possibility of pure collagen prosthesis. A 2 mm (outer diameter) collagen vessel, seeded with both endothelial and smooth muscle cells, remained patent, *in vivo*, after 12 weeks [149].

Ultimately, collagen I and its blends outperform many synthetic polymers by providing an extracellular matrix that is beneficial to cell differentiation and proliferation, with adequate mechanical behavior, given certain conditions are met [150]. The greatest application of collagen seems to be associated with enhancing other polymer grafts in a "supporting" role. Collagen shows therefore great potential; a construct consisting solely of collagen with no harmful crosslinking agent and adequate mechanical compliance and hemocompatibility would be a serious competitor in vascular tissue engineering.

Elastin

Elastin is a hydrophobic connective tissue protein polymer consisting of post-translational modified and cross-linked tropoelastin monomers. As its name suggests it is elastic and allows tissues to retain shape memory, dictating tissue mechanics at low strains and preventing tissue creep [151]. At higher mechanical strains collagen then assumes the role of providing mechanical resistance, due to the low maximum tensile strength of elastin.   Elastin is the dominant extracellular matrix protein in arterial walls; organized as concentric rings around the medial layer of arteries and making up roughly

50% of their dry weight [152]. Elastin exhibits low thrombogenicity and several vascular devices, coated with elastin-based polypeptides, demonstrated reduced platelet adhesion and activation, overall improving *in vivo* patency [153, 154]. Additionally, elastin is an autocrine regulator of smooth muscle cell (SMC) activity that has an essential role in preventing fibrocellular pathology and regulating proliferation [155].

The importance of the elastic properties and SMC regulatory activity has led to many studies aimed at inducing elastin biosynthesis in tissue-engineered vascular grafts. Several studies, using static collagen scaffolds seeded with SMC, did not show adequate elastin production [156-158]. However, further studies have shown that elastogenesis can be significantly improved by changing the scaffold substrate [151, 159], providing a mechanical stimuli [160-163] and also by the use of growth factors [151]. These cell seeding approaches have shown some success in promoting elastin deposition, the end result being the intended improvement in mechanical behavior, biocompatibility and hemocompatibility.

Besides cell seeding, several methods of producing vascular grafts that incorporate elastin have been studied [164, 165]. Collagen [166], polyurethane [167], polydioxanone[168], PCL [169], gelatin and recently polyethylene glycol [170], and also combinations of these polymers [125], have all been electrospun into hybrid tubular grafts, with elastin, to produce viable vascular grafts. These approaches all have similar objectives, to limit the degradation rate and provide high mechanical resistance while allowing for the beneficial mechanical and chemotactic performance of elastin. As such, they have all shown potential in regards to mechanical, bio- and hemocompatibility.

Attempts of incorporating elastin in tissue-engineered products and designing biocompatible synthetic elastic polymers are, however, still insufficient. A major drawback of a viable elastin graft is cost related. Tropoelastin is hydrophilic and easily susceptible to proteolysis, it is hard to isolate and readily reacts with other monomers. The main source of elastin - extraction from animal tissues - provides small amounts of the polymer at relatively high cost due to its insolubility in water, which prevents the use of conventional wet-chemistry techniques [171]. Further studies are needed to understand elastin biosynthesis in order to produce adequate elastin-incorporating and/or elastin-based grafts at cost-efficient methods.

Fibrin

Fibrin is the end-product of the coagulation cascade, produced by the conversion of fibrinogen to fibrin monomers, which polymerizes into an insoluble fibrin hydrogel network [172]. Fibrin seems an ideal scaffold for tissue regeneration since, *in vivo*, it acts as a "physiological scaffold" and plays a role in hemostasis, inflammation, wound healing and angiogenesis [173-175]. It has also been shown to promote cell migration into tissue-engineered constructs, the cells then gradually replace the fibrin scaffold with native extra cellular matrix [176, 177].

Fibrinogen can be isolated from the same patient that would receive the graft, thus lowering the risks of body reaction and infection [172, 178]. Conventionally fibrinogen is isolated from platelet poor plasma after freezing and thawing. However, this method of isolation has disadvantages: the quantity yield is relatively low (20-25%) and the production process is time consuming (2 days) [179]. The low yields would require large amounts of donor blood which is not a viable option. Alternative precipitation methods have been studied and, among them; ethanol precipitation, was found to be the most efficient with ~80% of fibrinogen precipitated [180].

Fibrin has been used as a coating in vascular prosthetics in order to enhance the hemo- and biocompatibility of synthetic grafts [181]. Fibrin based vascular grafts have been studied towards applications in coronary and peripheral artery bypass, arterio-venous access grafts or for congenital pulmonary artery reconstruction in children [179]. However, the fibrin gel lacks suitable mechanical properties. The grafts generally contain a supporting, bioresorbable, macroporous mesh. The meshes provide the required mechanical support while prior cell seeding remodels the fibrin matrix. Polylactide [182] and polyglactin [183] have been used as support structures. The tubular prosthesis is then generally seeded with different combinations of EC, SMC and myofibroblasts and incubated before implantation [182] and have been shown to remain patent for up to 6 months [184]. The major drawback with these approaches is the extremely long production time for the graft (circa 22 days) which prevents its application as an immediate alternative to current synthetic alternatives ePTFE and PET.

Silk

Silk is a natural protein polymer composed of two proteins: fibroin, the insoluble protein that is the main structural center of the silk fiber; and sericin, a water soluble protein that forms a gum coating the fibers and allowing them to stick to each other. Most of the silk produced and used worldwide is obtained from the pupating larvae of the mulberry silkworm *Bombyx mori*. The cocoons are then soaked in boiling water, to soften the sericin, and the fibers unwound to produce a continuous silk thread. Fibroin and sericin are separated in a degumming process. The resulting silk fibroin forms protein fibers with high tensile strength and high toughness, which have long found a home in medicine as a suture. From aqueous or organic solutions of silk fibroin it's also possible to form films, sponges, powder, gels and the regenerated fibers.

Silk fibroin has many of the requirements of a good biomaterial: it has good mechanical properties, biocompatibility, hemocompatibility, low immunogenicity and is biodegradable [185-187]. This has led to it being extensively studied for biomedical applications [186, 188-195]. For vascular grafts, in particular, the biocompatibility of silk is extremely important. Cell adhesion and growth on silk scaffolds has been shown to be very good [196-199] and, with the aid of recent biotechnology developments, improvements can be made further enhancing cell adhesion [200]. The inclusion of cell-adhesive sequences into the fibroin amino-acid sequence has been shown to enhance cell adhesion [195, 199, 201]. This cytocompatibility of silk fibroin has even led it to be studied as a coating for other polymeric materials in order to enhance cell adhesion [202].

As vascular grafts, silk fibroin can be woven [203], knitted [204], braided [205] or electrospun (using polyethylene oxide as an additive) [199] in order to produce tubular grafts with an open porous structure, this can easily be controlled through control of the flow rate [206]. Knitting and braiding require coating with an aqueous solution of silk fibroin, and usually another polymer such as poly(propylene glycol) dimethyl ether, in order to seal the graft and control permeability, mechanical behavior and pore size [204]. Some studies have already shown that vascular grafts of silk fibroin can be successful in small diameter applications [199, 204, 205]. A 1.5mm (inner diameter) by 10mm (length) graft was sutured, end-to-end, to a rat abdominal aorta and was shown to remain patent for 12 weeks in 85% of the cases [205]. The patency of the silk graft was largely due to

the almost complete cell coverage of the luminal surface, which was achieved after 9 weeks [205]. A similar study was also performed on the carotid artery of a canine model using 3mm diameter tubes and showing of up to one year in one of the implanted grafts [204].

Next Steps for Polymeric Grafts

The future of synthetic vascular graft development seems very promising. The field is every growing and the lack of a clear optimal polymer has led, and continues to lead, to many potential options. Either by further development and research into the already existing grafts (PET and ePTFE), the further development of new non-degradable grafts (PU, PVA and BC) or researching and developing temporary grafts that ultimately allow for a tissue engineered solution, either by prior cell-seeding or allowing for native cell migration, attachment and ingrowth, ultimately producing a new vessel out of native tissue (collagen, fibrin, elastin, silk and PCL).

In further years research seems like it will focus on the end development and fine tuning of either a nanocomposite or surface modified solution, with bioactive molecules, through *in vivo* testing. The nanocomposites approach seems to be the most common trend in the development of a tissue-engineered vessel. This method offers the possibility of combining the favorable properties of one polymer with the favorable properties of another, usually providing positive results with little or none of the drawbacks.

Those that have been mentioned here are the basis of the research that is currently ongoing and each has a beneficial aspect to contribute to the field. Alternatively, the surface modification of some of the above mentioned polymers may provide a viable alternative for a ready and off-the-shelf solution. The efforts of all the researchers in these fields will almost certainly provide a new graft that can out-perform the current standards and vastly improve the quality of life for millions.

References

[1] Go AS, Mozaffarian D, Roger VL, Benjamin EJ, Berry JD, Borden WB, et al. Heart Disease and Stroke Statistics—2013 Update A Report From the American Heart Association. Circulation. 2012.

[2] Defraigne J-O. Development of Atherosclerosis for the Vascular Surgeon. In: Liapis C, Balzer K, Benedetti-Valentini F, Fernandes e Fernandes J, editors. Vascular Surgery: Springer Berlin Heidelberg; 2007. p. 23-34.

[3] Rajagopalan S, Kurz S, Munzel T, Tarpey M, Freeman BA, Griendling KK, et al. Angiotensin II-mediated hypertension in the rat increases vascular superoxide production via membrane NADH/NADPH oxidase activation. Contribution to alterations of vasomotor tone. J Clin Invest. 1996;97:1916-23.

[4] Ohara Y, Peterson TE, Harrison DG. Hypercholesterolemia increases endothelial superoxide anion production. J Clin Invest. 1993;91:2546-51.

[5] Tesfamariam B, Cohen RA. Free radicals mediate endothelial cell dysfunction caused by elevated glucose. Am J Physiol. 1992;263:H321-6.

[6] Fuster V, Badimon JJ, Chesebro JH. Atherothrombosis: mechanisms and clinical therapeutic approaches. Vasc Med. 1998;3:231-9.

[7] Yusuf S, Hawken S, Ounpuu S, Dans T, Avezum A, Lanas F, et al. Effect of potentially modifiable risk factors associated with myocardial infarction in 52 countries (the INTERHEART study): case-control study. Lancet. 2004;364:937-52.

[8] Norgren L, Hiatt WR, Dormandy JA, Nehler MR, Harris KA, Fowkes FG. Inter-Society Consensus for the Management of Peripheral Arterial Disease (TASC II). Journal of vascular surgery. 2007;45 Suppl S:S5-67.

[9] Rutherford RB. Vascular Surgery, 2 Volume Set. Philadelphia, PA: W.B. Saunders Company; 2000.

[10] Panneton JM, Hollier LH, Hofer JM. Multicenter randomized prospective trial comparing a pre-cuffed polytetrafluoroethylene graft to a vein cuffed polytetrafluoroethylene graft for infragenicular arterial bypass. Ann Vasc Surg. 2004;18:199-206.

[11] Nguyen LL, Conte MS, Menard MT, Gravereaux EC, Chew DK, Donaldson MC, et al. Infrainguinal vein bypass graft revision: factors affecting long-term outcome. Journal of vascular surgery. 2004;40:916-23.

[12] White CJ, Gray WA. Endovascular Therapies for Peripheral Arterial Disease: An Evidence-Based Review. Circulation. 2007;116:2203-15.

[13] Mughal NA, Russell DA, Ponnambalam S, Homer-Vanniasinkam S. Gene therapy in the treatment of peripheral arterial disease. The British journal of surgery. 2012;99:6-15.

[14] Bradbury AW, Adam DJ, Bell J, Forbes JF, Fowkes FG, Gillespie I, et al. Bypass versus Angioplasty in Severe Ischaemia of the Leg (BASIL) trial: Analysis of amputation free and overall survival by treatment received. Journal of vascular surgery. 2010;51:18S-31S.

[15] Bisdas T, Wilhelmi M, Haverich A, Teebken OE. Cryopreserved arterial homografts vs silver-coated Dacron grafts for abdominal aortic infections with intraoperative evidence of microorganisms. Journal of vascular surgery. 2011;53:1274-81 e4.

[16] Moawad J, Gagne P. Adjuncts to improve patency of infrainguinal prosthetic bypass grafts. Vasc Endovascular Surg. 2003;37:381-6.

[17] Fabiani JN, Julia P, Chemla E, Birnbaum PL, Chardigny C, D'Attellis N, et al. Is the incidence of recurrent carotid artery stenosis influenced by the choice of the surgical technique? Carotid endarterectomy versus saphenous vein bypass. Journal of vascular surgery. 1994;20:821-5.

[18] Veldenz HC, Kinser R, Yates GN. Carotid graft replacement: a durable option. Journal of vascular surgery. 2005;42:220-6.

[19] de Valence S, Tille JC, Mugnai D, Mrowczynski W, Gurny R, Moller M, et al. Long term performance of polycaprolactone vascular grafts in a rat abdominal aorta replacement model. Biomaterials. 2012;33:38-47.

[20] Engler AJ, Sen S, Sweeney HL, Discher DE. Matrix elasticity directs stem cell lineage specification. Cell. 2006;126:677-89.

[21] Sperling C, Fischer M, Maitz MF, Werner C. Blood coagulation on biomaterials requires the combination of distinct activation processes. Biomaterials. 2009;30:4447-56.

[22] Fink H, Faxalv L, Molnar GF, Drotz K, Risberg B, Lindahl TL, et al. Real-time measurements of coagulation on bacterial cellulose and conventional vascular graft materials. Acta biomaterialia. 2010;6:1125-30.

[23] Andrade FK, Silva JP, Carvalho M, Castanheira EM, Soares R, Gama M. Studies on the hemocompatibility of bacterial cellulose. Journal of biomedical materials research Part A. 2011;98:554-66.

[24] Leitão AF, Gupta S, Silva JP, Reviakine I, Gama M. Hemocompatibility study of a bacterial cellulose/polyvinyl alcohol nanocomposite. Colloids and Surfaces B: Biointerfaces. 2013;111:493-502.

[25] Godo MN, Sefton MV. Characterization of transient platelet contacts on a polyvinyl alcohol hydrogel by video microscopy. Biomaterials. 1999;20:1117-26.

[26] Sheppard JI, McClung WG, Feuerstein IA. Adherent platelet morphology on adsorbed fibrinogen: Effects of protein incubation time and albumin addition. Journal of Biomedical Materials Research. 1994;28:1175-86.

[27] Northolt MG, den Decker P, Picken SJ, Baltussen JJM, Schlatmann R. The Tensile Strength of Polymer Fibres. Polymeric and Inorganic Fibers: Springer Berlin Heidelberg; 2005. p. 1-108.

[28] Rajendran S, Anand SC. DEVELOPMENTS IN MEDICAL TEXTILES. jotp. 2002;32:1-42.

[29] Ventura A, Terzaghi C, Legnani C, Borgo E, Albisetti W. Synthetic grafts for anterior cruciate ligament rupture: 19-year outcome study. Knee. 2010;17:108-13.

[30] Bodugoz-Senturk H, Macias CE, Kung JH, Muratoglu OK. Poly(vinyl alcohol)-acrylamide hydrogels as load-bearing cartilage substitute. Biomaterials. 2009;30:589-96.

[31] Buchensk J, Slomkowski S, Tazbir JW, Sobolewska E. Poly(ethylene terephthalate) yarn with antibacterial properties. Journal of biomaterials science Polymer edition. 2001;12:55-62.

[32] Zieren J, Neuss H, Paul M, Müller J. Introduction of polyethylene terephthalate mesh (KoSa hochfest<sup>®</sup>) for abdominal hernia repair: An animal experimental study. Bio-Medical Materials and Engineering. 2004;14:127-32.

[33] Menu P, Stoltz JF, Kerdjoudj H. Progress in vascular graft substitute. Clinical Hemorheology and Microcirculation. 2013;53:117-29.

[34] Prager MR, Hoblaj T, Nanobashvili J, Sporn E, Polterauer P, Wagner O, et al. Collagen-versus gelatine-coated Dacron versus stretch PTFE bifurcation grafts for aortoiliac occlusive disease: Long-term results of a prospective, randomized multicenter trial. Surgery. 2003;134:80-5.

[35] Nevelsteen A, Wouters L, Suy R. Long-term patency of the aortofemoral Dacron graft. A graft limb related study over a 25-years period. J Cardiovasc Surg (Torino). 1991;32:174-80.

[36] Hanson SR, Kotze HF, Savage B, Harker LA. Platelet interactions with Dacron vascular grafts. A model of acute thrombosis in baboons. Arteriosclerosis, Thrombosis, and Vascular Biology. 1985;5:595-603.

[37] Salacinski HJ, Goldner S, Giudiceandrea A, Hamilton G, Seifalian AM, Edwards A, et al. The mechanical behavior of vascular grafts: a review. Journal of biomaterials applications. 2001;15:241-78.

[38] Holmberg M, Hou X. Competitive protein adsorption of albumin and immunoglobulin G from human serum onto polymer surfaces. Langmuir. 2010;26:938-42.

[39] Hake U, Gabbert H, Iversen S, Jakob H, Schmiedt W, Oelert H. Evaluation of the healing of precoated vascular dacron prostheses. Langenbecks Archiv für Chirurgie. 1991;376:323-9.

[40] Van Damme H, Deprez M, Creemers E, Limet R. Intrinsic Structural Failure of Polyester (Dacron) Vascular Grafts. A General. Acta chir belg. 2005;105:249-55.

[41] Vogt PR, Brunner-LaRocca HP, Lachat M, Ruef C, Turina MI. Technical details with the use of cryopreserved arterial allografts for aortic infection: influence on early and midterm mortality. Journal of vascular surgery. 2002;35:80-6.

[42] Cziperle DJ, Joyce KA, Tattersall CW, Henderson SC, Cabusao EB, Garfield JD, et al. Albumin impregnated vascular grafts: albumin resorption and tissue reactions. J Cardiovasc Surg (Torino). 1992;33:407-14.

[43] Scott SM, Gaddy LR, Sahmel R, Hoffman H. A collagen coated vascular prosthesis. J Cardiovasc Surg (Torino). 1987;28:498-504.

[44] Koromila G, Michanetzis GP, Missirlis YF, Antimisiaris SG. Heparin incorporating liposomes as a delivery system of heparin from PET-covered metallic stents: effect on haemocompatibility. Biomaterials. 2006;27:2525-33.

[45] Lev EI, Assali AR, Teplisky I, Rechavia E, Hasdai D, Sela O, et al. Comparison of outcomes up to six months of Heparin-Coated with noncoated stents after percutaneous coronary intervention for acute myocardial infarction. Am J Cardiol. 2004;93:741-3.

[46] Kowalik Z, Kucharski A, Hobot J. Use of dacron vascular prosthesis impregnated with salts of silver, in treatment of extraanatomical axilla-femoral by-pass's infection. Infections in vascular surgery. Polim Med. 2002;32:80-4.

[47] Jeanmonod P, Laschke MW, Gola N, von Heesen M, Glanemann M, Dold S, et al. Silver acetate coating promotes early vascularization of Dacron vascular grafts without inducing host tissue inflammation. Journal of vascular surgery. 2013.

[48] Noel S, Liberelle B, Yogi A, Moreno MJ, Bureau MN, Robitaille L, et al. A non-damaging chemical amination protocol for poly (ethylene terephthalate)–application to the design of functionalized compliant vascular grafts. Journal of Materials Chemistry B. 2013;1:230-8.

[49] Li P, Cai X, Wang D, Chen S, Yuan J, Li L, et al. Hemocompatibility and anti-biofouling property improvement of poly(ethylene terephthalate) via self-polymerization of dopamine and covalent graft of zwitterionic cysteine. Colloids and Surfaces B: Biointerfaces. 2013;110:327-32.

[50] Guidoin R, Chakfe N, Maurel S, How T, Batt M, Marois M, et al. Expanded polytetrafluoroethylene arterial prostheses in humans: histopathological study of 298 surgically excised grafts. Biomaterials. 1993;14:678-93.

[51] Chlupac J, Filova E, Bacakova L. Blood vessel replacement: 50 years of development and tissue engineering paradigms in vascular surgery. Physiol Res. 2009;58 Suppl 2:S119-39.

[52] Grigioni M, Daniele C, D'avenio G, Barbaro V. Biomechanics and hemodynamics of grafting. Billerica, MA: WIT Press, 2003. 2003:41-82.

[53] Lee JM, Wilson GJ. Anisotropic tensile viscoelastic properties of vascular graft materials tested at low strain rates. Biomaterials. 1986;7:423-31.

[54] Soyer T, Lempinen M, Cooper P, Norton L, Eiseman B. A new venous prosthesis. Surgery. 1972;72:864-72.

[55] Norton L, Eiseman B. Replacement of portal vein during pancreatectomy for carcinoma. Surgery. 1975;77:280-4.

[56] Roll S, Muller-Nordhorn J, Keil T, Scholz H, Eidt D, Greiner W, et al. Dacron vs. PTFE as bypass materials in peripheral vascular surgery--systematic review and meta-analysis. BMC Surg. 2008;8:22.

[57] Greisler HP. New biologic and synthetic vascular prostheses: R.G. Landes Co.; 1991.

[58] Veith FJ, Gupta SK, Ascer E, White-Flores S, Samson RH, Scher LA, et al. Six-year prospective multicenter randomized comparison of autologous saphenous vein and expanded polytetrafluoroethylene grafts in infrainguinal arterial reconstructions. Journal of vascular surgery. 1986;3:104-14.

[59] van Det RJ, Vriens BH, van der Palen J, Geelkerken RH. Dacron or ePTFE for femoro-popliteal above-knee bypass grafting: short- and long-term results of a multicentre randomised trial. European journal of vascular and endovascular surgery : the official journal of the European Society for Vascular Surgery. 2009;37:457-63.

[60] Pevec WC, Darling RC, L'Italien GJ, Abbott WM. Femoropopliteal reconstruction with knitted, nonvelour Dacron versus expanded polytetrafluoroethylene. Journal of vascular surgery. 1992;16:60-5.

[61] Jensen LP, Lepantalo M, Fossdal JE, Roder OC, Jensen BS, Madsen MS, et al. Dacron or PTFE for above-knee femoropopliteal bypass. a multicenter randomised study. European

journal of vascular and endovascular surgery : the official journal of the European Society for Vascular Surgery. 2007;34:44-9.

[62] Lu S, Sun X, Zhang P, Yang L, Gong F, Wang C. Local hemodynamic disturbance accelerates early thrombosis of small-caliber expanded polytetrafluoroethylene grafts. Perfusion. 2013.

[63] Zilla P, Brink J, Human P, Bezuidenhout D. Prosthetic heart valves: catering for the few. Biomaterials. 2008;29:385-406.

[64] Berger K, Sauvage LR, Rao AM, Wood SJ. Healing of arterial prostheses in man: its incompleteness. Ann Surg. 1972;175:118-27.

[65] Clowes AW, Kirkman TR, Reidy MA. Mechanisms of arterial graft healing. Rapid transmural capillary ingrowth provides a source of intimal endothelium and smooth muscle in porous PTFE prostheses. Am J Pathol. 1986;123:220-30.

[66] Cameron BL, Tsuchida H, Connall TP, Nagae T, Furukawa K, Wilson SE. High porosity PTFE improves endothelialization of arterial grafts without increasing early thrombogenicity. J Cardiovasc Surg (Torino). 1993;34:281-5.

[67] Laube HR, Duwe J, Rutsch W, Konertz W. Clinical experience with autologous endothelial cell-seeded polytetrafluoroethylene coronary artery bypass grafts. J Thorac Cardiovasc Surg. 2000;120:134-41.

[68] Venkatraman S, Boey F, Lao LL. Implanted cardiovascular polymers: Natural, synthetic and bio-inspired. Progress in Polymer Science. 2008;33:853-74.

[69] Heyligers JM, Lisman T, Verhagen HJ, Weeterings C, de Groot PG, Moll FL. A heparin-bonded vascular graft generates no systemic effect on markers of hemostasis activation or detectable heparin-induced thrombocytopenia-associated antibodies in humans. Journal of vascular surgery. 2008;47:324-9; discussion 9.

[70] Hoshi RA, Van Lith R, Jen MC, Allen JB, Lapidos KA, Ameer G. The blood and vascular cell compatibility of heparin-modified ePTFE vascular grafts. Biomaterials. 2013;34:30-41.

[71] Zarge JI, Gosselin C, Huang P, Vorp DA, Severyn DA, Greisler HP. Platelet deposition on ePTFE grafts coated with fibrin glue with or without FGF-1 and heparin. J Surg Res. 1997;67:4-8.

[72] Kapfer X, Meichelboeck W, Groegler FM. Comparison of carbon-impregnated and standard ePTFE prostheses in extra-anatomical anterior tibial artery bypass: a prospective randomized multicenter study. European journal of vascular and endovascular surgery : the official journal of the European Society for Vascular Surgery. 2006;32:155-68.

[73] Akers DL, Du YH, Kempczinski RF. The effect of carbon coating and porosity on early patency of expanded polytetrafluoroethylene grafts: an experimental study. Journal of vascular surgery. 1993;18:10-5.

[74] Pedersen G, Laxdal E, Ellensen V, Jonung T, Mattsson E. Improved patency and reduced intimal hyperplasia in PTFE grafts with luminal immobilized heparin compared with standard PTFE grafts at six months in a sheep model. J Cardiovasc Surg (Torino). 2010;51:443-8.

[75] Saxon RR, Chervu A, Jones PA, Bajwa TK, Gable DR, Soukas PA, et al. Heparin-bonded, Expanded Polytetrafluoroethylene-lined Stent Graft in the Treatment of Femoropopliteal Artery Disease: 1-Year Results of the VIPER (Viabahn Endoprosthesis with Heparin Bioactive Surface in the Treatment of Superficial Femoral Artery Obstructive Disease) Trial. Journal of Vascular and Interventional Radiology. 2013;24:165-73.

[76] Zilla P, Bezuidenhout D, Human P. Prosthetic vascular grafts: wrong models, wrong questions and no healing. Biomaterials. 2007;28:5009-27.

[77] Peckham SM, Turitto VT, Glantz J, Puryear H, Slack SM. Hemocompatibility studies of surface-treated polyurethane-based chronic indwelling catheters. Journal of Biomaterials Science, Polymer Edition. 1997;8:847-58.

[78] He W, Hu Z, Xu A, Liu R, Yin H, Wang J, et al. The Preparation and Performance of a New Polyurethane Vascular Prosthesis. Cell Biochem Biophys. 2013:1-12.

[79] Maya ID, Weatherspoon J, Young CJ, Barker J, Allon M. Increased risk of infection associated with polyurethane dialysis grafts. Semin Dial. 2007;20:616-20.

[80] Meng J, Cheng X, Kong H, Yang M, Xu H. Preparation and biocompatibility evaluation of polyurethane filled with multiwalled carbon nanotubes. Journal of nanoscience and nanotechnology. 2013;13:1467-71.

[81] Hu Z-j, Li Z-l, Hu L-y, He W, Liu R-m, Qin Y-s, et al. The in vivo performance of small-caliber nanofibrous polyurethane vascular grafts. BMC Cardiovascular Disorders. 2012;12:1-11.

[82] Han J, Farah S, Domb A, Lelkes P. Electrospun Rapamycin-Eluting Polyurethane Fibers for Vascular Grafts. Pharm Res. 2013;30:1735-48.

[83] Wong CS, Liu X, Xu Z, Lin T, Wang X. Elastin and collagen enhances electrospun aligned polyurethane as scaffolds for vascular graft. J Mater Sci: Mater Med. 2013:1-10.

[84] Nguyen T-H, Padalhin AR, Seo HS, Lee B-T. A hybrid electrospun PU/PCL scaffold satisfied the requirements of blood vessel prosthesis in terms of mechanical properties, pore size, and biocompatibility. Journal of Biomaterials Science, Polymer Edition. 2013:1-15.

[85] Zhang Z, Marois Y, Guidoin RG, Bull P, Marois M, How T, et al. Vascugraft polyurethane arterial prosthesis as femoro-popliteal and femoro-peroneal bypasses in humans: pathological, structural and chemical analyses of four excised grafts. Biomaterials. 1997;18:113-24.

[86] Stachelek SJ, Alferiev I, Fulmer J, Ischiropoulos H, Levy RJ. Biological stability of polyurethane modified with covalent attachment of di-tert-butyl-phenol. Journal of biomedical materials research Part A. 2007;82:1004-11.

[87] Glickman MH, Stokes GK, Ross JR, Schuman ED, Sternbergh Iii WC, Lindberg JS, et al. Multicenter evaluation of a polyurethaneurea vascular access graft as compared with the expanded polytetrafluoroethylene vascular access graft in hemodialysis applications. Journal of vascular surgery. 2001;34:465-73.

[88] Chu KC, Rutt BK. Polyvinyl alcohol cryogel: An ideal phantom material for MR studies of arterial flow and elasticity. Magnetic Resonance in Medicine. 1997;37:314-9.

[89] Bourke SL, Al-Khalili M, Briggs T, Michniak BB, Kohn J, Poole-Warren LA. A photo-crosslinked poly(vinyl alcohol) hydrogel growth factor release vehicle for wound healing applications. AAPS PharmSci. 2003;5:E33.

[90] Takeuchi H, Kojima H, Yamamoto H, Kawashima Y. Polymer coating of liposomes with a modified polyvinyl alcohol and their systemic circulation and RES uptake in rats. J Control Release. 2000;68:195-205.

[91] Laurent A, Wassef M, Saint Maurice JP, Namur J, Pelage JP, Seron A, et al. Arterial distribution of calibrated tris-acryl gelatin and polyvinyl alcohol microspheres in a sheep kidney model. Invest Radiol. 2006;41:8-14.

[92] Pal K, Banthia AK, Majumdar DK. Preparation and characterization of polyvinyl alcohol-gelatin hydrogel membranes for biomedical applications. AAPS PharmSciTech. 2007;8:21.

[93] Yang S-H, Lee Y-SJ, Lin F-H, Yang J-M, Chen K-s. Chitosan/poly(vinyl alcohol) blending hydrogel coating improves the surface characteristics of segmented polyurethane urethral catheters. Journal of Biomedical Materials Research Part B: Applied Biomaterials. 2007;83B:304-13.

[94] Walker J, Young G, Hunt C, Henderson T. Multi-centre evaluation of two daily disposable contact lenses. Cont Lens Anterior Eye. 2007;30:125-33.

[95] Chaouat M, Le Visage C, Baille WE, Escoubet B, Chaubet F, Mateescu MA, et al. A Novel Cross-linked Poly(vinyl alcohol) (PVA) for Vascular Grafts. Advanced Functional Materials. 2008;18:2855-61.

[96] Millon LE, Wan WK. The polyvinyl alcohol-bacterial cellulose system as a new nanocomposite for biomedical applications. J Biomed Mater Res B Appl Biomater. 2006;79:245-53.

[97] Millon LE, Guhados G, Wan W. Anisotropic polyvinyl alcohol-Bacterial cellulose nanocomposite for biomedical applications. J Biomed Mater Res B Appl Biomater. 2008;86:444-52.

[98] Mohammadi H. Nanocomposite biomaterial mimicking aortic heart valve leaflet mechanical behaviour. Proc Inst Mech Eng H. 2011;225:718-22.

[99] Chuang WY, Young TH, Yao CH, Chiu WY. Properties of the poly(vinyl alcohol)/chitosan blend and its effect on the culture of fibroblast in vitro. Biomaterials. 1999;20:1479-87.

[100] Koyano T, Minoura N, Nagura M, Kobayashi K-i. Attachment and growth of cultured fibroblast cells on PVA/chitosan-blended hydrogels. Journal of Biomedical Materials Research. 1998;39:486-90.

[101] Mathews DT, Birney YA, Cahill PA, McGuinness GB. Vascular cell viability on polyvinyl alcohol hydrogels modified with water-soluble and -insoluble chitosan. Journal of Biomedical Materials Research Part B: Applied Biomaterials. 2008;84B:531-40.

[102] Tudorachi N, Cascaval CN, Rusu M, Pruteanu M. Testing of polyvinyl alcohol and starch mixtures as biodegradable polymeric materials. Polymer Testing. 2000;19:785-99.

[103] Leitão A, Silva J, Dourado F, Gama M. Production and Characterization of a New Bacterial Cellulose/Poly(Vinyl Alcohol) Nanocomposite. Materials. 2013;6:1956-66.

[104] Andrade F, Pertile R, Douradoa F. Bacterial cellulose: properties, production and applications. Cellulose: structure and properties, derivatives and industrial uses Nova Science Publishers, Inc. 2010:427-58.

[105] Jia S, Tang W, Yang H, Jia Y, Zhu H. Preparation and Characterization of Bacterial Cellulose Tube. Bioinformatics and Biomedical Engineering, 2009 ICBBE 2009 3rd International Conference on: IEEE; 2009. p. 1-4.

[106] Kaźmierczak D, Kazimierczak J. Biosynthesis of modified bacterial cellulose in a tubular form. Fibres & Textiles in Eastern Europe. 2010;18:82.

[107] Bäckdahl H, Risberg B, Gatenholm P. Observations on bacterial cellulose tube formation for application as vascular graft. Materials Science and Engineering: C. 2011;31:14-21.

[108] Klemm D, Schumann D, Udhardt U, Marsch S. Bacterial synthesized cellulose — artificial blood vessels for microsurgery. Progress in Polymer Science. 2001;26:1561-603.

[109] Svensson A, Nicklasson E, Harrah T, Panilaitis B, Kaplan DL, Brittberg M, et al. Bacterial cellulose as a potential scaffold for tissue engineering of cartilage. Biomaterials. 2005;26:419-31.

[110] Alvarez O, Patel M, Booker J, Markowitz L. Original Research Effectiveness of a Biocellulose Wound Dressing for the Treatment of Chronic Venous Leg Ulcers: Results of a Single Center Randomized Study Involving 24 Patients. Wounds. 2004;16:224-33.

[111] Czaja W, Krystynowicz A, Bielecki S, Brown Jr RM. Microbial cellulose—the natural power to heal wounds. Biomaterials. 2006;27:145-51.

[112] Solway DR, Consalter M, Levinson DJ. Microbial cellulose wound dressing in the treatment of skin tears in the frail elderly. Wounds. 2010;22:17-9.

[113] Fontana JD, de Souza AM, Fontana CK, Torriani IL, Moreschi JC, Gallotti BJ, et al. Acetobacter cellulose pellicle as a temporary skin substitute. Appl Biochem Biotechnol. 1990;24-25:253-64.

[114] Backdahl H, Helenius G, Bodin A, Nannmark U, Johansson BR, Risberg B, et al. Mechanical properties of bacterial cellulose and interactions with smooth muscle cells. Biomaterials. 2006;27:2141-9.

[115] Mello LR, Feltrin LT, Fontes Neto PT, Ferraz FAP. Duraplasty with biosynthetic cellulose: an experimental study. Journal of Neurosurgery. 1997;86:143-50.

[116] Wippermann J, Schumann D, Klemm D, Kosmehl H, Salehi-Gelani S, Wahlers T. Preliminary results of small arterial substitute performed with a new cylindrical biomaterial composed of bacterial cellulose. European journal of vascular and endovascular surgery : the official journal of the European Society for Vascular Surgery. 2009;37:592-6.

[117] Andrade FK, Costa R, Domingues L, Soares R, Gama M. Improving bacterial cellulose for blood vessel replacement: Functionalization with a chimeric protein containing a cellulose-binding module and an adhesion peptide. Acta Biomater. 2010;6:4034-41.

[118] Schumann DA, Wippermann J, Klemm DO, Kramer F, Koth D, Kosmehl H, et al. Artificial vascular implants from bacterial cellulose: preliminary results of small arterial substitutes. Cellulose. 2009;16:877-85.

[119] Fink H, Faxalv L, Molnar GF, Drotz K, Risberg B, Lindahl TL, et al. Real-time measurements of coagulation on bacterial cellulose and conventional vascular graft materials. Acta Biomater. 2010;6:1125-30.

[120] Fink H, Hong J, Drotz K, Risberg B, Sanchez J, Sellborn A. An in vitro study of blood compatibility of vascular grafts made of bacterial cellulose in comparison with conventionally-used graft materials. Journal of biomedical materials research Part A. 2011.

[121] Flynn CN, Byrne CP, Meenan BJ. Surface modification of cellulose via atmospheric pressure plasma processing in air and ammonia–nitrogen gas. Surface and Coatings Technology. 2013.

[122] Fernandes SCM, Sadocco P, Alonso-Varona A, Palomares T, Eceiza A, Silvestre AJD, et al. Bioinspired Antimicrobial and Biocompatible Bacterial Cellulose Membranes Obtained by Surface Functionalization with Aminoalkyl Groups. ACS Applied Materials & Interfaces. 2013;5:3290-7.

[123] Lee SJ, Liu J, Oh SH, Soker S, Atala A, Yoo JJ. Development of a composite vascular scaffolding system that withstands physiological vascular conditions. Biomaterials. 2008;29:2891-8.

[124] Ju YM, Choi JS, Atala A, Yoo JJ, Lee SJ. Bilayered scaffold for engineering cellularized blood vessels. Biomaterials. 2010;31:4313-21.

[125] McClure MJ, Sell SA, Simpson DG, Walpoth BH, Bowlin GL. A three-layered electrospun matrix to mimic native arterial architecture using polycaprolactone, elastin, and collagen: a preliminary study. Acta Biomater. 2010;6:2422-33.

[126] Ye L, Wu X, Mu Q, Chen B, Duan Y, Geng X, et al. Heparin-Conjugated PCL Scaffolds Fabricated by Electrospinning and Loaded with Fibroblast Growth Factor 2. Journal of biomaterials science Polymer edition. 2010.

[127] Pektok E, Nottelet B, Tille JC, Gurny R, Kalangos A, Moeller M, et al. Degradation and healing characteristics of small-diameter poly(epsilon-caprolactone) vascular grafts in the rat systemic arterial circulation. Circulation. 2008;118:2563-70.

[128] Mugnai D, Tille JC, Mrowczynski W, de Valence S, Montet X, Moller M, et al. Experimental noninferiority trial of synthetic small-caliber biodegradable versus stable vascular grafts. J Thorac Cardiovasc Surg. 2012.

[129] Walpoth B, Mugnai D, de Valence S, Mrowczynski W, Tille J, Montet X, et al. Non-inferiority of synthetic small-calibre biodegradable vs. stable ePTFE vascular prosthesis after long-term implantation in the rat aorta. The Thoracic and Cardiovascular Surgeon. 2013;61:OP56.

[130] Singh S, Wu BM, Dunn JC. Accelerating vascularization in polycaprolactone scaffolds by endothelial progenitor cells. Tissue Eng Part A. 2011;17:1819-30.

[131] Tillman BW, Yazdani SK, Lee SJ, Geary RL, Atala A, Yoo JJ. The in vivo stability of electrospun polycaprolactone-collagen scaffolds in vascular reconstruction. Biomaterials. 2009;30:583-8.

[132] Mun CH, Kim S-H, Jung Y, Kim S-H, Kim A-k, Kim D-I, et al. Elastic, double-layered poly(l-lactide-co-ε-caprolactone) scaffold for long-term vascular reconstruction. Journal of Bioactive and Compatible Polymers. 2013.

[133] Diban N, Haimi S, Bolhuis-Versteeg L, Teixeira S, Miettinen S, Poot A, et al. Hollow fibers of poly(lactide-co-glycolide) and poly(ε-caprolactone) blends for vascular tissue engineering applications. Acta Biomater. 2013;9:6450-8.

[134] Yuan S, Xiong G, Roguin A, Teoh SH, Choong C. Amelioration of Blood Compatibility and Endothelialization of Polycaprolactone Substrates by Surface-Initiated Atom Transfer Radical Polymerization. 2013.

[135] Del Gaudio C, Ercolani E, Galloni P, Santilli F, Baiguera S, Polizzi L, et al. Aspirin-loaded electrospun poly(ε-caprolactone) tubular scaffolds: potential small-diameter vascular grafts for thrombosis prevention. J Mater Sci: Mater Med. 2013;24:523-32.

[136] Wang S, Mo XM, Jiang BJ, Gao CJ, Wang HS, Zhuang YG, et al. Fabrication of small-diameter vascular scaffolds by heparin-bonded P(LLA-CL) composite nanofibers to improve graft patency. Int J Nanomedicine. 2013;8:2131-9.

[137] Lu G, Cui SJ, Geng X, Ye L, Chen B, Feng ZG, et al. Design and preparation of polyurethane-collagen/heparin-conjugated polycaprolactone double-layer bionic small-diameter vascular graft and its preliminary animal tests. Chin Med J (Engl). 2013;126:1310-6.

[138] Lodish H, Berk A, Zipursky SL, Matsudaira P, Baltimore D, Darnell J. Collagen: The Fibrous Proteins of the Matrix. 2000.

[139] Olsen D, Yang C, Bodo M, Chang R, Leigh S, Baez J, et al. Recombinant collagen and gelatin for drug delivery. Adv Drug Deliv Rev. 2003;55:1547-67.

[140] Smith M, McFetridge P, Bodamyali T, Chaudhuri JB, Howell JA, Stevens CR, et al. Porcine-Derived Collagen as a Scaffold for Tissue Engineering. Food and Bioproducts Processing. 2000;78:19-24.

[141] Kose GT, Korkusuz F, Ozkul A, Soysal Y, Ozdemir T, Yildiz C, et al. Tissue engineered cartilage on collagen and PHBV matrices. Biomaterials. 2005;26:5187-97.

[142] Sell SA, McClure MJ, Garg K, Wolfe PS, Bowlin GL. Electrospinning of collagen/biopolymers for regenerative medicine and cardiovascular tissue engineering. Adv Drug Deliv Rev. 2009;61:1007-19.

[143] Amarnath LP, Srinivas A, Ramamurthi A. In vitro hemocompatibility testing of UV-modified hyaluronan hydrogels. Biomaterials. 2006;27:1416-24.

[144] Miyata T, Taira T, Noishiki Y. Collagen engineering for biomaterial use. Clin Mater. 1992;9:139-48.

[145] Wissink MJ, Beernink R, Pieper JS, Poot AA, Engbers GH, Beugeling T, et al. Immobilization of heparin to EDC/NHS-crosslinked collagen. Characterization and in vitro evaluation. Biomaterials. 2001;22:151-63.

[146] Wilner GD, Nossel HL, LeRoy EC. Activation of Hageman factor by collagen. J Clin Invest. 1968;47:2608-15.

[147] McClure MJ, Simpson DG, Bowlin GL. Tri-layered vascular grafts composed of polycaprolactone, elastin, collagen, and silk: Optimization of graft properties. Journal of the Mechanical Behavior of Biomedical Materials. 2012;10:48-61.

[148] Kumar VA, Caves JM, Haller CA, Dai E, Li L, Grainger S, et al. Acellular Vascular Grafts Generated from Collagen and Elastin Analogues. Acta Biomater. 2013.

[149] Wu H, Fan J, Chu CC, Wu J. Electrospinning of small diameter 3-D nanofibrous tubular scaffolds with controllable nanofiber orientations for vascular grafts. J Mater Sci Mater Med. 2010;21:3207-15.

[150] Berglund JD, Mohseni MM, Nerem RM, Sambanis A. A biological hybrid model for collagen-based tissue engineered vascular constructs. Biomaterials. 2003;24:1241-54.

[151] Long JL, Tranquillo RT. Elastic fiber production in cardiovascular tissue-equivalents. Matrix Biology. 2003;22:339-50.

[152] Karnik SK, Brooke BS, Bayes-Genis A, Sorensen L, Wythe JD, Schwartz RS, et al. A critical role for elastin signaling in vascular morphogenesis and disease. Development. 2003;130:411-23.

[153] Jordan SW, Haller CA, Sallach RE, Apkarian RP, Hanson SR, Chaikof EL. The effect of a recombinant elastin-mimetic coating of an ePTFE prosthesis on acute thrombogenicity in a baboon arteriovenous shunt. Biomaterials. 2007;28:1191-7.

[154] Woodhouse KA, Klement P, Chen V, Gorbet MB, Keeley FW, Stahl R, et al. Investigation of recombinant human elastin polypeptides as non-thrombogenic coatings. Biomaterials. 2004;25:4543-53.

[155] Li DY, Brooke B, Davis EC, Mecham RP, Sorensen LK, Boak BB, et al. Elastin is an essential determinant of arterial morphogenesis. Nature. 1998;393:276-80.

[156] Weinberg CB, Bell E. A blood vessel model constructed from collagen and cultured vascular cells. Science. 1986;231:397-400.

[157] L'Heureux N, Germain L, Labbe R, Auger FA. In vitro construction of a human blood vessel from cultured vascular cells: a morphologic study. Journal of vascular surgery. 1993;17:499-509.

[158] Hirai J, Matsuda T. Venous reconstruction using hybrid vascular tissue composed of vascular cells and collagen: tissue regeneration process. Cell Transplant. 1996;5:93-105.

[159] Ramamurthi A, Vesely I. Evaluation of the matrix-synthesis potential of crosslinked hyaluronan gels for tissue engineering of aortic heart valves. Biomaterials. 2005;26:999-1010.

[160] Ziegler T, Alexander RW, Nerem RM. An endothelial cell-smooth muscle cell co-culture model for use in the investigation of flow effects on vascular biology. Ann Biomed Eng. 1995;23:216-25.

[161] Kolpakov V, Rekhter MD, Gordon D, Wang WH, Kulik TJ. Effect of mechanical forces on growth and matrix protein synthesis in the in vitro pulmonary artery. Analysis of the role of individual cell types. Circ Res. 1995;77:823-31.

[162] Kim BS, Mooney DJ. Scaffolds for engineering smooth muscle under cyclic mechanical strain conditions. J Biomech Eng. 2000;122:210-5.

[163] Kim BS, Nikolovski J, Bonadio J, Mooney DJ. Cyclic mechanical strain regulates the development of engineered smooth muscle tissue. Nat Biotechnol. 1999;17:979-83.

[164] Berglund JD, Nerem RM, Sambanis A. Incorporation of intact elastin scaffolds in tissue-engineered collagen-based vascular grafts. Tissue engineering. 2004;10:1526-35.

[165] Sell S, McClure MJ, Barnes CP, Knapp DC, Walpoth BH, Simpson DG, et al. Electrospun polydioxanone–elastin blends: potential for bioresorbable vascular grafts. Biomedical Materials. 2006;1:72.

[166] Caves JM, Kumar VA, Martinez AW, Kim J, Ripberger CM, Haller CA, et al. The use of microfiber composites of elastin-like protein matrix reinforced with synthetic collagen in the design of vascular grafts. Biomaterials. 2010;31:7175-82.

[167] Sarkar S, Schmitz-Rixen T, Hamilton G, Seifalian AM. Achieving the ideal properties for vascular bypass grafts using a tissue engineered approach: a review. Medical & biological engineering & computing. 2007;45:327-36.

[168] Smith MJ, McClure MJ, Sell SA, Barnes CP, Walpoth BH, Simpson DG, et al. Suture-reinforced electrospun polydioxanone–elastin small-diameter tubes for use in vascular tissue engineering: a feasibility study. Acta Biomater. 2008;4:58-66.

[169] Wise SG, Byrom MJ, Waterhouse A, Bannon PG, Ng MK, Weiss AS. A multilayered synthetic human elastin/polycaprolactone hybrid vascular graft with tailored mechanical properties. Acta Biomater. 2011;7:295-303.

[170] Chuang T-H, Stabler C, Simionescu A, Simionescu DT. Polyphenol-stabilized tubular elastin scaffolds for tissue engineered vascular grafts. Tissue Engineering Part A. 2009;15:2837-51.

[171] Mecham RP. Methods in elastic tissue biology: elastin isolation and purification. Methods. 2008;45:32-41.

[172] Weisel JW. Fibrinogen and fibrin. Adv Protein Chem. 2005;70:247-99.

[173] Laurens N, Koolwijk P, de Maat MP. Fibrin structure and wound healing. Journal of thrombosis and haemostasis : JTH. 2006;4:932-9.

[174] Lominadze D, Dean WL. Involvement of fibrinogen specific binding in erythrocyte aggregation. FEBS Letters. 2002;517:41-4.

[175] Grassl ED, Oegema TR, Tranquillo RT. A fibrin-based arterial media equivalent. Journal of biomedical materials research Part A. 2003;66:550-61.

[176] Ahmed TA, Dare EV, Hincke M. Fibrin: a versatile scaffold for tissue engineering applications. Tissue engineering Part B, Reviews. 2008;14:199-215.

[177] Koroleva A, Gittard S, Schlie S, Deiwick A, Jockenhoevel S, Chichkov B. Fabrication of fibrin scaffolds with controlled microscale architecture by a two-photon polymerization-micromolding technique. Biofabrication. 2012;4:015001.

[178] Kaijzel EL, Koolwijk P, van Erck MG, van Hinsbergh VW, de Maat MP. Molecular weight fibrinogen variants determine angiogenesis rate in a fibrin matrix in vitro and in vivo. Journal of thrombosis and haemostasis : JTH. 2006;4:1975-81.

[179] Jockenhoevel S, Zund G, Hoerstrup SP, Chalabi K, Sachweh JS, Demircan L, et al. Fibrin gel -- advantages of a new scaffold in cardiovascular tissue engineering. European journal of cardio-thoracic surgery : official journal of the European Association for Cardio-thoracic Surgery. 2001;19:424-30.

[180] Dietrich M, Heselhaus J, Wozniak J, Weinandy S, Mela P, Tschoeke B, et al. Fibrin-based tissue engineering: comparison of different methods of autologous fibrinogen isolation. Tissue Eng Part C Methods. 2013;19:216-26.

[181] Hasegawa T, Okada K, Takano Y, Hiraishi Y, Okita Y. Autologous fibrin-coated small-caliber vascular prostheses improve antithrombogenicity by reducing immunologic response. J Thorac Cardiovasc Surg. 2007;133:1268-76, 76 e1.

[182] Tschoeke B, Flanagan TC, Koch S, Harwoko MS, Deichmann T, Ella V, et al. Tissue-engineered small-caliber vascular graft based on a novel biodegradable composite fibrin-polylactide scaffold. Tissue Eng Part A. 2009;15:1909-18.

[183] Aper T, Teebken OE, Steinhoff G, Haverich A. Use of a fibrin preparation in the engineering of a vascular graft model. European journal of vascular and endovascular surgery : the official journal of the European Society for Vascular Surgery. 2004;28:296-302.

[184] Koch S, Tschoeke B, Deichmann T, Ella V, Gronloh N, Gries T, et al. Fibrin-based tissue engineered vascular graft in carotid artery position-the first in vivo experiences. The Thoracic and Cardiovascular Surgeon. 2010;58:MP25.

[185] Santin M, Motta A, Freddi G, Cannas M. In vitro evaluation of the inflammatory potential of the silk fibroin. J Biomed Mater Res. 1999;46:382-9.

[186] Demura M, Asakura T. Porous membrane of Bombyx mori silk fibroin: structure characterization, physical properties and application to glucose oxidase immobilization. Journal of Membrane Science. 1991;59:39-52.

[187] Asakura T, Kitaguchi M, Demura M, Sakai H, Komatsu K. Immobilization of glucose oxidase on nonwoven fabrics with bombyx mori silk fibroin gel. Journal of Applied Polymer Science. 1992;46:49-53.

[188] Demura M, Asakura T. Immobilization of glucose oxidase with Bombyx mori silk fibroin by only stretching treatment and its application to glucose sensor. Biotechnol Bioeng. 1989;33:598-603.

[189] Mhuka V, Dube S, Nindi M, Torto N. Fabrication and structural characterization of electrospun nanofibres from Gonometa Postica and Gonometa Rufobrunnae regenerated silk fibroin. Macromolecular Research. 2013;21:995-1003.

[190] Tamada Y. New process to form a silk fibroin porous 3-D structure. Biomacromolecules. 2005;6:3100-6.

[191] Meinel L, Hofmann S, Karageorgiou V, Zichner L, Langer R, Kaplan D, et al. Engineering cartilage-like tissue using human mesenchymal stem cells and silk protein scaffolds. Biotechnol Bioeng. 2004;88:379-91.

[192] Altman GH, Diaz F, Jakuba C, Calabro T, Horan RL, Chen J, et al. Silk-based biomaterials. Biomaterials. 2003;24:401-16.

[193] Zhang X, Wang X, Keshav V, Johanas JT, Leisk GG, Kaplan DL. Dynamic culture conditions to generate silk-based tissue-engineered vascular grafts. Biomaterials. 2009;30:3213-23.

[194] Makaya K, Terada S, Ohgo K, Asakura T. Comparative study of silk fibroin porous scaffolds derived from salt/water and sucrose/hexafluoroisopropanol in cartilage formation. J Biosci Bioeng. 2009;108:68-75.

[195] Enomoto S, Sumi M, Kajimoto K, Nakazawa Y, Takahashi R, Takabayashi C, et al. Long-term patency of small-diameter vascular graft made from fibroin, a silk-based biodegradable material. Journal of vascular surgery. 2010;51:155-64.

[196] Rockwood DN, Gil ES, Park SH, Kluge JA, Grayson W, Bhumiratana S, et al. Ingrowth of human mesenchymal stem cells into porous silk particle reinforced silk composite scaffolds: An in vitro study. Acta Biomater. 2011;7:144-51.

[197] Mauney JR, Sjostorm S, Blumberg J, Horan R, O'Leary JP, Vunjak-Novakovic G, et al. Mechanical stimulation promotes osteogenic differentiation of human bone marrow stromal cells on 3-D partially demineralized bone scaffolds in vitro. Calcif Tissue Int. 2004;74:458-68.

[198] Li C, Vepari C, Jin H-J, Kim HJ, Kaplan DL. Electrospun silk-BMP-2 scaffolds for bone tissue engineering. Biomaterials. 2006;27:3115-24.

[199] Lovett M, Eng G, Kluge J, Cannizzaro C, Vunjak-Novakovic G, Kaplan DL. Tubular silk scaffolds for small diameter vascular grafts. Organogenesis. 2010;6:217-24.

[200] Marelli B, Achilli M, Alessandrino A, Freddi G, Tanzi MC, Farè S, et al. Collagen-Reinforced Electrospun Silk Fibroin Tubular Construct as Small Calibre Vascular Graft. Macromolecular Bioscience. 2012;12:1566-74.

[201] Maskarinec SA, Tirrell DA. Protein engineering approaches to biomaterials design. Curr Opin Biotechnol. 2005;16:422-6.

[202] Liu H, Li X, Niu X, Zhou G, Li P, Fan Y. Improved hemocompatibility and endothelialization of vascular grafts by covalent immobilization of sulfated silk fibroin on poly (lactic-co-glycolic acid) scaffolds. Biomacromolecules. 2011;12:2914-24.

[203] Yang X, Wang L, Guan G, King MW, Li Y, Peng L, et al. Preparation and evaluation of bicomponent and homogeneous polyester silk small diameter arterial prostheses. Journal of biomaterials applications. 2013.

[204] Aytemiz D, Sakiyama W, Suzuki Y, Nakaizumi N, Tanaka R, Ogawa Y, et al. Small-Diameter Silk Vascular Grafts (3 mm Diameter) with a Double-Raschel Knitted Silk Tube Coated with Silk Fibroin Sponge. Advanced healthcare materials. 2012.

[205] Nakazawa Y, Sato M, Takahashi R, Aytemiz D, Takabayashi C, Tamura T, et al. Development of small-diameter vascular grafts based on silk fibroin fibers from bombyx mori for vascular regeneration. Journal of Biomaterials Science, Polymer Edition. 2011;22:195-206.

[206] Soffer L, Wang X, Zhang X, Kluge J, Dorfmann L, Kaplan DL, et al. Silk-based electrospun tubular scaffolds for tissue-engineered vascular grafts. Journal of Biomaterials Science, Polymer Edition. 2008;19:653-64.

Chapter 2

Hemocompatibility study of a bacterial cellulose/polyvinyl alcohol nanocomposite

Bacterial cellulose (BC) has been suggested to be a suitable biomaterial for the development of cardiovascular grafts. The combination of BC with polyvinyl alcohol (PVA) results in nanocomposites with improved properties. Surprisingly, there are very few studies on the BC-blood interaction. This is the focus of this paper. We present the first thorough assessment of the hemocompatibility of the BC/PVA nanocomposite. Whole blood clotting time, plasma recalcification, Factor XII activation, platelet adhesion and activation, hemolytic index and complement activation are all determined. The platelet activation profiles on BC and BC/PVA surfaces are comprehensively characterized. BC and BC/PVA outperformed ePTFE - used as a point of comparison - thus evidencing their suitability for cardiovascular applications.

Introduction

With the increase in the prevalence of cardiovascular diseases in the adult population, cardiovascular surgeries are becoming more and more common in operating rooms across the world. Among the most prevalent cardiovascular diseases is atherosclerosis which is generally treated by performing a bypass surgery. The procedure requires the application of a biological or a synthetic graft that will allow the blood flow to be redirected around an occluded portion of the vessel. Biological grafts deteriorate over time due to the natural progression of the patients' disease or may be unavailable [1]. Therefore, synthetic grafts are used. These are commonly made of polyethylene terephthalate (PET, commercially known as Dacron) or expanded polytetrafluoroethylene (ePTFE). However, they do not perform well in medium or small-caliber vessels such as coronary arteries [1]. In larger-caliber vessels characterized by high shear rates these materials do provide good mechanical compliance. However, they have a strong affinity for proteins, which adsorb on the surface of the material. This results in a layer, the pseudo-intima, which promotes platelet adhesion and activation and consequent clot formation [2, 3]. In low caliber vessels the protein build-up on the luminal surface and platelet activity ultimately lead to thrombosis. There is therefore a strong need for new materials for the construction of vascular grafts for small-caliber vessel applications, and a large amount of work has been aimed at finding natural alternatives to the synthetic polymer materials for making grafts.

In order to be suitable for this application, the material has to be hemocompatible, i.e., it must be able to remain in contact with blood without inducing toxicity or activating the intrinsic and extrinsic coagulation cascades or the complement system [4]. By triggering these blood reactions, foreign materials cause thrombosis and inflammation at the graft site or embolism. Emboli that occur due to the detachment of thrombi from the graft site or their formation downstream of the implant are the main cause of synthetic grafts failure [2].

One promising candidate is bacterial cellulose (BC). This polymer is a highly pure linear polysaccharide, consisting of β (1→4)–linked D-glucose monomers. It is secreted by bacteria of the *Gluconacetobacter* genus. Once secreted, it forms a fibrous network hydrogel. BC has been extensively studied for biomedical applications due to its

morphology, high purity, water-holding capacity, tensile strength, malleability and biocompatibility [5-7] and has been proposed for applications such as wound dressings [8], artificial skin [9] or blood vessels [6, 10-12] and as a scaffold for tissue engineering [7, 13-15].

Polyvinyl alcohol (PVA) has also been studied for potential biomedical applications. Its uncomplicated structure allows crosslinking of the polymer chains by either chemical agents or by physical crosslinking through thermal cycling [16]. The hydrogels formed by PVA generally present good tensile strength, flexibility and elasticity [17], allied with high water retention capability, non-toxicity and non-carcinogenicity. PVA has been studied for applications in tissue reconstruction and replacements, drug delivery, cardiovascular stents and wound covering bandages, among others [16, 18].

BC has high tensile strength but somewhat limited elasticity. On the other hand, PVA is highly elastic but its tensile strength is limited. A compromise would be ideal for potential applications in cardiovascular surgery: sufficient tensile strength allied with enough elasticity to allow for greater mechanical compliance. The BC/PVA nanocomposites indeed meet these criteria, as we and others reported [16, 19, 20]. We described previously one such nanocomposite, consisting of an interpenetrated polymer network of PVA fibers entangled inside the BC matrix, bridging gaps and linking individual BC fibers. The mechanical properties of the BC/PVA nanocomposites can be adjusted by thermal cycling. This allows tailoring of the nanocomposite mechanical properties to better mimic those of the arterial vessel walls.

While the potential of BC as a biomaterial for cardiovascular applications has been reported [6, 10-12] its interactions with blood have not been carefully characterized [10, 11]. Therefore, in this study, we assess the hemocompatibility of BC and of a BC/PVA nanocomposite.

Experimental Section

Bacterial Cellulose and Bacterial Cellulose/Polyvinyl Alcohol

Gluconacetobacter xylinus (ATCC 700178) was grown in a modified Hestrin-Schramm medium, supplemented with 2% Corn Steep Liquor (Sigma Aldrich, Germany) and 0.6%

ethanol, at pH 5.0. The medium was inoculated and then added to 24-well polystyrene microtitter plates. The plates were then incubated at 30°C for 7 days.

The resulting BC membranes were then washed thoroughly with distilled water and further purified with 4% NaOH at 60°C for 90min. The membranes were then, again, thoroughly washed until neutral pH was achieved.

For BC/PVA production, purified BC membranes were immersed in a 10% PVA (M$_w$= 31,000-50,000 g/mol) (Sigma Aldrich, Germany) solution for 24hr at 80°C. The membranes were then frozen at -20°C for 24hr, after which they were thawed at room temperature in distilled water and washed to remove any polymerized PVA particles on the surface of the membranes.

All membranes were sterilized by washing in 70% (v/v) ethanol for 24hr and then with ultrapure autoclaved water in a vertical laminar air flow hood chamber until ethanol was fully removed.

Preparation of Blood Samples

Whole blood was collected from healthy donors at Hospital São João (Oporto, Portugal) with citrated (3.2%) 1.8ml vacuum blood-collection tubes and transported on ice. The blood samples were then, unless mentioned otherwise, centrifuged at 2000g for 10min at 4°C to obtain Platelet Poor Plasma (PPP), which was then used in the plasma recalcification and Factor XII activation assays.

Whole Blood Clotting Times

Whole blood kinetic clotting times of wet and dried BC and BC/PVA membranes were determined as previously described by Motlagh [21]. Clotting was induced by addition of 360μl of 0.1M CaCl$_2$ to 3.6ml of whole blood. The BC and BC/PVA membranes along with glass microspheres (positive control) and empty wells of a 24-well polystyrene microtitter plate (negative control) were incubated for 0, 5, 10, 15, 25 and 35min at room temperature (16-18°C) with 150μl of the activated whole blood for each time point. At

the end of each time point 3ml of distilled water was added to the well and incubated for 5min, in order to lyse the red blood cells which were not trapped in the thrombus, and release hemoglobin.

The concentration of released hemoglobin was measured by transferring 200μl of the supernatant to a 96-well microtiter plate followed by spectrophotometric analysis at λ=540nm. The clot formation is followed by a reduction in the absorbance value. All samples, including ePTFE as a control, were analyzed in triplicate.

Plasma Recalcification Profiles

Plasma recalcification times for BC and BC/PVA membranes, along with empty polystyrene plate wells with (positive control) and without $CaCl_2$ (negative control) were determined by the method described by Mortagh [21]. Samples containing 500μl of Platelet Poor Plasma (PPP) were incubated for 1hr, at 37°C, on an orbital shaker. After the incubation period, 100μl of the PPP from each sample well was transferred to a 96-well plate and 100ml of $CaCl_2$ was added to each well (except the previously mentioned negative control). The 96-well microtiter plate was then immediately placed in a plate reader, and the kinetics of the clotting measured and monitored by changes in the absorption at λ=405nm, every 30sec for 45min (curves generally stabilized after 30min). The measure of thrombogenicity was given by the time it took to achieve half maximum absorbance (EC50). Each sample was measured in triplicate (3 donors per sample) and averaged; ePTFE was also analyzed in the same way.

Hemolysis Index

Hemolysis studies were conducted in accordance with the procedures described by the American Society for Testing and Materials (ASTM F756-00, 2000). BC samples were equilibrated in phosphate buffer saline (PBS) and then transferred to a tube containing 7ml of PBS. 1ml of diluted blood (hemoglobin concentration of 10 mg/ml) was added and incubated at 37°C for 3hr in a water bath. The tubes were gently inverted every 30min to promote contact between blood and samples. The membranes were then removed with

sterile tweezers and the diluted blood centrifuged at 750g for 15min. Then, 1ml of Drabkin's reagent (Sigma-Aldrich, Germany) was added to 1ml of supernatant and incubated for 15 min at room temperature, and finally the absorbance was read at λ=540nm.

Hemoglobin concentration was calculated using a calibration curve previously prepared with human hemoglobin (Sigma-Aldrich, Germany) and calculated using the formula: HC=A×m×d (A, Absorbance; m Slope of the hemoglobin curve; d, Dilution) and presented as percentage. Ultrapure water and PBS served as the positive and negative controls, respectively. ePTFE was analyzed in the same manner as control materials.

Complement System Activation

To determine whether the biomaterials activate the complement cascade, we performed the protocol described by the NCL (Nanotechnology Characterization Laboratory) for qualitative determination of total complement activation by Western blot analysis (http://ncl.cancer.gov/working_assay-cascade.asp) with slight modifications. Human plasma, from healthy donors, was incubated with BC and BC/PVA membranes in the presence of veronal buffer. Equal volumes (100μL) of plasma, buffer and sample were mixed together and incubated at 37°C for 60 min. Cobra venom factor (CVF) from Quidel Corporation (San Diego, CA, USA), and PBS were used as positive and negative controls, respectively.

In order to determine if complement proteins could have unspecific adsorption on the BC and BC/PVA membranes, several pre-incubations were performed:

1. Preincubation for 2 hr at 37°C with a pool of active plasma followed by a 1 hr incubation with plasma and veronal buffer at 37°C.

2. Preincubation for 2 hr at 37°C with a pool of inactive plasma and then 1 hr incubation with plasma and veronal buffer at 37°C.

3. Incubation for 1 hr with a pool of plasma and veronal buffer for 1 hr at 37°C.

4. Incubation of 3 hr with a pool of plasma at 37°C.

5. Incubation of 3 hr with a pool of plasma and veronal buffer at 37°C.

Proteins were resolved using 10% SDS-PAGE, and then transferred to a membrane (Immun-Blot PVDF Membrane, Biorad, Hercules, USA) using the transblot semidry apparatus BioRad transfer equipment (Trans blot SD, BioRad, Hercules, USA). The membranes were incubated for 90 min with a mouse monoclonal antibody against human C3, diluted to 1:1000 (Abcam, Cambridge, UK). The membranes were then washed and incubated with secondary polyclonal goat anti-mouse IgG antibodies conjugated with alkaline phosphatase, diluted to 1:2000 (Dako, Glostrup, Denmark). The membranes were finally revealed with 5-Bromo-4-Chloro-3-Indolyl Phosphate (BCIP) (Sigma Aldrich, Germany).

Factor XII Activation

Both free and adhered Factor XII (FXII) activation was determined by a method adapted from Sperling et al [22]. For the determination of free Factor XII activation BC and BC/PVA membranes were incubated with 300μl of PPP for 1, 5, 10 and 20 min at room temperature (16-18°C). Then, 30μl of the plasma was added to 200μl of 0.3M chromogenic substrate S-2302 (Chromogenix, Italy) in 50mM 4-(2-hydroxyethyl)-1-piperazineethanesulfonic acid buffer (HEPES) and 120mM NaCl at pH 7.4; the absorbance was immediately measured at λ=405nm for 30min (every 30sec). An empty polystyrene well and glass microspheres were used as the negative and positive controls. The slope of the resulting curves was calculated and used to compare Factor XII activation. All samples were analyzed in triplicate along with ePTFE.

Additionally, to determine the activation of Factor XII adhered to the surface of BC and BC/PVA, samples incubated with PPP for the same time periods as above (1, 5, 10 and 20 min) were immersed in 300μl of 0.3M chromogenic substrate S-2302 (Chromogenix) in 50mM HEPES and 120mM NaCl at pH 7.4 for 30 min, the reaction was then stopped with 75μl of 20% (v/v) acetic acid and 200μl of the reaction volume and the absorbance measured on a 96-well microtitter plate at λ=405nm.

Platelet Isolation, Characterization and Surface Activation Studies

Platelet rich plasma (PRP) and purified platelets were obtained by centrifugation of sodium citrate-anticoagulated human blood [23]. Blood collection was organized by the Biobanco Vasco para la Investigación (Basque Biobank for Research, Galdakao, Spain) and performed with informed consent according to the appropriate legal and ethical guidelines. Donors were healthy volunteers without any history of exposure to medication (such as aspirin) or to alcohol in the two weeks prior to blood collection. Purified platelets were suspended in the buffer (145mM NaCl, 5mM Glucose, 1mM $MgCl_2$, 10mM HEPES, 5mM KCl, pH 7.4), with (Plt+Ca^{2+}) or without (Plt-Ca^{2+}) 2mM calcium. Platelet concentration was adjusted to $\approx 1 \times 10^8$ cells per ml.

Flow cytometry was used to test platelets for their purity, state of activation in platelet rich plasma (PRP)/purified platelet suspensions and their ability to respond to agonists such as TRAP (thrombin receptor-activating peptide, Sigma-Aldrich, Madrid, Spain) or PMA (phorbol 12-myristate 13-acetate, Sigma-Aldrich, Madrid, Spain). Fluorescently labelled monoclonal antibodies specific for well-known platelet activation markers (CD62P, CD63, active form of GPIIb/IIIa) and fluorescent-annexin 5 (A5) that binds to phosphatidylserine (PS) were used in the flow cytometry experiments. Platelets were identified by staining with anti-CD41a (platelet specific marker). All antibodies and fluorescent markers were purchased from BD Biosciences (Madrid, Spain). Light scatter and fluorescence data from 10,000 events were collected with all the detectors in the logarithmic mode. Flow Jo software (Tree Star Inc, Oregon, USA) was used to determine the percentage of platelets positive for antibody binding for different platelet activation markers. Mean fluorescence intensity for the positive and negative events was determined to obtain the level of expression of various platelet activation markers.

Once platelets were confirmed to be in a quiescent state, as well as responsive to agonists, purified platelets, with and without extracellular Ca^{2+} (Plt+Ca^{2+}; Plt-Ca^{2+}) or PRP were incubated with clean and sterile BC, BC/PVA and ePTFE membranes. For these experiments, the membranes were cut and deposited into autoclaved eppendorf tube caps. Purified platelets or PRP preparations were incubated with these materials for various time periods (10, 30, 50 and 180min) at 37°C. The entire set up was put inside a clean and covered Petri dish, which was then placed inside a 37°C incubator to avoid any

contamination. After incubation, the supernatants were removed and collected in an eppendorf tube for immediate analysis by flow cytometry. The non-adherent platelets in the supernatant from each sample were stained for the same markers (CD62P, CD63, PS and activated GPIIb/IIIa) to check for their activation state. The surface adhered platelets were fixed with 2.5% glutaraldehyde and stained with the antibodies specific for CD41a, CD62P and CD63, for their analysis by confocal microscopy to assess platelet adhesion and activation.

Results and Discussion

Whole Blood Clotting Time

Whole blood was used to determine clotting times and provide information on the thrombogenicity and pro-coagulative activity of each biomaterial. In this assay, whole blood is allowed to clot in contact with a biomaterial. As clotting occurs, more red blood cells are retained in the clot, and therefore less hemoglobin is released by lysis upon addition of distilled water. A hemocompatible material will therefore maintain a higher absorbance value over time. Results show (Figure 2-1) that ePTFE and polystyrene (negative control) are the least thrombogenic; conversely, the glass microspheres present the quickest clotting time. BC appears more thrombogenic than either ePTFE or polystyrene, consistent with the results of Andrade et al [24]. The results for BC/PVA show no statistical difference ($p \geq 0.05$) compared to those of BC alone. Andrade and colleagues [24] observed, in agreement with others [25], that whole blood clotting time is related - to some extent - to the surface area of the material. The surface area of the bottom of the microtitter plate well is $1.21 cm^2$. The ePTFE samples were cut and stretched in order to sit flush and cover the well bottom and so surface of contact was similar to that of the negative control. In the case of both BC and BC/PVA, these hydrogels are porous and present a dome shaped structure that does not sit flush to the bottom of the microtitter wells. This increases the surface of biomaterial-blood contact which may adversely affect the comparative analysis of the results. Once dried, BC and BC/PVA membranes lose most of their original thickness (from 3mm down to 0,068mm in the case of BC), hence they are less porous. The resulting dried membranes present a similar surface of contact to that of ePTFE and the negative control. As expected, the clotting time
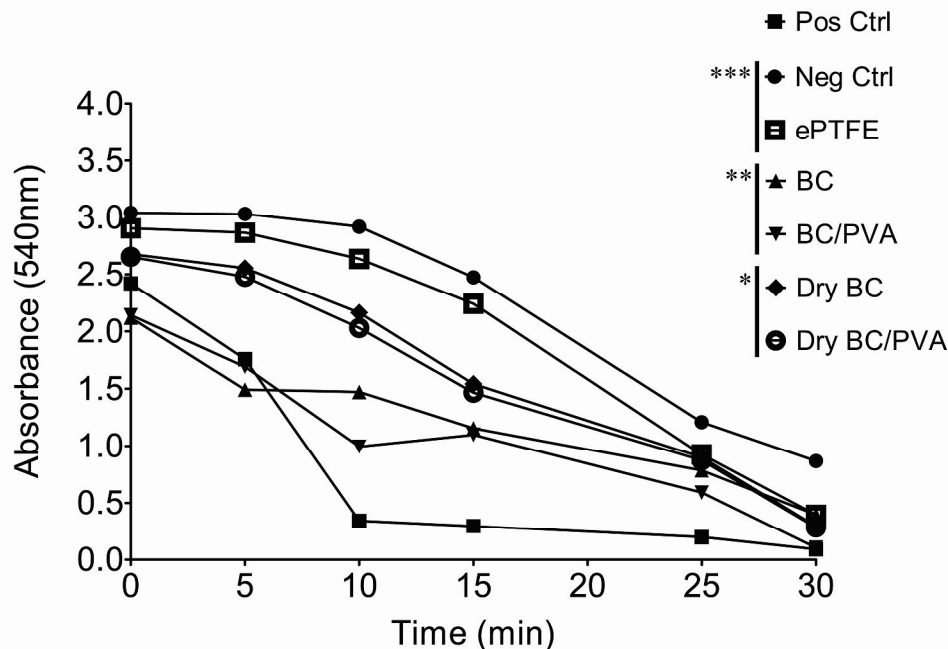
Figure 2-1 - Whole Blood Clotting Time for wet and dry bacterial cellulose (BC), bacterial cellulose/polyvinyl alcohol (BC/PVA) and expanded polytetrafluoroethylene (ePTFE). The positive (+) Control used were glass microspheres and the negative (-) control the polystyrene microtitter plate.

observed on the dried membranes was closer to that of both the negative control and ePTFE. Once again, no significant difference was observed between BC and BC/PVA.

Plasma Recalcification Profile

The plasma recalcification profile obtained in response to PPP contact to a material is often used as a measure of activation of the intrinsic pathway [21, 26]. As plasma becomes more turbid due to the accumulation of clotting by-products, absorbance increases. The measure of pro-coagulative activity in this test is given by the time it takes to achieve half the maximum absorbance; the higher this value, the less thrombogenic the material. For this assay (Figure 2-2) glass microspheres serve as a positive control. The glass microspheres are generally accepted as positive controls in this respect due to their negatively charged surface that triggers protein adsorption and activates coagulation factors.
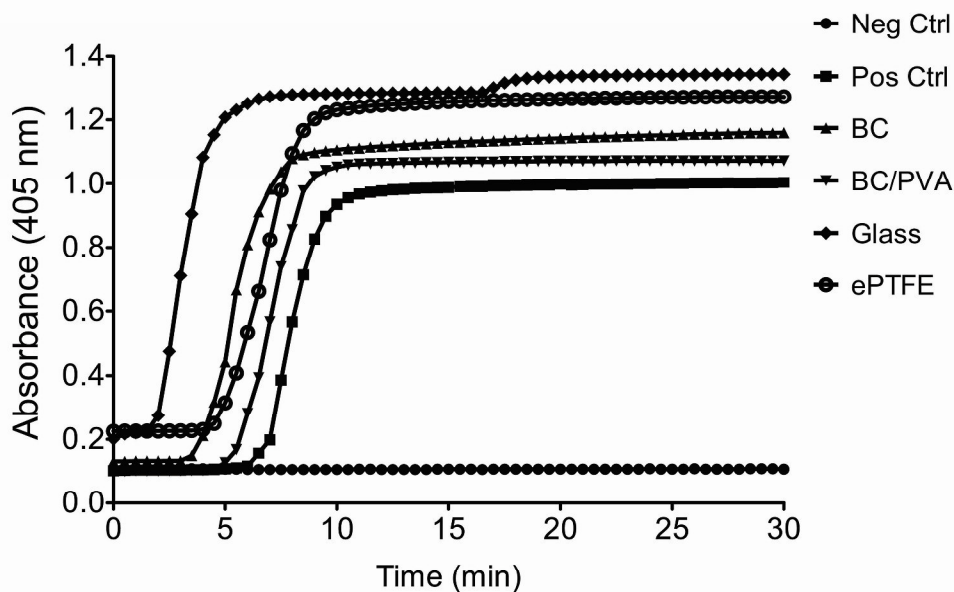
Figure 2-2 - Plasma Recalcification Profile of Platelet Poor Plasma (PPP) in the presence of bacterial cellulose (BC), bacterial cellulose/polyvinyl alcohol (BC/PVA) and expanded polytetrafluoroethylene (ePTFE) along with glass micoshperes. The positive control was obtained by addition CaCl₂ to PPP in a polystyrene plate.

The positive control was found to be significantly different (p<0.05), with no statistical differences found among the other tested samples. Similarly to what was reported by Andrade [24], ePTFE presents a lower pro-coagulating activity than BC (higher half maximum absorbance time - 6.5 versus 5.5min, respectively). Of particular note is the result for BC/PVA, which outperforms ePTFE. This suggests that the incorporation of PVA improves the performance of BC, as may be inferred from the higher half maximum absorbance time (7min).

Factor XII Activation

In order to further characterize the activation of the intrinsic pathway, direct quantification of the catalytic activity of both free (Figure 2-3) and adhered (Figure 2-4) activated Factor XII was performed using a chromogenic substrate. The chromogenic substrate (S-2302) is broken down, specifically, by the activated form of Factor XII (Factor XIIa). The results are expressed as the Factor XII activation upon exposure to the Materials, normalized to the value obtained using the positive control (glass microspheres).
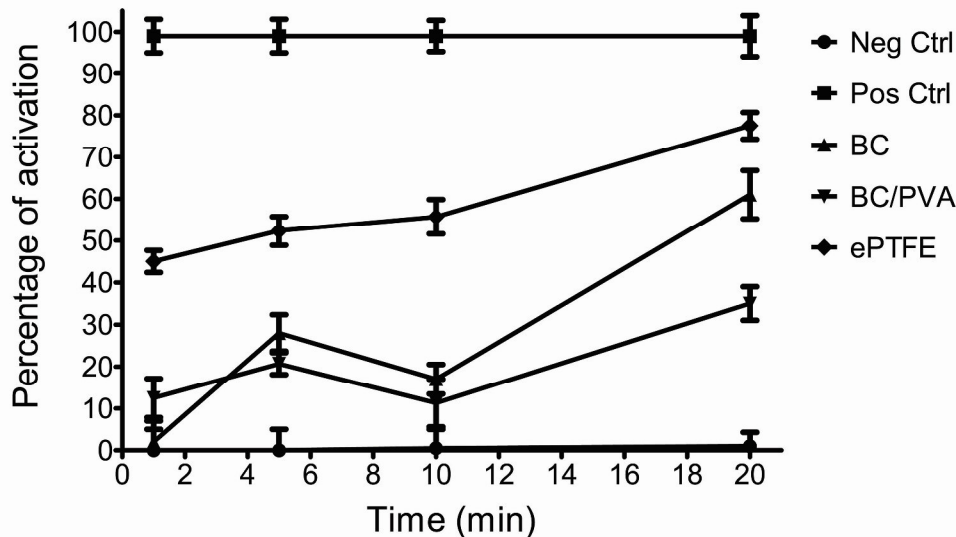
Figure 2-3 - Percentage of Factor XII Activation, as compared to glass microspheres (+ Control), over time of bacterial cellulose (BC), bacterial cellulose/polyvinyl alcohol (BC/PVA), expanded polytetrafluoroethylene (ePTFE) and polystyrene plate (- control). Measurements were obtained from absorbance of chromogenic substrate S-2302 (chromogenix).

The results obtained with BC and BC/PVA present no statistical differences ($p \geq 0.05$). The thrombogenicity of both materials is however different from that of ePTFE: they induce less free Factor XII activation; the differences are statistically significant (Figure 2-3).

All of the materials showed some adhered Factor XIIa (Figure 2-4). Similar amounts are detected on BC and ePTFE, with no statistical difference between them ($p \geq 0.05$). On the other hand, BC/PVA presents significantly ($p < 0.05$) lower values for adhered Factor XIIa than the other two materials. Overall, BC/PVA seems to be triggering the lowest response of the intrinsic coagulation cascade. Thus, again, PVA seems to a have a beneficial impact on the BC hemocompatibility.

It is generally accepted that synthetic materials with a negatively charged surfaces trigger the activation of Factor XII via conformational change to a Factor XIIa-similar molecule [4, 27-29]. We expect that the surface charges on BC, BC/PVA, and ePTFE are similar and small compared to the highly charged glass spheres. Therefore the differences we observe in the propensity of these materials to activate FXII are not related to differences in their surface charge but to their hydrophilicity/hydrophobicity. Indeed, while some authors suggest that there is little difference in terms of FXII activation between
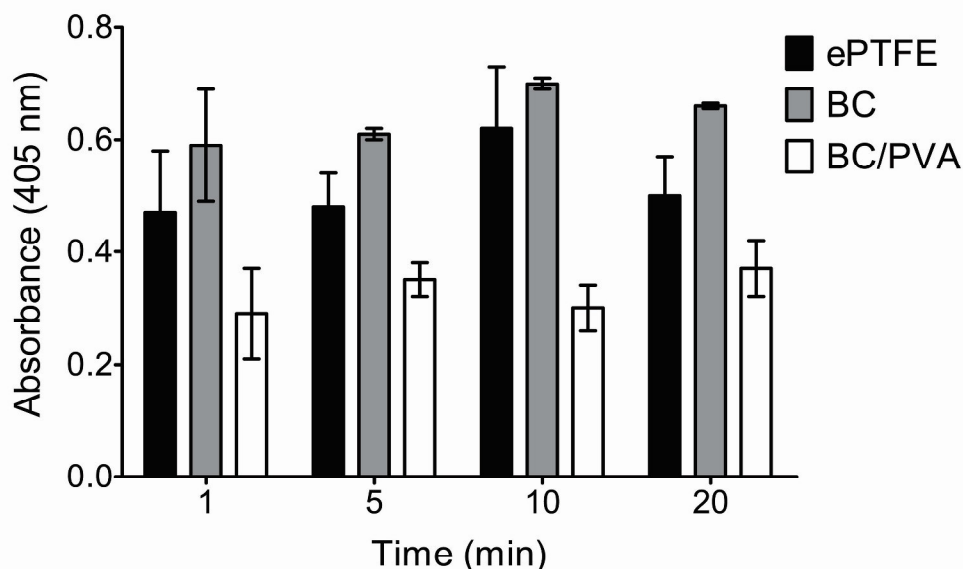
Figure 2-4 - Absorbance of Adhered Factor XII on the surface of bacterial cellulose (BC), bacterial cellulose/polyvinyl alcohol (BC/PVA) and expanded polytetrafluoroethylene (ePTFE) over time. The activity of Factor XII was measures by use of chromogenic substrate S-2302 (chromogenix).

hydrophobic and hydrophilic surfaces [27], others assert that hydrophilic surfaces are more prone to induce Factor XII activation [22]. This is thought to happen due to the so-called adsorption-dilution that occurs on the hydrophobic surfaces, where more proteins adsorb in general and FXII is diluted [27]. We observe the opposite: the more hydrophilic BC and BC/PVA hydrogels are less effective in activating FXII than the hydrophobic ePTFE.

It must be realized, however, that activation of Factor XII does not suffice for the activation of the intrinsic pathway, the complex interactions between several proteins on the surface of the materials may result in more or less effective amplification [30].

Platelet Adhesion and Activation Studies

While platelet adhesion to BC [31] and PVA grafts [32] has already been described in the literature, the detailed characterization of platelet response on these surfaces, especially the newly developed PVA-modified BC surface, has not been done. Here we studied the

adhesion and activation of platelets upon interaction with the BC-based materials. To do so, we exposed BC and BC/PVA membranes to PRP for different time periods—10, 30, 50 and 180min—at 37°C and assayed for the expression of the activation markers on the surface-adhered platelets and on the platelets in the bulk solution above the surfaces by immunostaining.

We studied four classical markers of platelet activation: transmembrane proteins CD62P (P-selectin) and CD63 (present in the membranes of the granules stored inside the resting platelets and brought to the surface upon activation), active conformation of the integrin complex GPIIb-IIIa, (constitutively expressed on platelet surfaces but undergoes conformation changes upon activation), and phospholipid phosphatidyl serine (located in the cytoplasmic leaflet of the cell membrane in the resting platelets but is brought to the outer leaflet upon activation) [33]. Surface-adhering platelets were studied using confocal laser scanning microscopy (CLSM). The results of these experiments, performed with BC, BC/PVA and ePTFE are shown in Figure 2-5. After 10min, very few platelets adhered on either BC or BC/PVA as compared to ePTFE, which showed a higher level of platelet adhesion (c.f. the number of platelets on the various surfaces in Figure 2-5A). More platelets were found on BC and BC/PVA surfaces after 50min of incubation, while no significant difference in the number of platelets between 10 and 50min was observed on ePTFE (Figure 2-5B); larger patches/clusters could sometimes be observed after 50 min (arrowhead in Figure 2-5B). Surface-adhered platelets were found to be activated (expressed CD62P and CD63) on BC and ePTFE surfaces both after 10 and 50min (Figure 2-5-A, B). Judging from the level of fluorescence intensity, the level of expression of CD62P and CD63 was higher on ePTFE than on BC. BC/PVA-adhered platelets were activated only after 50min (Figure 2-5B). The level of activation in this case was also lower than that observed on ePTFE. Similar results were obtained for purified platelets incubated with surfaces in the absence of calcium (data not shown). Platelet response observed on ePTFE is consistent with the literature where it has been stated that protein adsorption on the ePTFE surface leads to adhesion and activation of platelets [34].

In order to have a better understanding of the interactions between platelets and these materials, we further studied the behavior of platelets in the bulk solution, above the biomaterial surface. Previous studies have shown that in addition to platelets adhering to the material surface, the non-adherent platelets may get activated upon blood-biomaterial interaction [34, 35]. These fluid-phase activated platelets contribute to
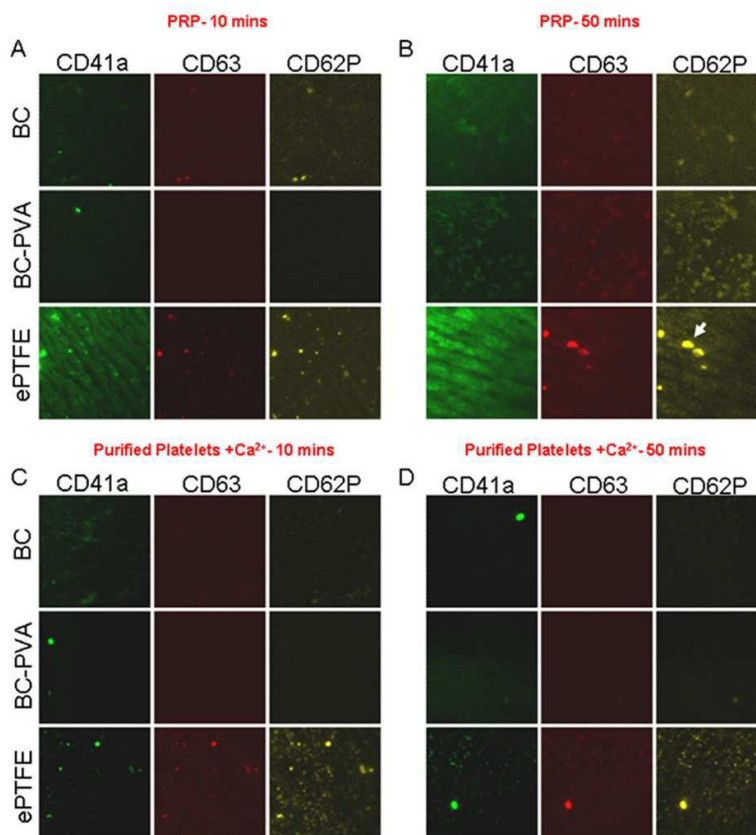
Figure 2-5 - Images obtained by confocal laser scanning microscopy of the surfaces of bacterial cellulose (BC), bacterial cellulose/polyvinyl alcohol nanocomposite (BC/PVA) and ePTFE after incubation with platelet rich plasma (PRP) for 10 and 50 minutes. The platelets were marked with antibodies for CD41a (a platelet marker) and the activated platelet markers CD63 and CD62P.

thrombotic and inflammatory reactions at a distance from the original implantation site [36-38]. The activation of non-adherent platelets was investigated using flow cytometry [39]. The results for these experiments are shown in Figure 2-6 and 2-7. We determined the percentage of cells positive for a particular surface marker (Figure 2-6) and also the level of expression of that marker (calculated from mean fluorescence intensity) on the positive cells (Figure 2-7). The degree of non-adhered platelet activation upon contact with the surface is here presented as an increase in the expression of a particular marker as compared to the freshly isolated resting platelets (Figure 2-7, Mean fluorescence intensities ratio, MFIR). Both PRP and purified platelets were used in the experiments. For PRP, CD62P and CD63 expression were used to monitor activation, while for purified platelets all four activation markers (CD62P, CD63, PS and activated GPIIb/IIIa) were used. This is because detection of PS and activated GPIIb/IIIa expression requires extracellular Ca [40, 41], which would induce clotting when using PRP.

Freshly isolated platelets were in their quiescent state (Figure 2-7) and showed negligible expression of the activation markers until stimulation with TRAP or PMA (positive controls). Following incubation with PRP, no discernible difference in the expression of the activation markers CD62P and CD63 was observed for all 3 biomaterials at time points of 10, 30 and 50min (Figure 2-7A, B). However, a significant difference in the CD62P and CD63 expression was observed after 180 min: ePTFE showed a 13 fold increase in CD62P expression level as compared to BC and BC/PVA, which showed a modest 2-3 fold increase relative to the quiescent platelets (Figure 2-7A). Similarly, the increase in CD63 expression was 9 fold for ePTFE and 2 fold for BC and BC/PVA (Figure 2-7B). Additionally, the results for percentage of cells (Figure 2-6) positive for these 2 markers were also in accordance with the trends obtained for their expression levels. For BC and BC/PVA, only 16% and 18% of cells, respectively, showed CD62P expression whereas for ePTFE it was almost much higher (67%) of BC and BC/PVA (Figure 2-6A). Again, for CD63, ePTFE presented much more CD63 positive cells (Figure 2-6B) as compared to BC materials (80% and 40%, respectively). These results support our claim that, in the presence of plasma proteins, BC and BC/PVA prove to be more hemocompatible as compared to ePTFE in terms of plasma recalcification profiles, Factor XII activation, platelet adhesion and activation (both in bulk and on surface of the biomaterials).

To complement the results obtained with PRP, we also studied the activation of purified platelets in the presence, as well as in the absence, of calcium. Direct effects of bare surfaces on platelets have previously been reported [24, 42-46]. The results obtained with surface adhered platelets were already discussed above (Figure 2-5), while the results of platelet activation in solution are shown in Figure 2-6 and 2-7 together with those of PRP. The non-adherent platelets incubated with ePTFE showed almost no CD62P/CD63 expression, both in the presence and absence of calcium, for all time points (Figure 2-7-A,B). After 180min, in the absence of calcium, platelets incubated with BC and BC/PVA showed roughly a 2 fold increases in CD62P and CD63 expression, further increased by about 8 and 2 fold, in the presence of calcium, for the same markers. Similarly, BC and BC/PVA presented higher percentage of cells positive for CD62P and CD63 as compared to ePTFE (Figure 2-6-A,B).

In the case of purified platelets, we could also study the effect of surface interaction on the expression of PS and the active form of GPIIb/IIIa. No increase in the expression of
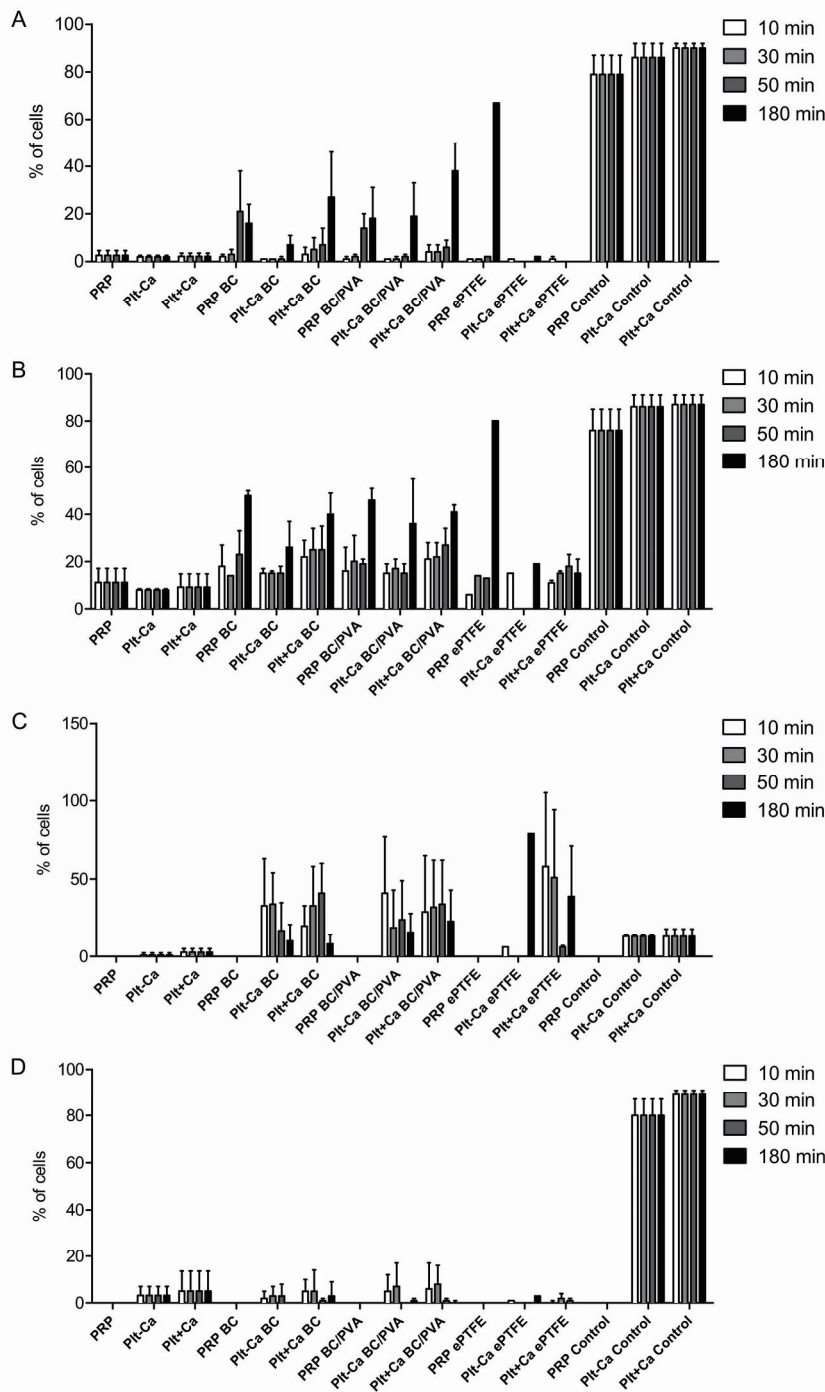
Figure 2-6 - Percentage of platelets (Plt) with a positive marking for CD62P (A), CD63 (B), PS (C) and GPIIB/IIIa (D), as counted using a flow cytometer, on platelet surfaces exposed to bacterial cellulose (BC), of a bacterial cellulose/polyvinyl alcohol nanocomposite (BC/PVA) and ePTFE. The samples were incubated for 10, 30, 50 and 180 minutes with platelet rich plasma (PRP) and also a platelet solution with (Plt+Ca) and without (Plt-Ca) 2mM Ca added to the solution.

activated form of GPIIb/IIIa relative to that in quiescent platelets was observed for any of the three surfaces (Figure 2-6D and 7D). PS expression was found to fluctuate (Figure
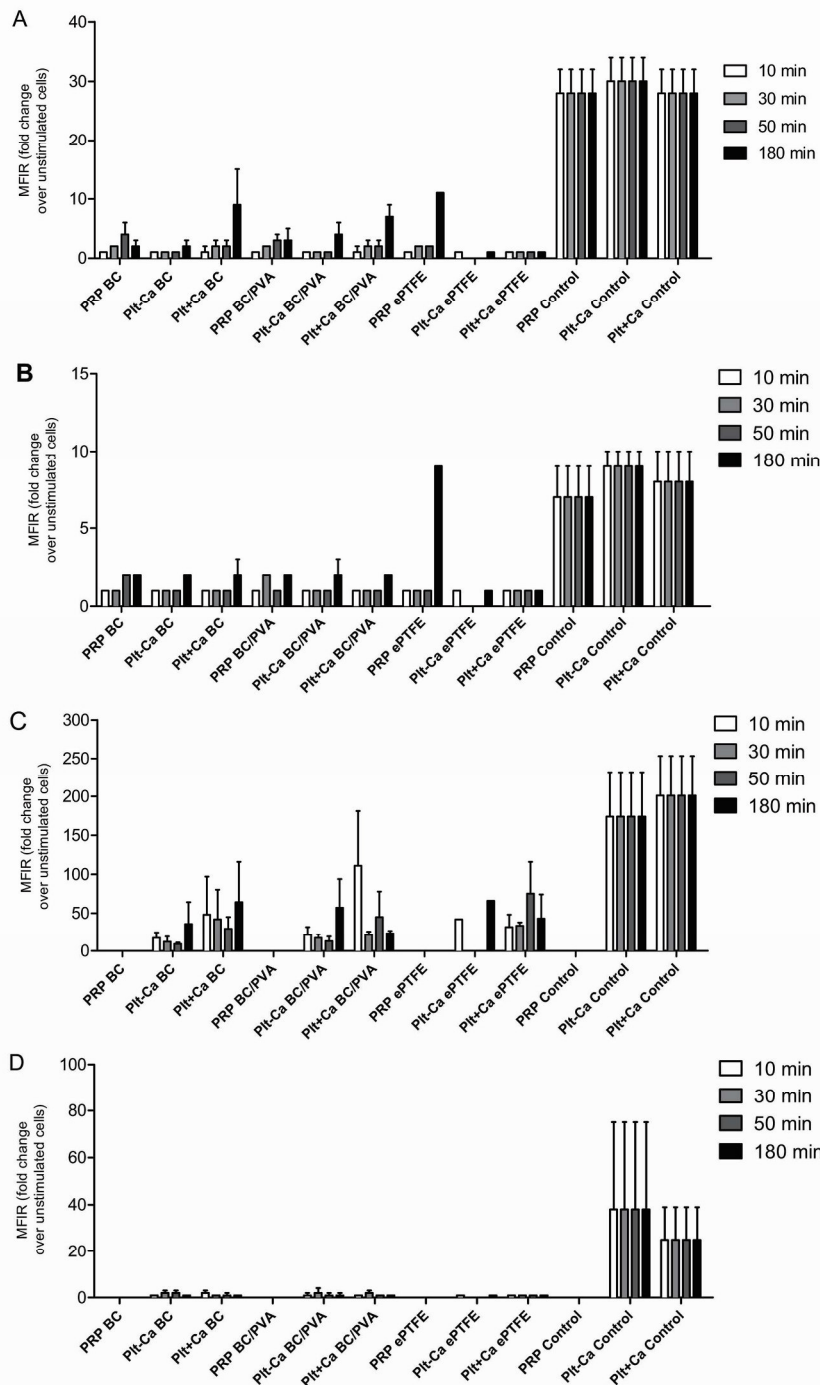
Figure 2-7 - Mean fluorescence intensities (MFIR) , as obtained by flow cytometry, for the expression of CD62P (A), CD63 (B), PS (C) and GPIIB/IIIa (D) on platelet surface after exposure to BC, PC/PVA and ePTFE for 10, 30, 50 and 180 minutes. The surface were incubated with platelet rich plasma (PRP) and also a platelet solution with (Plt+Ca) and without (Plt-Ca) 2mM Ca added to the solution.

2-7C). After 180min, the PS expression is lower (25 fold increase) for BC/PVA as compared to BC (60 fold increase) and ePTFE (50 fold).

The observed PS fluctuations are interesting, but their significance is not altogether clear. They may be related to platelet activation or reflect the loss of PS in the microparticles generated upon activation. The consensus is that PS exposure on the platelet surface is necessary for thrombin generation, but whether it is sufficient for the pro-coagulant function of platelets is still debated [47]. Moreover, there are inconsistencies in literature regarding PS detection, because annexin A5 binding may be interfered with by other PS binding proteins, including the factors of the clotting cascade. Some authors suggest that activation leads to different platelet subpopulations, only some of which expressing PS [48].

In summary, it appears that in the absence of plasma proteins (that is, when using purified platelets), BC and BC/PVA surfaces activate platelets in the bulk more efficiently than ePTFE. Therefore, their superior performance noted in PRP (which better mimic the in vivo conditions) is most likely due to a passivating layer of plasma proteins.

As noted above, the hydrophilic surface of BC and BC/PVA does not favor protein unfolding/conformational changes, hence not leading to Factor XII activation and not causing as much platelet activation as protein layers on other surfaces. These results are also in accordance with the findings of Sperling and colleagues [22] who showed that platelet adhesion and activation was favored by highly hydrophobic surfaces.

Hemolytic Index

The hemolytic index is a direct measure of free hemoglobin present in plasma after exposure to a given material or stressor. An isotonic solution (PBS) served as the negative control and distilled water as the corresponding positive control, inducing osmotic stress that ruptures red blood cells. The assay was performed as according to the Standard Practice for Assessment of Hemolytic Properties of Materials from the American Society for Testing and Materials (ASTM F756-00, 2000); the standard classifies the material as non-hemolytic (0-2% of hemolysis), slightly hemolytic (2-5% of hemolysis) and hemolytic (>5% of hemolysis). Our results (Table 1) show that both BC and BC/PVA are classified, as according to the standard, as non-hemolytic while, ePTFE is classified as slightly hemolytic.

Table 2-1 - Hemoglobin index blood after contact with of bacterial cellulose (BC), bacterial cellulose/polyvinyl alcohol (BC/PVA) and expanded polytetrafluoroethylene (ePTFE).

Sample	%
PBS	1.84
mQ H_2O (C+)	95.34
BC	1.85
BC/PVA	1.94
ePTFE	2.42

Complement System Activation

In order to further study the blood/material interaction, we also looked at the activation of the complement system by BC and BC/PVA. Among the three possible mechanisms the alternative activation pathway is of particular importance. In blood/biomaterial interactions the alternative activation pathway is triggered directly by foreign surfaces that do not provide adequate down-regulation of the protease C3-convertase.

We determined the overall percentage of C3 cleavage products, by semi-quantitative Western blot analysis, in order to determine the degree of activation of the complement system. The results are presented as the percentage of cleaved products as compared to the positive control, obtained by addition of cobra venom factor to the plasma. Our results show that both BC and BC/PVA significantly activate complement (Figure 2-8). Complement activation of the BC samples presents an average of 64.5±4.2%. The effect is slightly mitigated in the case of BC/PVA with an average of 55.6±5.0% activation. Considering the negative control presents an average 39.6±4.0% this means an increase of 24.9% for BC and 16.0% for BC/PVA. Additionally, dry BC was also tested (results not shown) and was found not to activate the complement system, the values obtained were lower than those of the negative control.

The mechanisms by which complement is activated are still not fully understood but it is well established that different biomaterial surfaces have different complement-activating properties. Physical properties such as hydrophobicity affect the activating ability. Hydrophobic surfaces are more potent activators than hydrophilic ones, and incorporation of chemical groups such as $-NH_2$, -OH or -COOH influences the activation
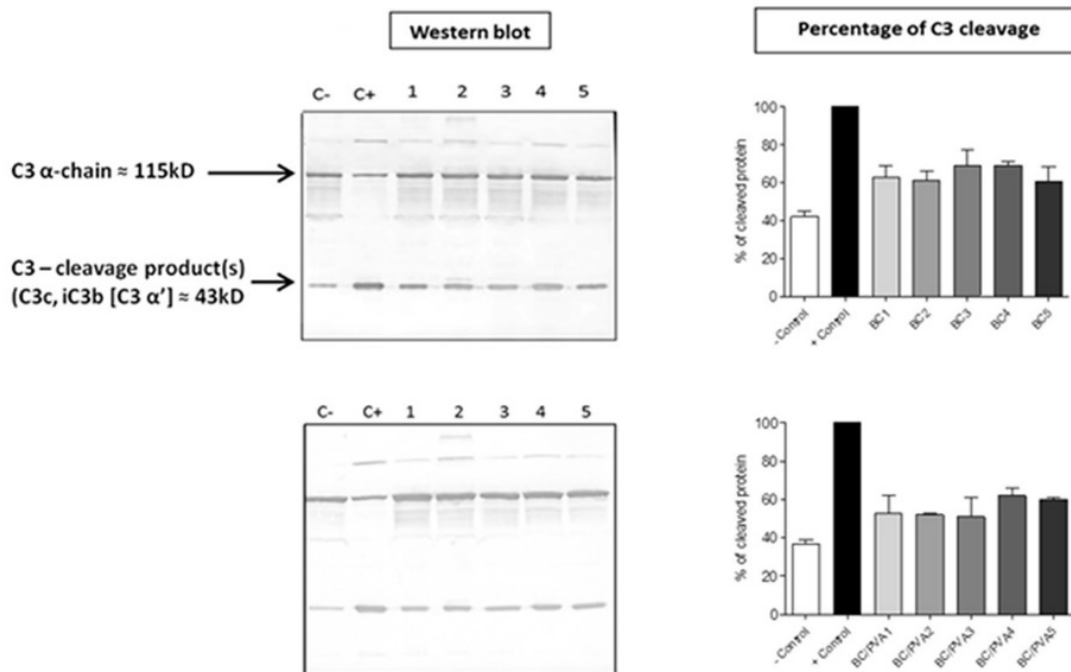
Figure 2-8 - Representative images of Western Blot and Percentage of C3 Cleavage for BC and BC/PVA. Both BC and BC/PVA were tested under 5 conditons: (1) 2 hour preincubation at 37ºC with active plasma and then 1 hour incubation with plasma and Veronal buffer at 37ºC; (2)) 2 hour preincubation at 37ºC with inactive plasma and then 1 hour incubation with plasma and Veronal buffer at 37ºC, (3) 1 hour incubation with plasma and Veronal buffer for 1hour at 37ºC, (4) 3 hour incubation with plasma at 37ºC and (5) 3 hour incubation with plasma and Veronal buffer at 37ºC.

of complement [49]. Both BC and BC/PVA have many surface -OH groups which would in turn activate the complement system to some extent. However, the total increase of C3 cleavage products is relatively low, as compared to the negative control.

Interestingly, in both the presence of PVA and in the dry BC membranes, complement system activation is mitigated or canceled out. This may be due to a probable reduction of the total number of free surface -OH groups, resulting in reduced biomaterial derived C3 cleavage [49].

Conclusions

BC and PVA have been extensively studied by various research groups for biomedical applications in blood contacting materials. This is the first study, to our knowledge, to present extensive results on the hemocompatibility of a nanocomposite of BC impregnated with PVA, namely in regards to platelet activation profiles on BC and the

BC/PVA nanocomposite. The results consistently show that these materials have a good hemocompatibility, probably due to both low activation of platelets and Factor XII.

The results for platelet adhesion and activation profiles demonstrate that both BC and BC/PVA exhibit superior performance as compared to ePTFE. Platelet activation on ePTFE seems to be mediated by plasma proteins. It appears that, on ePTFE, activation of the intrinsic pathway (higher Factor XII activation, Figure 2-3) leads to higher thrombin generation and this could explain the high level of platelet activation observed on this surface. The indication that platelets can be activated by BC and BC/PVA is relevant; however, it seems to be mitigated by the presence of other plasma constituents. BC appears thus as a suitable material for the development of cardiovascular grafts.

References

[1] Chlupac J, Filova E, Bacakova L. Blood vessel replacement: 50 years of development and tissue engineering paradigms in vascular surgery. Physiol Res. 2009;58 Suppl 2:S119-39.

[2] Tsai WB, Grunkemeier JM, Horbett TA. Human plasma fibrinogen adsorption and platelet adhesion to polystyrene. J Biomed Mater Res. 1999;44:130-9.

[3] Schopka S, Schmid T, Schmid C, Lehle K. Current Strategies in Cardiovascular Biomaterial Functionalization. Materials. 2010;3:638-55.

[4] Colman RW, Schmaier AH. Contact system: a vascular biology modulator with anticoagulant, profibrinolytic, antiadhesive, and proinflammatory attributes. Blood. 1997;90:3819-43.

[5] van der Zijpp YJ, Poot AA, Feijen J. Endothelialization of small-diameter vascular prostheses. Archives of physiology and biochemistry. 2003;111:415-27.

[6] Klemm D, Schumann D, Udhardt U, Marsch S. Bacterial synthesized cellulose — artificial blood vessels for microsurgery. Progress in Polymer Science. 2001;26:1561-603.

[7] Svensson A, Nicklasson E, Harrah T, Panilaitis B, Kaplan DL, Brittberg M, et al. Bacterial cellulose as a potential scaffold for tissue engineering of cartilage. Biomaterials. 2005;26:419-31.

[8] Alvarez O, Patel M, Booker J, Markowitz L. Original Research Effectiveness of a Biocellulose Wound Dressing for the Treatment of Chronic Venous Leg Ulcers: Results of a Single Center Randomized Study Involving 24 Patients. Wounds. 2004;16:224-33.

[9] Fontana JD, de Souza AM, Fontana CK, Torriani IL, Moreschi JC, Gallotti BJ, et al. Acetobacter cellulose pellicle as a temporary skin substitute. Appl Biochem Biotechnol. 1990;24-25:253-64.

[10] Wippermann J, Schumann D, Klemm D, Kosmehl H, Salehi-Gelani S, Wahlers T. Preliminary Results of Small Arterial Substitute Performed with a New Cylindrical Biomaterial Composed of Bacterial Cellulose. European Journal of Vascular and Endovascular Surgery. 2009;37:592-6.

[11] Andrade FK, Costa R, Domingues L, Soares R, Gama M. Improving bacterial cellulose for blood vessel replacement: Functionalization with a chimeric protein containing a cellulose-binding module and an adhesion peptide. Acta Biomater. 2010;6:4034-41.

[12] Bäckdahl H, Risberg B, Gatenholm P. Observations on bacterial cellulose tube formation for application as vascular graft. Materials Science and Engineering: C. 2011;31:14-21.

[13] Andrade FK, Moreira SM, Domingues L, Gama FM. Improving the affinity of fibroblasts for bacterial cellulose using carbohydrate-binding modules fused to RGD. Journal of biomedical materials research Part A. 2010;92:9-17.

[14] Andrade F, Pertile R, Douradoa F. Bacterial cellulose: properties, production and applications. Cellulose: structure and properties, derivatives and industrial uses Nova Science Publishers, Inc. 2010:427-58.

[15] Backdahl H, Helenius G, Bodin A, Nannmark U, Johansson BR, Risberg B, et al. Mechanical properties of bacterial cellulose and interactions with smooth muscle cells. Biomaterials. 2006;27:2141-9.

[16] Millon LE, Wan WK. The polyvinyl alcohol-bacterial cellulose system as a new nanocomposite for biomedical applications. J Biomed Mater Res B Appl Biomater. 2006;79:245-53.

[17] Hassan C, Peppas N. Structure and Applications of Poly(vinyl alcohol) Hydrogels Produced by Conventional Crosslinking or by Freezing/Thawing Methods. Biopolymers · PVA Hydrogels, Anionic Polymerisation Nanocomposites: Springer Berlin Heidelberg; 2000. p. 37-65.

[18] Mori Y, Tokura H, Yoshikawa M. Properties of hydrogels synthesized by freezing and thawing aqueous polyvinyl alcohol solutions and their applications. Journal of Materials Science. 1997;32:491-6.

[19] Chu KC, Rutt BK. Polyvinyl alcohol cryogel: An ideal phantom material for MR studies of arterial flow and elasticity. Magnetic Resonance in Medicine. 1997;37:314-9.

[20] Leitão A, Silva J, Dourado F, Gama M. Production and Characterization of a New Bacterial Cellulose/Poly(Vinyl Alcohol) Nanocomposite. Materials. 2013;6:1956-66.

[21] Motlagh D, Yang J, Lui KY, Webb AR, Ameer GA. Hemocompatibility evaluation of poly(glycerol-sebacate) in vitro for vascular tissue engineering. Biomaterials. 2006;27:4315-24.

[22] Sperling C, Fischer M, Maitz MF, Werner C. Blood coagulation on biomaterials requires the combination of distinct activation processes. Biomaterials. 2009;30:4447-56.

[23] Gupta S, Reviakine I. Platelet activation profiles on TiO2: effect of Ca^{2+} binding to the surface. Biointerphases. 2012;7:28.

[24] Andrade FK, Silva JP, Carvalho M, Castanheira EM, Soares R, Gama M. Studies on the hemocompatibility of bacterial cellulose. Journal of biomedical materials research Part A. 2011;98:554-66.

[25] Beal CB, Nguyen TT, Stewart DL. A method of determining the clotting time of blood and particulate reagents therefor. Google Patents; 1985.

[26] Vroman L. The life of an artificial device in contact with blood: initial events and their effect on its final state. Bulletin of the New York Academy of Medicine. 1988;64:352-7.

[27] Zhuo R, Siedlecki CA, Vogler EA. Autoactivation of blood factor XII at hydrophilic and hydrophobic surfaces. Biomaterials. 2006;27:4325-32.

[28] Chen X, Wang J, Paszti Z, Wang F, Schrauben JN, Tarabara VV, et al. Ordered adsorption of coagulation factor XII on negatively charged polymer surfaces probed by sum frequency generation vibrational spectroscopy. Analytical and bioanalytical chemistry. 2007;388:65-72.

[29] Fink H, Hong J, Drotz K, Risberg B, Sanchez J, Sellborn A. An in vitro study of blood compatibility of vascular grafts made of bacterial cellulose in comparison with conventionally-used graft materials. Journal of biomedical materials research Part A. 2011.

[30] Park JH, Bae YH. Hydrogels based on poly(ethylene oxide) and poly(tetramethylene oxide) or poly(dimethyl siloxane): synthesis, characterization, in vitro protein adsorption and platelet adhesion. Biomaterials. 2002;23:1797-808.

[31] Fink H, Faxalv L, Molnar GF, Drotz K, Risberg B, Lindahl TL, et al. Real-time measurements of coagulation on bacterial cellulose and conventional vascular graft materials. Acta Biomater. 2010;6:1125-30.

[32] JIN Gu, Qi-zhi Y, Li-quan D, Feng M. PEG-grafted PVA Membrane and Its Blood Compatibility. CHEMICAL RESEARCH IN CHINESE UNIVERSITIES. 2011;27:1078-82.

[33] Jennings LK. Mechanisms of platelet activation: need for new strategies to protect against platelet-mediated atherothrombosis. Thrombosis and haemostasis. 2009;102:248-57.

[34] Gemmell CH. Activation of platelets by in vitro whole blood contact with materials: increases in microparticle, procoagulant activity, and soluble P-selectin blood levels. Journal of biomaterials science Polymer edition. 2001;12:933-43.

[35] Wang S, Gupta AS, Sagnella S, Barendt PM, Kottke-Marchant K, Marchant RE. Biomimetic fluorocarbon surfactant polymers reduce platelet adhesion on PTFE/ePTFE surfaces. Journal of biomaterials science Polymer edition. 2009;20:619-35.

[36] He Q, Gong K, Ao Q, Ma T, Yan Y, Gong Y, et al. Positive charge of chitosan retards blood coagulation on chitosan films. Journal of biomaterials applications. 2013;27:1032-45.

[37] Ratner BD, Bryant SJ. Biomaterials: where we have been and where we are going. Annual review of biomedical engineering. 2004;6:41-75.

[38] Ratner BD. Blood compatibility--a perspective. Journal of biomaterials science Polymer edition. 2000;11:1107-19.

[39] Ratner BD. The catastrophe revisited: blood compatibility in the 21st Century. Biomaterials. 2007;28:5144-7.

[40] Shattil S, Cunningham M, Hoxie J. Detection of activated platelets in whole blood using activation- dependent monoclonal antibodies and flow cytometry1987.

[41] Shattil SJ, Hoxie JA, Cunningham M, Brass LF. Changes in the platelet membrane glycoprotein IIb.IIIa complex during platelet activation. The Journal of biological chemistry. 1985;260:11107-14.

[42] Gerke V, Moss SE. Annexins: from structure to function. Physiological reviews. 2002;82:331-71.

[43] Goodman SL, Cooper SL, Albrecht RM. Integrin receptors and platelet adhesion to synthetic surfaces. J Biomed Mater Res. 1993;27:683-95.

[44] Smith BS, Yoriya S, Grissom L, Grimes CA, Popat KC. Hemocompatibility of titania nanotube arrays. Journal of biomedical materials research Part A. 2010;95:350-60.

[45] Aldenhoff YB, Koole LH. Platelet adhesion studies on dipyridamole coated polyurethane surfaces. European cells & materials. 2003;5:61-7; discussion 7.

[46] Nurdin N, Francois P, Mugnier Y, Krumeich J, Moret M, Aronsson BO, et al. Haemocompatibility evaluation of DLC- and SiC-coated surfaces. European cells & materials. 2003;5:17-26; discussion -8.

[47] Munnix IC, Kuijpers MJ, Auger J, Thomassen CM, Panizzi P, van Zandvoort MA, et al. Segregation of platelet aggregatory and procoagulant microdomains in thrombus formation: regulation by transient integrin activation. Arterioscler Thromb Vasc Biol. 2007;27:2484-90.

[48] Heemskerk JW, Mattheij NJ, Cosemans JM. Platelet-based coagulation: different populations, different functions. Journal of thrombosis and haemostasis : JTH. 2013;11:2-16.

[49] Ekdahl KN, Nilsson B, Gölander CG, Elwing H, Lassen B, Nilsson UR. Complement Activation on Radio Frequency Plasma Modified Polystyrene Surfaces. Journal of Colloid and Interface Science. 1993;158:121-8.

Chapter 3

Production and Characterization of a New Bacterial Cellulose/Poly(Vinyl Alcohol) Nanocomposite

Bacterial cellulose (BC) is characterized for its high water holding capacity, high crystallinity, an ultrafine fiber network and high tensile strength. This work demonstrates the production of a new interpenetrated polymer network nanocomposite obtained through the incorporation of poly(vinyl alcohol) (PVA) on the BC matrix and evaluates the effect of oven drying on the morphological, mechanical and mass transfer properties of the composite membranes. Both the addition of PVA and oven drying induce the appearance of larger pores (circa 1–3μm in average diameter) in dried BC/PVA membranes. Both types of treatments also affect the permeability of the composite, as assessed by the diffusion coefficients of polyethylene glycol (PEG) molecules (900, 8,000, 35,000 and 100,000Da) across the membranes. Finally, the Young's modulus of dry pristine BC decreases following PVA incorporation, resulting in a change from 3.5GPa to 1GPa and a five-fold loss in tensile strength.

Introduction

Bacterial cellulose (BC) is produced mainly by *Gluconacetobacter* strains as a hydrated membrane or pellicle at the air-medium interface and represents a promising biomaterial that has been the subject of intensive research and development. It is formed by repeated dimers of β-1,4 linked D-glucose units and reveals unique properties, including high water holding capacity, high crystallinity, an ultrafine fiber network, high tensile strength and a relatively simple, cost-efficient production [1, 2]. Moreover, its membrane morphology, along with its physicochemical properties, may be easily manipulated by controlling growth conditions (*in situ* modifications) and/or by chemical modifications (*ex situ* modifications) that allow the desired functionality [3].

For the past years, BC has gained interest in the field of tissue engineering, being studied by several research groups as a scaffold for cartilage [4, 5], wound dressing [6, 7], dental implants [8, 9], nerve regeneration [10] and vascular grafts [11-13]. The incorporation of living cells into the material is highly desirable; however, the limited porosity precludes proper tissue ingrowth.

Mass transfer limitations may have a major impact on cell growth and differentiation and even compromise the utility of the scaffold or its usage as a drug delivery device [14, 15]. Thus, it is important that a material, once implanted, allows the permeation of water, metabolic products and chemical signals in the aqueous physiological environment [16]. Mass transfer experiments previously conducted by Sokolnicki and colleagues [3], who aimed at determining the transport and interaction parameters of selected molecules through a hydrated BC system, indicated the presence of dual transport mechanisms, for solute transport through the continuous water phase and cellulose matrix, with some hindrance of molecular diffusion via fiber obstruction.

In addition to suitable mass transfer properties, the geometry of the material at the nano- and micro-scales has already been shown to affect cell behavior [17]. For example, the geometry of the microenvironment around osteoprogenitor cells has been shown to regulate the progress of osteoinduction in bone grafts and scaffolds [18]. Thus, the control of BC structure and porosity at the nano and microscales assumes great relevance for applications in which BC is used as a cell scaffold and has been a focus of research [17].

Poly(vinyl alcohol) (PVA) is a synthetic hydrophilic biocompatible homopolymer with desirable characteristics for biomedical applications, such as hemocompatibility and non-linear mechanical properties, both in tension and compression and viscoelastic behavior [19-21]. Additionally, it can be physically cross-linked by a low temperature thermal cycling process. This physical cross-linking has the advantage of not leaving residual amounts of any chemical cross-linking agent [22]. Moreover, its mechanical properties can be modified by regulating parameters, like the PVA concentration, the number of freeze/thaw cycles, thawing rate, the freezing holding time and freezing temperature [23]. The combination of PVA and BC has been previously proposed by Millon and Wan [23]; however, these authors used PVA as the matrix for their nanocomposite, adding BC fibers homogenates to the PVA solution. The PVA/BC suspension is then cast to a desired shape. It can then be fine-tuned to exhibit varying mechanical properties via the thermal cycle process [23].

Herein, we describe the PVA cross-linking on an intact BC membrane originating a double network where the PVA fibers fill the porous BC matrix. The composite obtained is therefore an interpenetrating polymer network. This composite has been reported before [24], but has remained relatively unstudied. The preparation method we adopted, in regards to impregnation of a BC hydrogel with a PVA solution, is similar to that one presented by Gea and colleagues [24]. However, our nanocomposite differs in terms of PVA concentration, impregnation time and the molecular size of the PVA used. In order to better understand the nanocomposite we are using, we have characterized the surface morphology, permeability, mass transfer and mechanical properties of the composite in this work. To our knowledge, this is the first study to present an interrelation between the morphology, mechanical properties and the permeability of a BC/PVA composite.

Experimental Section

Bacterial Cellulose and Bacterial Cellulose/Poly(Vinyl Alcohol)

Gluconacetobacter xylinus (ATCC 700178) was grown in a modified Hestrin-Schramm medium, supplemented with 2% Corn Steep Liquor and 0.6% ethanol, at pH 5.0. Inoculated Erlenmeyer flasks were then placed in an incubator, and the culture was

allowed to grow for 7 days, at 30°C, under static conditions. The resulting BC membranes were washed thoroughly with distilled water and further purified with 4% NaOH at 60°C for 90 min, after which they were again washed thoroughly with distilled water until the pH of the membranes was the same as that of distilled water. The membranes where then cut thinly into 2–3 mm thick membranes.

In order to produce the BC/PVA nanocomposite, the purified BC membranes were immersed in a 10% PVA solution (M_w = 30–50,000g/mol) for 24h at 80°C. The membranes were then frozen at −20 °C for 24 h, after which they were thawed at room temperature in distilled water and washed to remove any excess PVA from the membranes.

Dry BC and BC/PVA samples were obtained by thoroughly drying the samples in an incubator oven at 50°C for a minimum of 12h. The membranes obtained through this drying process suffer a significant loss in thickness as compared to the never dried membranes, while only slight variation in thickness was registered in the freeze-dried samples.

SEM Imaging

BC and BC/PVA samples were prepared in 2 ways: "dried" (*d*) at 50°C overnight, so as to remove all residual water, and then rehydrated before freeze-drying; or "never-dried" (*nd*), which were freeze-dried directly after production and then sputter-coated with a gold/palladium mixture. Each sample, whether dried first or maintained wet until freeze-drying, was initially 3mm thick. The sample's morphology was then observed with a Nova NanoSEM 200 Scanning Electron Microscope operating at 5kV (FEI Europe, Eindhoven, The Netherlands).

Stress-Strain Analysis

Dry BC and BC/PVA strips, with 5 × 1cm, were cut from a single sheet of each material and then analyzed using on a Shimadzu AG-X 50 kN at a traction speed of 5mm/min and

a load cell of 1kN. Each sheet was initially 1.5cm thick and then dried at 50°C overnight, so as to remove all the water. BC strips were on average 0.065 ± 0.005mm thick, whereas BC/PVA strips were on average 0.480 ± 0.050mm thick. Six replicates per sample material were tested in order to obtain a significant set of data. Special care was taken in order to attempt to prevent sample slipping from the hydraulic grips by using both fine grain sandpaper and construction paper.

Diffusion Assays

Diffusion assays were carried out using custom-built diffusion cells. Each cell consisted of a donor chamber and a receptor chamber separated by a membrane of either never-dried (*nd*) or dry (*d*) BC or BC/PVA with 9.61cm². Four different molecular mass polyethylene glycol (PEG) solutions were used in these assays: 900, 8000, 35,000 and 100,000Da at a concentration of 50mg/mL.

Each donor chamber was filled with 3.5mL of PEG solution and the receptor chamber with 3.5mL of distilled water. 100μL samples were taken at specific intervals to determine the retention time for each of the solutions. The refraction index of the samples was measured on a Knauer RI Detector K-2300 (Knauer) connected to Pharmacia LKB LCC-500 Plus FPLC (GE Healthcare Life Sciences) in order to obtain the diffusion profiles for each molecular weight PEG through n*d*BC, *d*BC, n*d*BC/PVA and *d*BC/PVA.

Membrane thickness (L) was determined with a standard outside micrometer at three different locations on each membrane and then averaged. The diffusion coefficients (D) were calculated by testing the retention time, estimated from the slope of the linear regressions in the diffusion curves (θ), before running into the balance state, according to the following equation:

$$D = L^2/6\theta$$

Reagents

All reagents used were acquired from Sigma-Aldrich Quimica, S.L. (Sintra, Portugal).

Results and Discussion

Morphology and Characterization of BC and BC/PVA Membranes

SEM imaging was used to reveal the morphological features of the BC and BC/PVA membranes. The three-dimensional structure of the BC hydrogel is well documented as a fibrous, porous network of un-oriented nanofibers [5, 25, 26]. The membranes were freeze-dried so that the three-dimensional morphology would be preserved as in a hydrated state, before and after an initial drying step. The scanning electron micrographs obtained (Figure 3-1) show the fibrous morphology of the network. All samples presented similar morphological characteristics in terms of the fiber thickness, randomness of fiber distribution and three-dimensional orientation.

The main and most noticeable differences have to do with the relative dimension and overall number of pores, which is associated with the preparation method and composition of the membrane. The incorporation of PVA (Figure 3-1B) is clearly noticeable in the composite membranes, although, other than some fibers that project from the membrane surface, the BC and PVA fibers where rather similar, slightly varying in thickness. It was possible to distinguish, to some degree, the PVA from BC fibers in two ways: BC fibers degraded slightly quicker under the electron beam of the SEM than PVA and, also, some from PVA fibers that project and loop from the surface of the BC membrane. These are PVA fibers that formed on top of the BC surface.

Previous work had shown that the BC/PVA nanocomposite was made up of interpenetrated fibers [24]. The molecular size and concentration of PVA used does not allow for a PVA hydrogel to form; therefore, rather than a PVA matrix embedding the BC fibers, we have found, as expected, PVA fiber wells integrated into the original BC hydrogel forming an interpenetrated network. The PVA fibers inside the BC membrane randomly bridge individual BC fibers, rising the overall density of the hydrogels. Comparison between the morphology of never-dried (*nd*) (Figure 3-1A, B) and dried (*d*) (Figure 3-1C, D) membranes showed clear and marked structural differences. Once BC membranes are dried, the overall thickness of the membranes greatly decreases, resulting in a higher fiber density and, consequently, a much less porous membrane, as
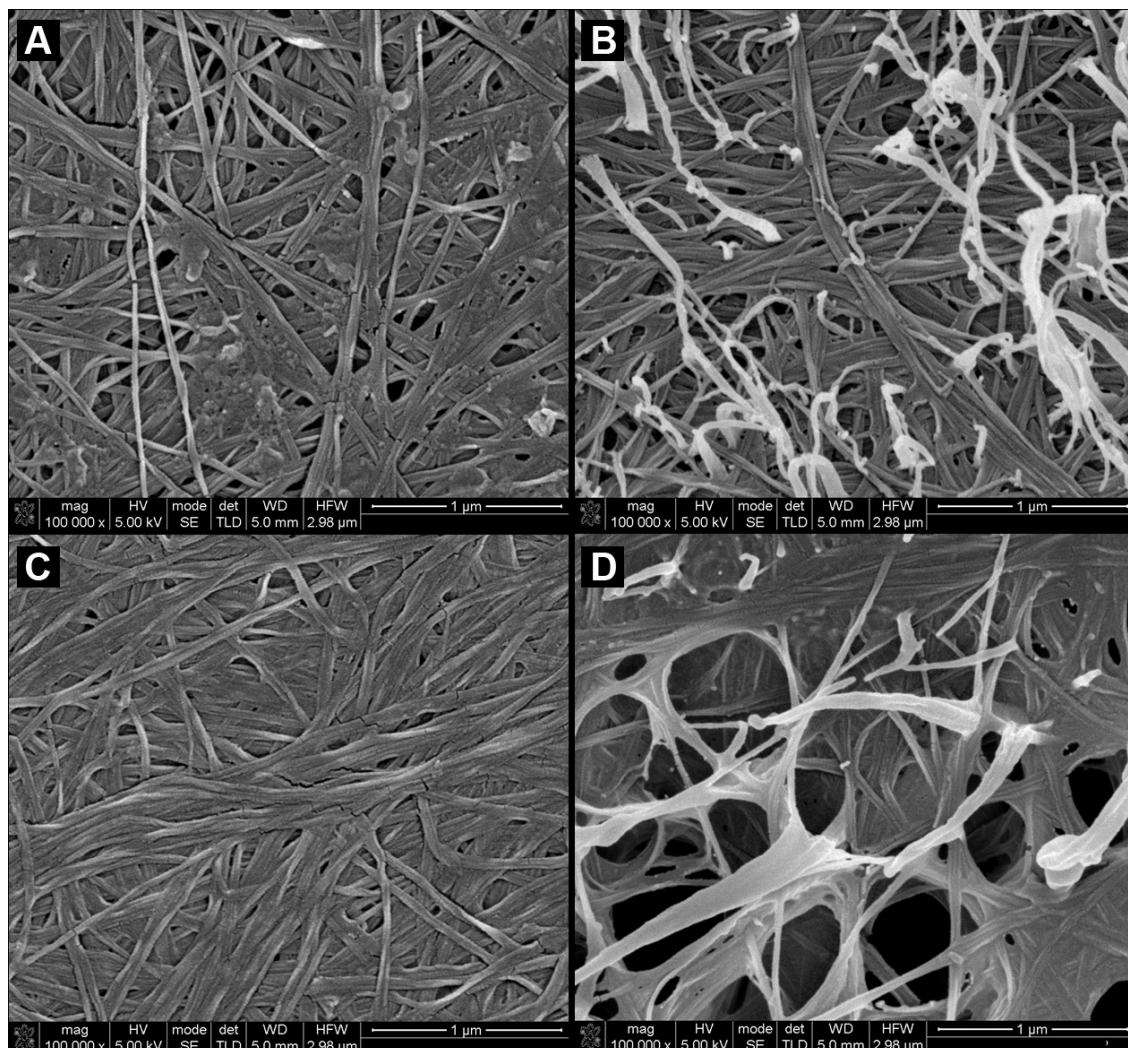
Figure 3-1 - SEM micrographs of (A) never-dried bacterial cellulose (BC); (B) never-dried BC/poly(vinyl alcohol) (PVA); (C) dried BC; and (D) BC/PVA at 100,000× magnification.

can be observed in Figure 3-1C, when compared to the *nd*BC membrane (Figure 3-1A). The most remarkable structural difference is observed in the morphology of the *d*BC/PVA membranes (Figures 3-1D and 3-2). In this case, there are two very clearly distinct regions comprised of different fiber structures. A large portion of the membrane contained large pores ranging from 500nm to 2μm in diameter (in *nd*BC, the largest measurable pores were 120nm in diameter) that are separated by very densely compacted regions with no discernible pore structures (Figure 3-2). PVA was largely present in the porous regions, with BC making up much of the denser regions. It should be noted, however, that both BC and PVA fibers could be observed across the entirety of the membrane.
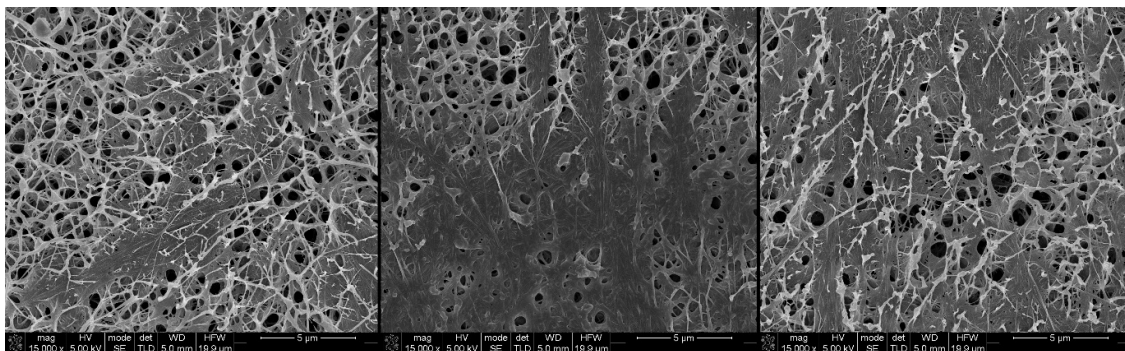
Figure 3-2 - Three SEM micrographs of the same dry BC/PVA membrane at 15,000× magnification with two very distinct regions of densely compacted fibers and regions with large pores.

The porous and densely compacted regions of the dried BC/PVA membranes (Figure 3-2) are due to the presence of PVA. When BC dries, the fibers collapse onto each other and, due to the lack of elasticity, should maintain their overall relative position. When PVA fibers dry or are heated, they contract [27]. As the PVA fibers contract inside the BC network and due to a non-uniform integration of PVA that is associated with the heterogeneity of the BC network, regions with a higher BC fiber density bundle together. The remaining spaces, where the overall number of BC fibers was lower, are bridged by PVA and a few random BC fibers originating in the porous regions.

Mechanical Characterization of Dry BC and Dry BC/PVA Membranes

BC is known for its high tensile strength, with a Young's modulus' ranging from 1MPa to 114GPa [24, 28-31], varying according to the membrane's density, dimensions, treatment and preparation methods. Generally, BC is regarded as lacking elastic properties, since hydrogen bonds formed between individual BC strands contribute to the stiffness of the hydrogel. PVA, on the other hand, is known for its elasticity and relatively low tensile strength [24]. As found by Gea and colleagues [24], the impregnation of PVA into the BC network affects the tensile strength of the nanocomposite. This occurs by steric hindrance, where the overall number of hydrogen bonds formed between individual BC fibers during the drying process lowers, due to the presence of PVA [31, 32].

Our findings are in accordance with this theory. *d*BC resisted better to tensile stress deforming, slightly before abruptly rupturing along the midriff of the strips, with no

discernible tearing prior rupture, at a tensile strength of 1.306 ± 0.297GPa. Whereas, *d*BC/PVA under lower tensile stress started to gradually rip, and so, consequently, tensile strength was nearly five-times lower, 0.271 ± 0.036GPa. The effect of PVA addition on the Young's modulus is also noticeable. The Young's modulus for *d*BC and *d*BC/PVA was, respectively, 3.5 ± 0.5GPa and 1 ± 0.3GPa (Figure 3-3).

SEM micrographs also present a supporting explanation for the loss in tensile strength. The uneven distribution of PVA across the nanocomposite contributes to the reduction in overall mechanical performance, due to the heterogeneity of the *d*BC/PVA membrane. The *d*BC/PVA membrane presents regions with large pores, which, as mentioned previously, have a lower fiber density, a large portion of which is PVA. The end results of the combination of large pores and high PVA content is that, ultimately, these are mechanically weaker than the surrounding, denser, regions. Therefore the membranes would rupture more easily across these areas. This also explains why the *d*BC/PVA rather than rupturing abruptly, as with *d*BC, tended to rip. The force applied would cause stress failure on the weaker regions, and the uneven impregnation of the BC hydrogel with PVA negatively affected the tensile strength and the Young's modulus of the nanocomposite. The same did not occur with the *d*BC membranes. In this case, the drying process does
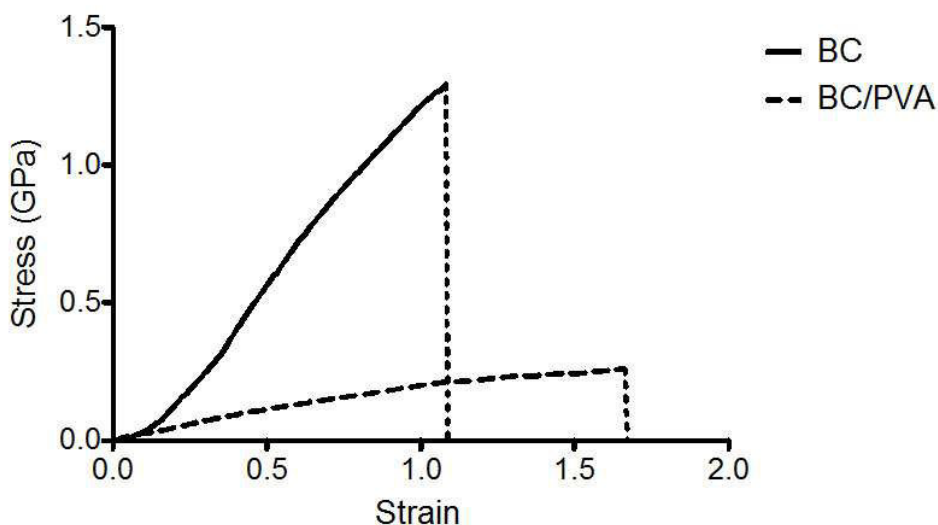
Figure 3-3 Stress-strain curves of dry strips of BC and BC/PVA. Each strip of 5 × 1 cm (length × width) was cut from a single sheet of material and measured multiple times (n = 6). The results here are the averaged curves obtained up to the rupture point.

not result in higher surface heterogeneity and/or pore distribution. The *d*BC membranes

present a uniform and non-oriented distribution of fibers (Figure 3-1C), which has the end-result of a greater tensile strength and Young's modulus.

Diffusion Assays

Solute transport has been classified according to two mechanisms: the pore and the partition (or sorption) mechanisms [33, 34]. The former states that solutes diffuse through micro-channels in the membrane; as for the partition mechanism, the solute dissolves or is adsorbed onto the membrane itself and diffuses through or along fibers. As described above, the BC and BC/PVA hydrogels are more porous in nature, forming a series of channels that would allow for solute diffusion across the membrane via the pore mechanism.

As to test the effect of the structural and morphological changes incurred by the drying process on the mass transfer properties, the diffusion across the never-dried (*nd*) and dry (*d*) states of the materials was tested using PEG probes and the diffusion coefficients determined using the time-retention method. It would be expected that the denser the membrane (as is the case with the dry membranes), the harder it would be for solutes to diffuse across the membrane, since the overall interconnection of pores and channels in the membrane would be much lower [35]. Additionally, molecule size would also effect diffusion across the membranes, given the low diffusion coefficient in the liquid phase and also because molecule collision with the fibers would increase with molecule size.

The higher the value for the diffusion coefficient, the more permeable the membrane is and the easier solutes pass through the membrane matrix. Our results show that in both the case of BC and BC/PVA, solute diffusion across the never-dried membranes is easier than in the dried membranes (Table 3 - 1). The *nd*BC membranes presented the highest diffusion coefficient values and, so, were the most permeable of the membranes with *nd*BC/PVA second, followed by *d*BC/PVA and, finally, *d*BC.

These results can mostly be explained due to the fiber density of the materials. A less dense material will have less fibers in the transport path [3]. *nd*BC was therefore expected to be the most permeable of the membranes. Similarly, the second least dense

Table 3-1 - Diffusion coefficients of four different M_w polyethylene glycol (PEG) in BC and BC/PVA samples.

PEG M_w	Diffusion Coefficient (cm²/sec)			
(Da)	*nd*BC	*d*BC	*nd*BC/PVA	*d*BC/PVA
900	7.40×10^{-5}	1.12×10^{-7}	4.48×10^{-5}	1.16×10^{-5}
8000	2.71×10^{-5}	1.79×10^{-8}	1.28×10^{-5}	1.88×10^{-6}
35000	2.27×10^{-5}	1.53×10^{-8}	1.10×10^{-5}	1.68×10^{-6}
100000	1.95×10^{-5}	1.41×10^{-8}	9.82×10^{-6}	1.50×10^{-6}

hydrogel was the *nd*BC/PVA nanocomposite that, despite the formation and entanglement of PVA nanofibers in the BC network (thus, adding to the overall number of fibers), still allows for a porous structure similar to that of *nd*BC. The two denser materials would be the dry membranes, due to the aforementioned collapse of fibers onto each other, thus blocking and reducing in number the pathways available for solute diffusion. However, in the case of the theoretically densest sample, *d*BC/PVA, the diffusion coefficient values present as the third least permeable material. As revealed by the SEM imaging (Figure 3-2), the two very distinct regions observed are the reason for this occurrence. While, in all the other cases, the pores, regardless of their number, distribution and size, are distributed randomly across the entirety of the 3D-structure of the membrane. Contrarily, on the *d*BC/PVA, there are very compact regions and others with very large pores. Solute diffusion is facilitated across these extremely porous regions, but hindered in the densely compacted regions. Apparently, the balance between densely compacted and porous regions must slightly tend towards the latter, due to the delay in retention time and, consequently, reduction of the diffusion coefficient.

Our results are similar to the findings of Sokolnicki [3], which tested the diffusion of dextran molecules and showed that molecular size has little effect on diffusion. Higher molecule size dictates collisions with the hydrogel fibers, temporary immobilization and/or possible rerouting around narrowed passages, according to each. The larger the molecule, the likelier it is for these interactions to occur, resulting in a delay in diffusion times. The overall number of pores and pathways across the materials, due to overall fiber number and density, seems to be the main factor responsible for a slower diffusion. This means that diffusion in these membranes is mainly governed by the pore mechanism.

Conclusions

Previous researchers had shown that a BC hydrogel impregnated with PVA had some potential in biomedicine, namely in cardiovascular applications. The work we present here shows the mechanical, permeability and morphology changes incurred by both incorporation of PVA, in a different concentration and molecular size than previously proposed, and the effect of drying the materials.

Both *nd*BC and *nd*BC/PVA are similar in terms of morphology of the hydrogels and fiber distribution, with an increase in overall fiber number in BC/PVA. When dried, the morphology of both materials change, BC fibers collapse, forming a denser membrane, which leads to a decrease in the permeability. Dry BC/PVA membranes suffer dramatic changes in terms of morphology, creating two distinct regions: densely compacted regions leaving other regions mostly consisting of PVA fibers with large pores. The dual nature of the dried BC/PVA membrane affects both the permeability and mechanical behavior of the material. The tensile strength of BC decreases, due to the presence of PVA impeding the interactions of BC fibers and creating large porous regions that are easier to rupture. Potentially, these large pores could serve in aiding cell migration into the material and nutrient diffusion across the membrane. Therefore, we here show that by promoting physical changes and/or altering the composition of a BC hydrogel, it is possible to alter its morphology, mechanical characteristics and permeability.

References

[1] Klemm D, Schumann D, Kramer F, Heßler N, Koth D, Sultanova B. Nanocellulose Materials – Different Cellulose, Different Functionality. Macromolecular Symposia. 2009;280:60-71.

[2] Czaja WK, Young DJ, Kawecki M, Brown RM, Jr. The future prospects of microbial cellulose in biomedical applications. Biomacromolecules. 2007;8:1-12.

[3] Sokolnicki AM, Fisher RJ, Harrah TP, Kaplan DL. Permeability of bacterial cellulose membranes. Journal of Membrane Science. 2006;272:15-27.

[4] Andersson J, Stenhamre H, Backdahl H, Gatenholm P. Behavior of human chondrocytes in engineered porous bacterial cellulose scaffolds. Journal of biomedical materials research Part A. 2010;94:1124-32.

[5] Svensson A, Nicklasson E, Harrah T, Panilaitis B, Kaplan DL, Brittberg M, et al. Bacterial cellulose as a potential scaffold for tissue engineering of cartilage. Biomaterials. 2005;26:419-31.

[6] Alvarez O, Patel M, Booker J, Markowitz L. Original Research Effectiveness of a Biocellulose Wound Dressing for the Treatment of Chronic Venous Leg Ulcers: Results of a Single Center Randomized Study Involving 24 Patients. Wounds. 2004;16:224-33.

[7] Luan J, Wu J, Zheng Y, Song W, Wang G, Guo J, et al. Impregnation of silver sulfadiazine into bacterial cellulose for antimicrobial and biocompatible wound dressing. Biomedical Materials. 2012;7:065006.

[8] Novaes Jr AB, Novaes AB. Bone formation over a TiAl6V4(IMZ) implant placed into an extraction socket in association with membrane therapy (Gengiflex). Clinical Oral Implants Research. 1993;4:106-10.

[9] dos Anjos B, Novaes AB, Jr., Meffert R, Barboza EP. Clinical comparison of cellulose and expanded polytetrafluoroethylene membranes in the treatment of class II furcations in mandibular molars with 6-month re-entry. J Periodontol. 1998;69:454-9.

[10] Klemm D, Heublein B, Fink H-P, Bohn A. Cellulose: Fascinating Biopolymer and Sustainable Raw Material. Angewandte Chemie International Edition. 2005;44:3358-93.

[11] Klemm D, Schumann D, Udhardt U, Marsch S. Bacterial synthesized cellulose — artificial blood vessels for microsurgery. Progress in Polymer Science. 2001;26:1561-603.

[12] Andrade FK, Costa R, Domingues L, Soares R, Gama M. Improving bacterial cellulose for blood vessel replacement: Functionalization with a chimeric protein containing a cellulose-binding module and an adhesion peptide. Acta Biomater. 2010;6:4034-41.

[13] Bäckdahl H, Risberg B, Gatenholm P. Observations on bacterial cellulose tube formation for application as vascular graft. Materials Science and Engineering: C. 2011;31:14-21.

[14] Grasso D, Strevett K, Fisher R. Uncoupling mass transfer limitations of gaseous substrates in microbial systems. The Chemical Engineering Journal and the Biochemical Engineering Journal. 1995;59:195-204.

[15] Serafica G, Mormino R, Bungay H. Inclusion of solid particles in bacterial cellulose. Applied Microbiology and Biotechnology. 2002;58:756-60.

[16] Hutchens SA, Benson RS, Evans BR, O'Neill HM, Rawn CJ. Biomimetic synthesis of calcium-deficient hydroxyapatite in a natural hydrogel. Biomaterials. 2006;27:4661-70.

[17] Petersen N, Gatenholm P. Bacterial cellulose-based materials and medical devices: current state and perspectives. Applied Microbiology and Biotechnology. 2011;91:1277-86.

[18] Habibovic P, Yuan H, van der Valk CM, Meijer G, van Blitterswijk CA, de Groot K. 3D microenvironment as essential element for osteoinduction by biomaterials. Biomaterials. 2005;26:3565-75.

[19] Bodugoz-Senturk H, Macias CE, Kung JH, Muratoglu OK. Poly(vinyl alcohol)-acrylamide hydrogels as load-bearing cartilage substitute. Biomaterials. 2009;30:589-96.

[20] Paradossi G, Cavalieri F, Chiessi E, Spagnoli C, Cowman MK. Poly(vinyl alcohol) as versatile biomaterial for potential biomedical applications. J Mater Sci Mater Med. 2003;14:687-91.

[21] Hwang MR, Kim JO, Lee JH, Kim YI, Kim JH, Chang SW, et al. Gentamicin-loaded wound dressing with polyvinyl alcohol/dextran hydrogel: gel characterization and in vivo healing evaluation. AAPS PharmSciTech. 2010;11:1092-103.

[22] Hassan C, Peppas N. Structure and Applications of Poly(vinyl alcohol) Hydrogels Produced by Conventional Crosslinking or by Freezing/Thawing Methods. Biopolymers · PVA Hydrogels, Anionic Polymerisation Nanocomposites: Springer Berlin Heidelberg; 2000. p. 37-65.

[23] Millon LE, Guhados G, Wan W. Anisotropic polyvinyl alcohol-Bacterial cellulose nanocomposite for biomedical applications. J Biomed Mater Res B Appl Biomater. 2008;86:444-52.

[24] Gea S, Bilotti E, Reynolds CT, Soykeabkaew N, Peijs T. Bacterial cellulose–poly(vinyl alcohol) nanocomposites prepared by an in-situ process. Materials Letters. 2010;64:901-4.

[25] Iguchi M, Yamanaka S, Budhiono A. Bacterial cellulose—a masterpiece of nature's arts. Journal of Materials Science. 2000;35:261-70.

[26] Nakagaito AN, Iwamoto S, Yano H. Bacterial cellulose: the ultimate nano-scalar cellulose morphology for the production of high-strength composites. Applied Physics A. 2005;80:93-7.

[27] Kudo S, Otsuka E, Suzuki A. Swelling behavior of chemically crosslinked PVA gels in mixed solvents. Journal of Polymer Science Part B: Polymer Physics. 2010;48:1978-86.

[28] George J, Ramana KV, Sabapathy SN, Bawa AS. Physico-Mechanical Properties of Chemically Treated Bacterial (Acetobacter xylinum) Cellulose Membrane. World Journal of Microbiology and Biotechnology. 2005;21:1323-7.

[29] Bodin A, Concaro S, Brittberg M, Gatenholm P. Bacterial cellulose as a potential meniscus implant. J Tissue Eng Regen Med. 2007;1:406-8.

[30] Tanpichai S, Quero F, Nogi M, Yano H, Young RJ, Lindström T, et al. Effective Young's Modulus of Bacterial and Microfibrillated Cellulose Fibrils in Fibrous Networks. Biomacromolecules. 2012;13:1340-9.

[31] Yamanaka S, Watanabe K, Kitamura N, Iguchi M, Mitsuhashi S, Nishi Y, et al. The structure and mechanical properties of sheets prepared from bacterial cellulose. Journal of Materials Science. 1989;24:3141-5.

[32] Soykeabkaew N, Sian C, Gea S, Nishino T, Peijs T. All-cellulose nanocomposites by surface selective dissolution of bacterial cellulose. Cellulose. 2009;16:435-44.

[33] Yasuda H, Lamaze CE, Peterlin A. Diffusive and hydraulic permeabilities of water in water-swollen polymer membranes. Journal of Polymer Science Part A-2: Polymer Physics. 1971;9:1117-31.

[34] Fisher RJ. Diffusion with immobilization in membranes: transport and failure mechanisms. Prog Clin Biol Res. 1989;292:129-51.

[35] Fang Y-E, Cheng Q, Lu X-B. Kinetics of in vitro drug release from chitosan/gelatin hybrid membranes. Journal of Applied Polymer Science. 1998;68:1751-8.

Chapter 4

A Novel Small-Caliber Bacterial Cellulose Vascular Prosthesis: Production, Characterization and Preliminary In vivo Testing

Vascular grafts are used to replace, bypass or maintain function of damaged, occluded or diseased blood vessels. Towards that end several polymers, of both synthetic and natural origin, have been studied as small caliber vascular graft alternatives. Bacterial cellulose (BC) is among one of those polymers, being studied as an off-the-shelf and ready to use vascular graft. Herein, we present a novel, facile and cost-effective method for the production of small caliber BC grafts with minimal processing or the requirement for complex bioreactor systems. The unique morphology of the graft wall translated into tensile strength above that of a native vessel while providing similar values of compliance, out-performing commercial alternatives in this regard. As an additional result of the production method the luminal surface of the graft presents similar topography to that of native vessels. We have also studied the in vivo behavior of these BC graft in a pig model in order to further demonstrate their viability. In these preliminary studies, 1 month patency was achieved, with the presence of neo-vessels and endothelial cells on the luminal surface of the graft; with no evident signs of a foreign body response or fibrosis.

Introduction

Data from the World Health Organization (WHO) suggests that the number of people that suffer from cardiovascular diseases (CVDs) will increase from 17.3, in 2008, to 23.3 million by 2030. In vascular surgery, surgical bypass is fundamental in the treatment of some diseases. Vascular grafts replace, bypass or maintain function of damaged, occluded or diseased blood vessels. The chosen conduit and its success depend on several factors such as availability, size, ease of handling and technical facility, thrombogenicity, resistance to infection and dilation, durability, long-term patency and price.

The most common, and generally considered ideal grafts, are autografts, i.e., vessels collected from the patient. There are generally two major downsides to the use of autografts. The first is the need for prior surgical interventions, before the actual bypass surgeries, in order to collect the autologous vessel. Along with this, the actual availability of these vessels may be limited, due to prior interventions. Secondly, these grafts are subject to the natural progression of the patient's disease which can lead to deterioration, over time, of the biological grafts [1] and so synthetic grafts have been used for potential application as cardiovascular grafts.

Polyethylene terephthalate (PET or Dacron) and expanded polytetrafluoroethylene (ePTFE) grafts are the gold standard, at the moment, for synthetic grafts in large and medium diameter (>6 mm) vessels. However, these synthetic alternatives are not yet the ideal solution. While demonstrating acceptable results in larger diameter grafts, as internal diameter decreases so does its long-term patency [2, 3]. These grafts ultimately fail under 6mm in diameter, due to surface adsorption of proteins to the luminal and consequent activation of platelet activity resulting in clot formation and subsequent thrombosis [4, 5].

A large amount of work has therefore been aimed at finding alternative solutions to these materials through either natural or synthetic polymer materials [6-8]. The field is ever growing and the lack of a clear optimal polymer has led, and continues to lead, to many potential options. By either, further development and research into the already existing grafts (PET and ePTFE) or the creation of new non-degradable grafts of polyurethane, polyvinyl alcohol or bacterial cellulose (BC). Another option is researching and developing temporary grafts that ultimately allow for a tissue engineered solution, either by prior cell-seeding or allowing for native cell migration, attachment and ingrowth. Ultimately these

tissue engineered grafts would end up producing a new vessel out of native tissue from a scaffold of collagen, fibrin, elastin, silk and polycaprolactone [9-12].

One promising candidate is BC. This polymer is a highly pure linear polysaccharide, consisting of β (1→4)–linked D-glucose monomers. It is secreted by bacteria of the Gluconacetobacter genus. Once secreted, it forms a fibrous network hydrogel that has been extensively studied for biomedical applications due to its morphology, high purity, water-holding capacity, tensile strength, malleability and biocompatibility [13-15] and has been proposed for applications such as wound dressings [16], artificial skin[17] or blood vessels [18-20] and as a scaffold for tissue engineering [15, 21, 22]. The hemocompatibility of BC has been comprehensively studied in our group, with rather promising results (19).

Many methods have been proposed and patented [23-30] for the production of BC tubular grafts. Generally, the methods employed take advantage of the way the BC hydrogel is produced at air-medium interfaces [14, 31]. However, these production methods require dedicated bioreactors specifically designed for graft production. By using an oxygen permeable scaffold upon which BC is produced there are limits to the thickness and density of the BC structures because the oxygen rich environment produced by the likes of silicone tubing is limited to the immediate vicinity of that tube. Additionally, the oxygen permeable scaffold must allow oxygen to permeate consistently and homogenously throughout its surface. Otherwise the BC on the material surface will not be produced in a homogenously. Also, some cases develop interconnected sheets or layers of BC in the wall of the graft. These sheets can potentially delaminate under arterial pressure resulting in pockets of pooled blood and pressure build-up which results in the graft ballooning and bursting. This heterogeneity in the BC structure translates to varying mechanical properties along and across a single BC tube. Meeting these conditions for heterogeneity, along with the logistic costs of producing and maintaining a series of graft producing bioreactors, oxygen to inflate the permeable scaffold, the oxygen permeable scaffold per se with appropriate characteristics and the inevitable optimization processes involved have yet to produce a viable model for large scale BC graft production.

As mentioned, BC has several properties that make it a good prospect as a biomaterial for biomedical applications and has shown potential as an in vivo vascular grafts [14, 18, 20, 23]. It is already widely produced commercially in membranes or sheets with varying thicknesses and scale depending on the producer and method adopted for production. We

believe these methods for graft production, as presented to date, have an inherent inability to assure an economically viable and reproducible approach to the graft production. In this paper we present a novel approach to small caliber BC graft (<6mm) production that is both easily reproducible and provides a graft with adequate mechanical and biocompatible properties and, through in vivo experimentation, has already demonstrated promising patency.

Material and Methods

Graft Fabrication

Bacterial cellulose was produced by *Gluconacetobacter xylinus* (ATCC 53582) in a modified Hestrin-Schramm medium, supplemented with 2% Corn Steep Liquor (Sigma Aldrich, Germany) and 0.6 % ethanol, at pH 5.0. The resulting BC membranes were then washed in 4% (w/v) NaOH. The membranes were then thoroughly washed with distilled water until pH was neutral. Finally, endotoxin removal was accomplished by further washing in 5% SDS (w/v). The water and detergent solutions were changed after 24 hours over the course of 2 days.

Endotoxin removal was performed as follows: quadruplicate BC samples (1.5 x 2.5 x 4cm (height x width x length) were placed in 200ml of distilled water (control) and 5% SDS (w/v). The water and detergent solutions were changed after every 24 hours over the course of 3 days. At each exchange, duplicate BC samples were taken and washed abundantly with distilled water and freeze-dried. The samples were subsequently cut into samples of the same weight 20 ± 4mg and rehydrated with 500µl of apyrogenic water. The concentration of endotoxin in each sample determined using the Pierce LAL Chromogenic Endotoxin Quantitation Kit and the standard protocol included (Thermo Scientific, Rockford, IL USA). Additionally, a non-washed BC graft was implanted in a single in vivo assay (as described ahead) and compared to the subsequent in vivo assays performed with the SDS washed BC grafts.

BC grafts were prepared by cutting large BC sheets (1.5x25x30cm) into 1.5 x 2.5 x 7cm (height x width x length) blocks. These were perforated along the center of the sample with a sharp 4mm (outer diameter) metallic needle and then dried by mass transfer of water from

the hydrogel to blotting paper until a final wall thickness of roughly 2mm was achieved. The resulting tubular structures were then freeze-dried and stored at room temperature until needed (see Figure 4-1). All grafts tested herein have a luminal caliber of 4mm and independently of the final length used in the varying assays were initially 7cm long. The BC grafts used for in vivo experimentation were rehydrated in sterile 0.9% (w/v) saline solution and autoclaved at 121ºC for 20 min 72 hours before surgery.

Surface Profilometry

BC grafts, created as previously described, were split open longitudinally and fixed with double-sided tape to glass slides. PFA, commercial ePTFE and Dacron grafts were also split longitudinally and affixed the same way (Dacron grafts were stretched as much as possible in order to remove the kinking inherent to the graft). The sample surface profiles were then measured 5 times along the same surface (each measurement roughly 1mm apart) with a KLC TENCOR D-100 profilometer along 20mm (for Porcine Femoral Artery, ePTFE and PET) and 30mm for BC at set speed of 0.2mm/second and a resolution of 2000 points per mm. The results were then plotted on a 3D graph so to convey an idea of the 3 dimensional surface of the each sample. Roughness was calculated as the amplitude between maximum peak height and minimum valley depth.

Cryo-SEM Imaging

Cross sections of the BC grafts were imaged via Cryo-SEM on a JEOL JSM 6301F/ Oxford INCA Energy 350/ Gatan Alto 2500. The graft samples were prepared as described above and then cut into 1mm wide sections and placed upright in a metallic support. The samples were then rapidly cooled by plunging them into sub-cooled nitrogen (slush nitrogen) and transferred under vacuum to the cold stage of the preparation chamber. The samples were then fractured, sublimated for 180 seconds at -90°C, and coated with Au/Pd by sputtering for 40 seconds. The samples were finally transferred into the SEM chamber and imaged at -150°C. Pore size was estimated from the micrographs using Image J software.

Mechanical Tests

Tensile Strength Determination

BC grafts along with untreated BC (these are grafts that were not freeze-dried and as such did not finish the graft processing), ePTFE and porcine femoral artery (PFA) were tested for their tensile strength in quintuplicate (n=5) on a Shimadzu AG-X 50 kN at a traction speed of 5mm/min and a load cell of 1kN. Each sample tested was split open longitudinally and the materials thickness and width was measured with digital calipers and accounted for in the calculations of the strength parameters. Special care was taken in order to prevent sample slipping from the hydraulic grips by using both fine grain sandpaper and construction paper.

Suture Retention Assay

BC grafts with 6 cm length (4mm internal diameter and 7mm external diameter) were fixed the top clamp of a Z2.5 Zwick/Roell (Zwick GmbH & Co. KG; Ulm; Germany). A 4-0 Prolene® suture (0.15mm diameter; Ethicon) was placed approximately 7mm from the edge of the prosthesis (measured with a digital micrometer) and looped around the bottom clamp before clamping. The assay was then carried out in quintuplicate, on both freeze-dried and non-freeze-dried bacterial cellulose prosthetics, at a set speed of 10mm/min and a 1N pre-load.

Compliance Characterization

Compliance characterization of BC grafts (n=5) was performed using the system and method described previously by Diamantouros and colleagues [32]. Briefly, the grafts were fixed into a chamber and initially exposed to a steady flow of purified water. A pulse (1Hz) was added by a linear magnetic actuator. The pressures were stabilized at 80-120mmHg. Variations in the outer diameter were measured by an optical micrometer sensor (LS-7030(M); Keyence Deutschland GmbH, Neu-Isenburg, Germany) placed perpendicularly to the graft. Pressures were recorded by pressure transducers (CODAN pvd Critical Care GmbH; Forstinning,

Germany). The measurements were realized for 30 seconds once the pressures were stable. Variations in the outer diameter and pressures were recorded by a LabVIEW™ application (National Instruments; Texas, USA). The circumferential compliance was then calculated with the following equation:

$$C = \frac{(D_{Syst} - D_{Diast})/D_{Diast}}{P_{Syst} - P_{Diast}} \; x \; 100$$

Where C is compliance (%/mmHg), D is diameter (μm) and P is pressure (mmHg). "Syst" and "Diast" stand for the systolic and diastolic phase respectively.

A slight addition to the method presented by Diamantouros, consisting of the use of ultrasound imaging equipment (Vivid I, GE Healthcare; Freiburg, Germany), allowed for the acquisition of video of the changes in internal diameter in response to pressure variation. The videos were then converted to still frames and the diameter of the lumen determined with Image J software on three points per image. Care was taken so that the measurements from each video would be performed at the same coordinates in each individual frame so as to account, as much as possible, for human error.

In vivo Experimentation and Histological Analysis

Surgical procedure

Four female domestic pigs (*Sus scrofa domesticus*) with weight ranging from 30-40kgs were restrained from food (24 hours) and water (6 hours) before each surgical procedure. All experiments were conducted according to the European Union Directive no.86/609/CEE for the use of animals in research and approved by the board for the ethical treatment of animals of the Faculty of Medicine of the University of Porto (ORBEA, FMUP, Oporto, Portugal). All procedures were performed under general anesthesia, with endotracheal intubation and spontaneous ventilation. A pre-anesthesia intramuscular injection of 32mg/ml azaperone (Stressnil®, Esteve Veterinaria) at a dose of 4 mg/kg reconstituted with 1mg/ml midazolam (Dormicum®, Roche) at a dose of 0.15–0.2ml/kg was administered. Venous access was obtained through an IV line placed in the marginal ear vein. Anesthesia was induced with 3μg/kg fentanyl (Fentanest®, Janssen-Cilag), and sodium thiopental (12.5 mg/kg IV initially

and then to effect Tiopental 0,5 B Braun®, B. Braun). After orotracheal intubation, the 7- to 7.5-mm tube was connected to the anesthetic equipment (Ohmeda, Boc Health Care), and anesthesia was maintained with a mixture of isoflurane (1.5% to 2.5%; Isoflo®, Esteve Veterinaria) in 100% oxygen and fentanyl at constant-rate infusion of 30-50 µg/kg/h. Afterwards an epidural analgesia protocol was implemented with application of 1 mg/kg morphine (Morfina 1% Braun®, B. Braunl). To address infection prophylaxis, all animals received intramuscular injection of 1g ceftriaxone (Rocephin®, Roche) before surgery. End-tidal CO_2, oxygen saturation, electrocardiography and temperature were monitored continuously (Cygnus 1000C Vet® Monitor, Servive Portugal). Pigs were placed in supine position and shaved, and electrocardiographic electrodes were attached to the chest for continuous evaluation of cardiac electrical function. Normal saline (2 to 4 mL/kg hourly) was infused through the venous cannula in the auricular vein during surgery, to maintain adequate preload stability.

Open surgery was then performed with isolation of the common femoral artery, the profunda femoris artery and the superficial artery. The BC grafts were anastomosed in the left hind limb in a homolateral -femoral artery bypass. Papaverine was administered topically to the artery to avoid arterial spasm. The animals were heparinized systemically with an intravenous bolus injection of 200units/kg of heparin (Heparina Sódica B.Braun®, B.Braun), five minutes before clamping of the target arteries. BC grafts were then anastomosed with continuous suturewith 6/0 monofilament polypropylene sutures (Prolene®, Ethicon). The femoral artery from the right hind limb was sham-operated with all the surgical procedures being equally performed, excluding the implantation of the graft.

After the surgery, the pigs were transported back to their quarters, only when arterial oxygen tension stabilized above 95%. Pigs were monitored until their body temperature normalized (with digital thermometers) and they were able to ambulate. They then were observed at least 2 or 3 times daily for locomotor activity, respiratory changes, body temperature, and food and water intake. Analgesia was maintained during the first 24 h after surgery by using meloxicam (0.5 mg/kg IM; Metacam, Boehringer Ingelheim). Acetylsalicylic acid (150mg/animal per os daily; Ácido Acetilsalicílico ratiopharm 100 mg, Ratiopharm) was given once daily until euthanasia, to prevent platelet aggregation.

After the designated times, the animals were sacrificed by IV KCl injection after sedation with azaperone reconstituted with midazolam administered IM prior to induction with sodium

thiopental (12.5 mg/kg IV initially and then to effect) and the grafts and sham-operated arteries were harvested and histologically evaluated for signs of chronic inflammation, infection, foreign body responses, clot formation, cell ingrowth, and diameter via electron microscopy.

Histology

Tissues were preserved in formalin for a minimum of 4 days and were embedded in paraffin in an automated tissue processor (Microm STP 120). Tissues were then transferred to embedding workstation to obtain paraffin blocks. From these, sections (2µm) were cut on a rotary microtome (Leica RM 2035) and stained with Hematoxylin and Eosin (H&E) for light microscopic examination. Observations and photographs were made using an Olympus BX51 microscope with an Olympus camera attached.

Immunohistochemistry

Immunostaining of endothelial cells was performed using the primary antibody – Mouse Anti Pig CD31 (AbD Serotec; Oxford, England). This is a mouse monoclonal antibody designed to detect porcine CD31. The slides were immersed in 10mM sodium citrate (pH 6.0) buffer, and and heated in a water bath (95-99°C) for antigen retrieval. Antigen visualization was done with the Novocastra Novolink Polymer Detection System (Leica Microsystems GmbH, Wetzlar, Germany) and involved the following steps: Sections were incubated with H_2O_2 (3%) for 10min to eliminate endogenous peroxidase activity followed by a 5min incubation with a protein blocking agent. Sections were subsequently incubated overnight at 4°C with the primary antibody diluted at 1:100 with BSA (5%), and on the following day, washed in TBS-buffered saline solution before incubation for 30min with the secondary antibody system using diaminobenzidine (DAB) as a chromogen.

Statistical Data Analysis

All data and statistical analysis was performed using both GraphPad Prism and Origin Pro 9 software. Statistical significances were determined via One-way and Two-Way ANOVA tests after verifying the Normal distribution ($p<0.05$) of the data.

Results

Graft Fabrication

The novel methodology presented herein for production of the BC graft is schematically outlined in Figure 4-1. The BC grafts were produced with needles that were purposely built, regularly sharpened and exchanged in order to assure consistent perforation. Special care was taken during perforation in order assure a smooth luminal channel. An unsharpened needle resulted in tears during the perforation with the appearance of "flaps" that could occlude or restrict flow through the graft. Also, while all grafts produced and presented in this work were 4mm in diameter we found that by using different diameter needles allows the production of grafts with different diameters.

The drying and shaping was performed with the needle in place with special care to avoid changes to the luminal diameter of the graft and an irregular topography of the external surface. Also, the grafts were found to dry quickly during the freeze-drying process (a maximum of 2 days is required for complete drying) and the least irregular grafts were obtained the quicker this process was performed.

Figure 4-1 - Schematic representation BC vascular graft formation process. From left to right: the BC perforated with a sharp metallic needle, dried by capillary action and shaped into a cylinder and finally freeze-dried.

Surface Profilometry

The surface profiles we present here were obtained by 5 consecutive measurements that were 1 mm spaced (side-by-side) and plotted together in a three-dimensional topological graph so as to convey an idea of the topography of the materials (see Figure 4-2). Our results

show that the surface roughness of BC is in the same range of that of porcine femoral artery, ranging roughly 300nm in both cases from highest peaks to lowest valley, with no statistically significant difference between them ($p>0.05$). On the other hand, both ePTFE and, to a greater extent, PET show a much greater surface roughness with a distance of approximately 600 and 1600 nm between peaks and valleys respectively.
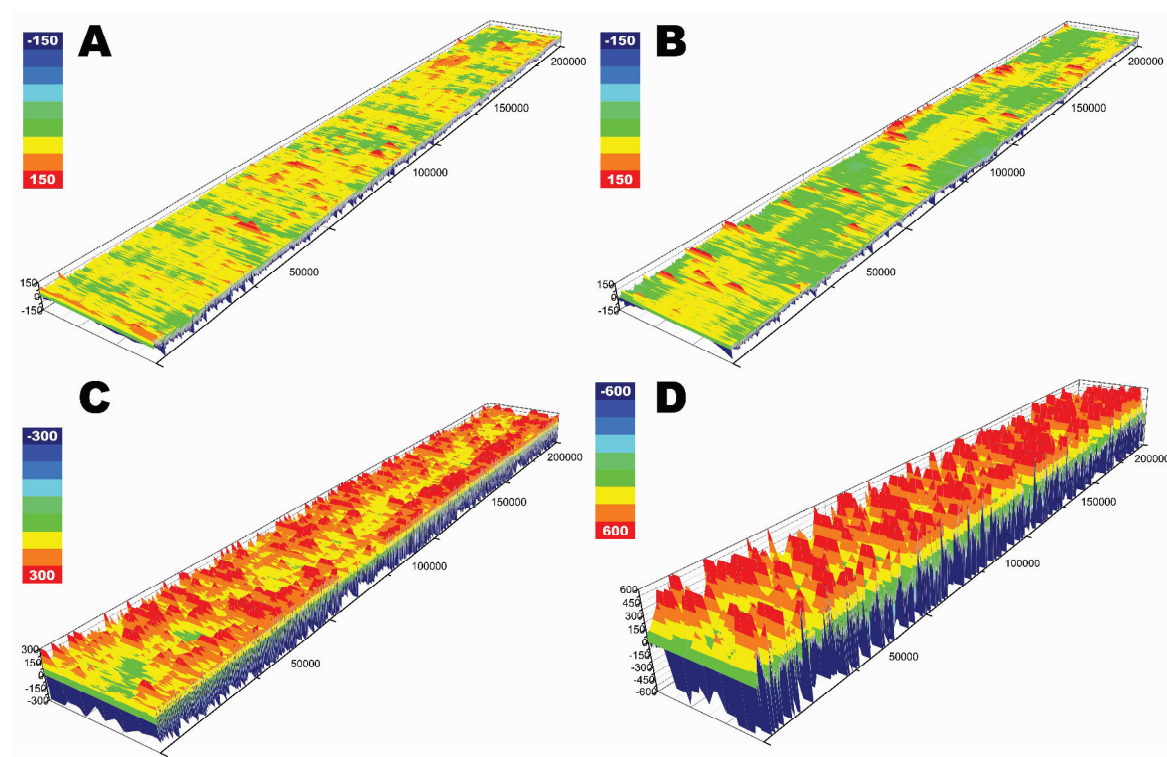
Figure 4-2 - Surface profiles of Porcine Femoral Artery (A), BC graft (B), ePTFE graft (C) and a PET graft (D). The plots were obtained from 5 separate linear measurements (2000 points/mm) over 2 cm (3cm for BC), spaced 1mm apart and plotted in a 3D graph.

Cryo-SEM Imaging

Several BC grafts samples, and several different regions of each graft, were observed via Cryo-SEM so as to maintain the hydrated three-dimensional structure of the grafts; the images presented here are representative of those observations (Figure 4-3). The fibril distribution inside of our grafts showed markedly different structures throughout the graft wall that are well distributed throughout. In lower magnifications dense sheets of BC fibers intersecting each other are visible and appear in wave-like patterns, parallel to the luminal surface of the graft (Figure 4-3A, B and C). Dense sheets are surrounded by low density open

porous regions (Figure 4-3D) with pore sizes ranging from 1 to 5 μm in diameter. Additionally, there seems to be a consistent and dense single layer of BC fibers over the entire luminal surface of the graft that is immediately followed by open porous regions (Figure 4-3E).
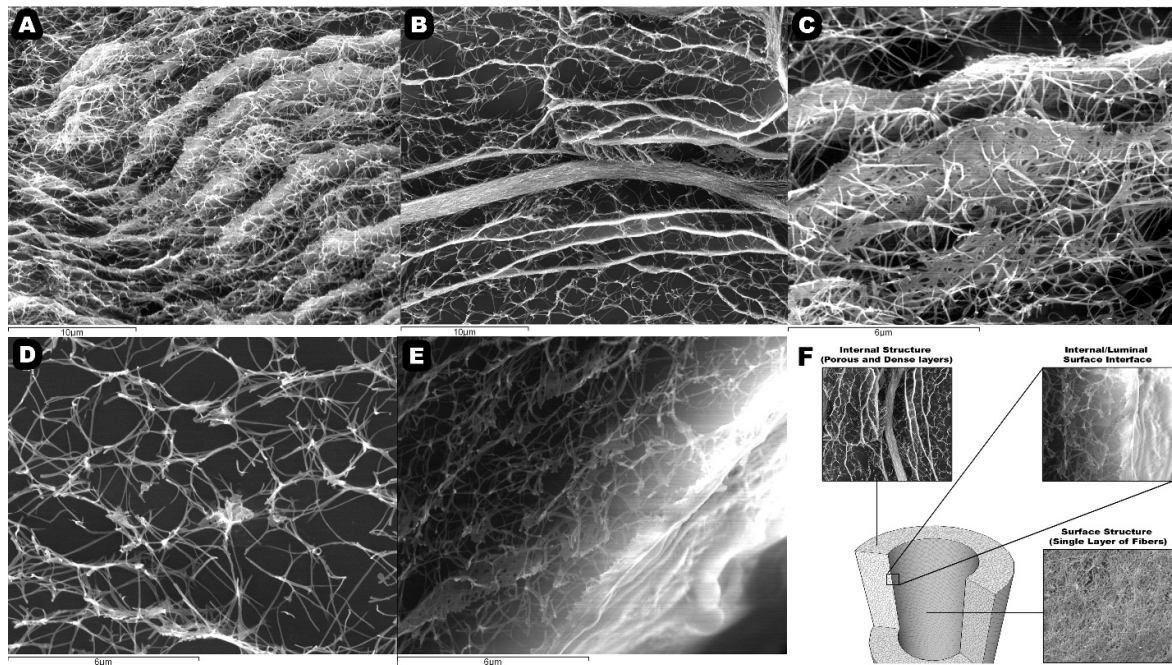
Figure 4-3 - Cryo-SEM images of a portion of the cross-section of the graft wall. (A) and (B) 4000x magnification with noticeable dense regions layered between open-pore structures; (C) 10000x magnification of the dense BC regions; (D) 10000x magnification of the open-pore structures and (E) 10000x magnification of the edge of the luminal surface of the graft. (F) is a schematic representation of the interface between the luminal surface and inner wall structure.

Endotoxin Removal Study

Endotoxin (Lipopolysaccharide; LPS) concentration on non-washed and SDS washed BC was determined with the Pierce LAL Chromogenic Endotoxin Quantitation Kit. Total LPS concentration on non-washed BC over the course of the study was 2.65 ± 0.27EU/ml (Endotoxin Units/ml) and dropped to 0.43 ± 0.15, 0.06 ± 0.04 and 0.003 ± 0.02EU/ml over the following 3 days (Figure 4-4). Total LPS concentration was shown to be significantly different between washed and non-washed BC ($p < 0.05$). Results also show a significant difference between a single and twice washed ($p < 0.05$) and no significant difference between the second and third washes.
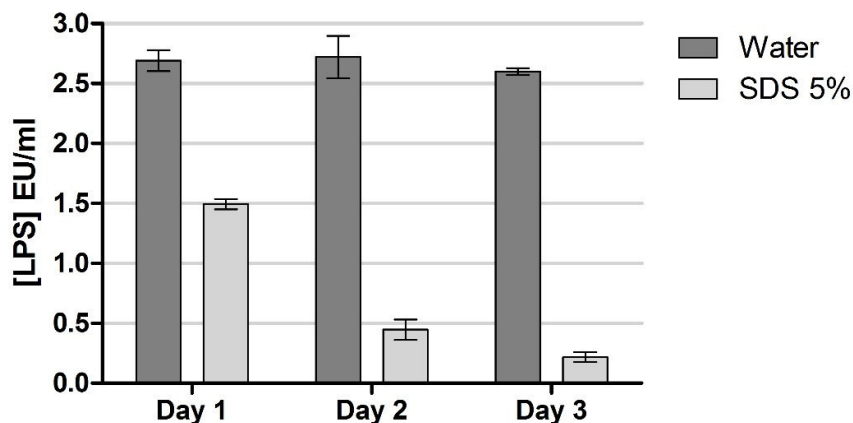
Figure 4-4 - Endotoxin (LPS) concentration in EU/ml (Endotoxin Units/ml) as determined over 3, 24 hour, washes in 5% SDS and water (negative control).

Mechanical Tests

Tensile Strength Determination

Mechanical testing demonstrated marked differences between porcine femoral artery (PFA), ePTFE and BC (both as a graft and untreated) - see Table 4–1. The BC graft and untreated BC show no statistically significant difference between them ($p > 0.05$) in regards to any of the parameters though. However, the BC graft did show higher values for maximum tensile strength (Max Force), maximum stress and strain. PFA, while mechanically weak as compared to the other materials in regards to strength, was by far the most elastic, deforming 133% before rupture. Also noteworthy, ePTFE was shown to be most rigid of the tested materials, with the highest values in all the parameters. The BC grafts thus better resembles the biological vessels than ePTFE, in the sense that it presents higher elasticity, translated in a Young modulus in the same order of magnitude as PFA´s.

Table 4-1 - Mechanical test results for Porcine Femoral Artery (PFA), ePTFE the BC Graft and unprocessed BC (n=5). Values marked with an asterisk (*) are not statistically different from each other in their respective columns (p>0.05). Data is presented as mean ± standard deviation.

Material	Young's Modulus (N/mm²)	Max Force (N)	Max Stress (N/mm²)	Max Strain (%)
PFA	2.58 ± 0.95	10.05 ± 3.39	1.15 ± 0.39*	133.46 ± 11.25
ePTFE	125.40 ± 24.33	198.54 ± 13.33	23.57 ± 1.00	40.62 ± 9.92*
BC Graft	10.56 ± 1.53*	95.92 ± 5.62*	2.75 ± 0.38*	41.08 ± 8.65*
BC	10.70 ± 2.23*	91.47 ± 16.33*	2.10 ± 0.26*	34.5 ± 4.27*

Suture Retention Strength

Results show that untreated BC and our BC grafts demonstrate suture retention strength of 3.94 ± 0.38 and 4.20 ± 0.99N respectively, with no statistically significant difference between them ($p>0.05$). The results demonstrate a superior performance of the BC grafts, as compared to most materials, presenting a suture retention strength comparable to that of ePTFE.

Table 4-2 - Suture Retention strength (N) of several autologous and synthetic grafts for Tissue Engineered Blood Vessels (TEBV), Internal Mammary Artery (IMA), Polytetrafluoroethylene (ePTFE), Fibrin and Fibrin/polylactic acid (PLA), Human Saphenous Vein (HSV), Collagen and Bacterial Cellulose (BC). Suture retention strength for the BC graft and untreated BC are not statistically different (p>0.05; n=4)

Graft Material	Retention Strength (N)	SD	References
IMA	1.35	± 0.49	29
HSV	2.60		30
TEBV	1.49	± 0.49	29
Fibrin	0.19	± 0.05	31
Fibrin/PLA	1.32	± 0.58	31
Collagen	0.82-2.87	± 0.12-0.09	32
ePTFE	4.70	± 0.50	33
BC graft	4.20	± 0.99	--
BC	3.94	± 0.38	--

Compliance Characterization Assay

We measured the compliance for our BC grafts externally via laser detector and estimated compliance internally by sonography imaging. Results show a significant difference between the compliance of the BC graft in regards to the internal and external measurements (see Table 4–3). Externally compliance was measured as being 0.4×10^{-2} %/mmHg while internally graft compliance was determined to be 9.5×10^{-2} %/mmHg. While the external compliance falls far from the results for the most of the other materials found in the literature internally compliance seems to be much better matching, in most regards, the compliance values found for autografts.

Table 4-3 - Compliance (presented as value x10-2 %/mmHg) with standard deviation (SD) as collected from the literature for Internal Mammary Artery (IMA), Human Saphenous Vein (HSV), Human Iliac Artery (HIA), Tissue Engineered Blood Vessel (TEBV), Polyurethane (PU), Polyethylene terephthalate (PET), expanded Polytetrafluoroethylene (ePTFE), Bacterial Cellulose/Chitosan blend (BC/Chi) and measurements for the compliance of the BC grafts as measured externally and internally (n=5).

Graft Material	Compliance (%/mmHg; x10^{-2})	SD	References
IMA	11.5	± 3.9	29
HSV	3.7-12.8	± 1.3-1.9	34
HIA	8	± 5.9	35
TEBV	1.5-3.4	± 0.3	29; 30
PU	8.1	± 0.4	35
PET	1.8	± 1.2	35
ePTFE	1.2-1.6	± 0.3	35; 36
BC/Chi	5.9	± 2.7	36
BC graft External	0.4	± 0.1	--
BC graft Internal	9.5	± 2.8	--

In vivo Experimentation and Histological Analysis

As a preliminary in vivo assay, 4 surgical procedures have been performed to date, with implantation of the BC graft in a femoral-femoral artery bridge on the left hind limb of female domestic pigs (see Figure 4-5A). The right femoral artery was also isolated in a sham-operated procedure and served as a control for the implanted graft. No significant changes to the arterial wall of the control vessel were detected.

During the first surgical intervention severe arterial spasm and contraction was noted during, and after, the procedure. There was noticeably reduced pulse immediately after graft implantation and the limb was found to be slightly cold to the touch 24 hours post-operatively both situations indirectly attributed to arterial contraction and restricted blood flow. All further procedures were performed with papaverine administration, via topical wash to the artery in order to facilitate anastomosis and avoid the transitory arterial spasms in the immediate moments post-op. The following three procedures resulted in 1 month patency that were all confirmed via Doppler ultrasound imaging (results not shown) being terminated at that point for explantation of the BC graft and subsequent histological analysis.

Histological analysis and Immunohistochemistry staining were performed on the grafts harvested after the experiments were terminated. The BC grafts that were recovered one
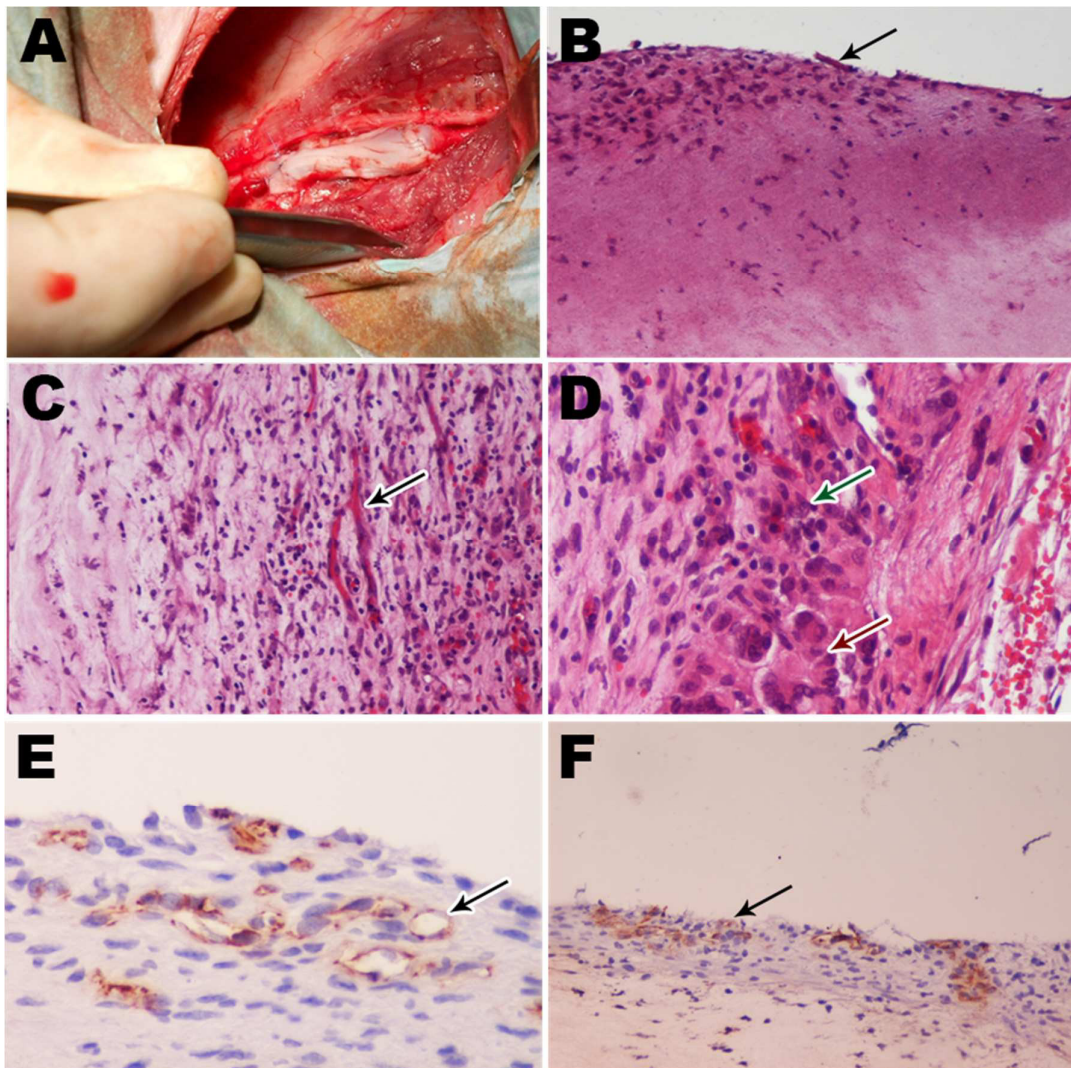
Figure 4-5 - Representative photographs of the microscopy images of in vivo tests. (A) Femoral-femoral artery BC graft placement, (B) luminal surface of the graft with cell adhesion on the surface of the graft along and some cell infiltration, (C) external surface of BC graft showing formation of neo-vessels (arrow), (D) Close-up detail of external surface of the graft with giant cells (red arrow) and macrophages (green arrow) among fibroblasts, (E) immunohistochemistry staining of CD31 positive cells forming neo-vessels on the luminal surface of the graft, (F) CD31 positive cell clusters on the luminal surface of the grafts.

month after surgical intervention were intact and well integrated into the surrounding tissue with no significant fibrosis or macroscopic evidence of inflammation. Later histological analysis showed a distinct, three-layered, structure with cellular adhesion and infiltration on both the luminal and adventitial surfaces of the graft and an unpopulated and larger BC central region. CD31 positive cells were detected on the luminal surface and are believed to be endothelial or progenitor endothelial cells that migrated from the adjoining femoral artery (Figure 4-5B and F). The presence of neo-vessel formation was detected in the cell population on both the adventitial and luminal surfaces (see Figure 4-5C and E). It should be

noted that a significant amount of background staining occurred due the unspecific staining of BC in the immunohistochemistry staining and so the exact extent of the CD31 positive cells cannot be accurately assessed. Figure 4-5D is representative of the cellular infiltration and population found on the adventitial surface of all the recovered grafts. The cell populations in the adventitial regions were determined to be composed, mostly, of fibroblasts, macrophages and some giant cells with a small population of lymphocytes also present.

Discussion

The method for BC graft production, as described herein, is hinged on its simplicity and a few crucial steps, namely: perforation, simultaneous drying and shaping and freeze-drying (Figure 4-1). By processing a single BC sheet this method can render multiple grafts while allowing fine control over the luminal diameter, thickness, and consequently density, of the graft wall.

Perforation of the graft by a sharp needle allows a precise control over the luminal diameter of the graft and directly affects the structure of the luminal surface of the graft (Figure 4-1). There seems to be a consistent and dense (and apparently single layer, see Figure 4-3E) of BC fibers over the entire luminal surface of the graft that is immediately followed by an open porous regions (discussed ahead). The uniform layer that forms the luminal wall results from the perforation process used to create the luminal canal. As the needle penetrates the cellulose block it pushes BC fibers out of its way and to the sides, the end result is a dense inner wall of BC fibers. This luminal surface plays an important role in containing the blood in the lumen of the graft while serving as a semi-permeable barrier to plasma and potentially adhered cells.

Additionally, the surface created by this layer of BC fibers is quite smooth and, in regards to its profile, similar to that of a native artery (Figure 4-2). Blood flow and shear stress have been shown to contribute to plaque formation due to non-uniform blood flow [41, 42]. Physiological levels of shear maintain the homeostatic functioning of vessels and so, ideally, grafts should aim for physiological levels of shear [43-47]. In this regard the topography of both ePTFE and Dacron are quite different from that of both BC and the artery (Figure 4-2). The similarities between the surface roughness/topography of the BC grafts and that of the

arterial wall should theoretically match and allow for an un-interrupted and consistent blood flow over the transition from artery to graft maintaining physiological levels which, in the end, is beneficial to graft performance.

The subsequent partial capillary drying, shaping and freeze-drying steps are largely responsible for the final structural and mechanical properties of the resulting grafts. The drying and shaping allows the BC block to be shaped into a cylindrical tube with 2mm in wall thickness. As a direct result the graft wall density is brought from $0.02g/cm^3$ to $0.09g/cm^3$. With the final freeze-drying step being required to eliminate the remaining water. This allows individual BC fibers to come into contact with each other and form H-bonds [48], while maintaining each individual fiber's spatial position. This step is essential in order to reduce swellability of the graft, which would otherwise cause the loss of the cylindrical shape, while retaining the malleability, flexibility, the degree of the water retaining capability of the BC hydrogel and, above all, the shape of the graft.

The contact and bonds created between fibers induced morphological changes in the BC hydrogel (Figure 4-3). BC has been extensively characterized as presenting an open porous structure that is relatively homogenous throughout the hydrogel [14, 48, 49]. Our grafts present a dual structure, presenting dense sheets, formed by the collapse of fibers onto each other in the drying and with bonds formed during freeze-drying, (Figure 4-3A and B) layered in between the characteristic open porous morphology of BC (Figure 4-3D). These two distinct regions/structures complement each other structurally and functionally. The dense regions observed at a micro/sub-micro scale provide a slight increase in mechanical support while allowing the graft to maintain the shape and structural integrity essential to a functional vascular graft. Simultaneously, the open-porous regions allow for void space and pore interconnectivity that in turn allows the graft to preserve its flexibility while allowing cellular migration from the adjoining tissues to the graft.

A final step in graft preparation was the removal of bacterial lipopolysaccharide (LPS or endotoxin) from the grafts by SDS wash. A significant amount of endotoxin (2.65 ± 0.27EU/ml) remains on BC after alkaline wash, a standard procedure in purifying BC, which has been shown to induce a strong inflammatory response [50]. The inflammatory response triggers coagulation mechanics and could subsequently cause thrombosis. A 24 hour wash was enough to significantly reduce the overall concentration of LPS in BC by over 83%, and a subsequent succession of three washes completely removes any presence of LPS.

In terms of tensile strength untreated BC and the BC grafts show no statistically significant difference between each other; though there seems to be a slight increase in the tensile strength of the BC grafts due to the higher number of bonds in the denser regions (95.92 vs 91.47N). Since, the total number of BC fibers in a given cross-section is essentially identical the higher strength of the graft does not translate to significantly higher values. BC fibers are characteristically strong yet inelastic [13] as opposed to the elastin in a native vessel which, has lower tensile strength though capable of great deformation and shape memory. This is evident when comparing the tensile strength (95.92 vs 10.05N) and elasticity, or deformation, (41 vs 133%) of the graft compared to a porcine vessel.

Similar to what happens with the tensile strength of the graft, suture retention of the BC graft is influenced by the inelasticity of the BC fibers when compared to that of native vessels. The large number of fibers, some organized in the stronger dense regions, provide a solid anchor point for the suture. This translates to a suture retention strength that is noticeably higher than that of native vessels, which as mentioned, tend to deform rather than resist the tensile stress. This suture retention strength is both comparable to that of much stronger and rigid materials like ePTFE, which can also be seen when comparing the tensile strength and deformation, and also, greatly outperforms other polymers that are being proposed as grafts materials (see Table 4–2).

Another important consequence, of the distribution and layered structure of the graft wall is the compliance behavior the graft. Intimal hyperplasia in both autologous saphenous vein and synthetic artery bypass grafts is a major reason for graft failure [40] and is closely associated with a mismatch in mechanical properties of the native vessel and the bypass graft. Diastolic and systolic pressure changes cause vessel walls to expand and contract. A mismatch in mechanical properties of native vessels and grafts adds direct stress to ingrown tissues. Specifically, at the point where the mechanical properties of the vessel wall changes. This can cause lesions to the cell layers which can expose underlying smooth muscle cells resulting in an abnormal migration and proliferation, along with the deposition of extracellular matrix, in the intimal layer (intimal hyperplasia). This leads to thickening of the vessel wall and causing a reduction in the lumen of the vessel, restricting blood flow which can eventually cause occlusion [51].

Therefore, mechanical compliance between the tissue and graft is paramount. The open porous regions of the graft, as mentioned, provide void spaces that allow for fiber movement

inside the graft wall. The void spaces of the pores allow fiber movement in response to pressure changes on the grafts luminal surface. The graft wall seems to absorb the pressure change and does not translate outward to the surface of the material. Hence the difference in compliance values for the outer (0.4×10^{-2} %/mmHg) and inner (9.5×10^{-2} %/mmHg) measurements. Though the method used for measuring the diameter changes of the luminal surface is not extremely precise, when compared to the precision of the laser detector, we are comfortable in the assessment that inner (luminal) compliance is significantly different from that of the outer (adventitial) compliance. While the BC grafts inner and outer surfaces comply differently, the end result is that the BC graft and native vessels present similar values of compliance on the blood-contacting surface. In this regard, the BC grafts greatly outperform the current synthetic materials available, such as ePTFE and PET, by a large margin (see Table 4–3). As a final supporting note, in regards to the mechanical behavior of the BC graft, the ANSI/AAMI VP20-2001 standards outlines that arterial constructs are required to withstand normal arterial pressures and have a burst strength above 1680mmHg. We have measured burst pressure of the BC grafts to be above 1900mmHg (results not shown).

As a result of the findings presented in this work and our prior work with BC [18, 19, 52], along with all that presented in the literature, there was reason to believe that the graft could perform well in vivo. Previous in vivo studies have used rats, sheep and pigs as in vivo models for the study of the performance of BC grafts [14, 53, 54]. Due to the similar anatomy and physiology, domestic pigs were chosen as a model for this work. Despite drawbacks such as the lack of cooperation, without full general anesthesia, and a propensity for rapid growth, pigs constitute an optimal, analogous, model for pre-clinical protocol development and studies [55]. In order to comply with the set parameter of a small caliber vessel (<6mm) the femoral artery was chosen as the sight for implantation of the graft as a femoral artery bridge.

The use of the pig model proved invaluable in determining surgical procedure and complications that could otherwise remain undetermined. Namely, failure associated with vessel occlusionavoiding due to muscular and arterial spasm and contraction; as was the case in the first surgical procedure performed. Normal and physiological Aarterial contraction occurred during surgery and persisted, in the immediate time frame, after implantation which led to a noticeably restricted blood flow before closing. We believe that

the restricted blood flow in these initial moments after implantation led to the collapse of the prosthesis and clot formation. The end result was an occluded vessel 15 days after surgery, though 24 hours after the procedure pulse was weak and the limb hypothermic. Papaverine is an antispasmodic drug commonly used in coronary artery bypass surgery [56] and, as a result of this initial experiment, was introduced as a procedural step to the implantation protocol. Papaverine has been shown to aid in venous graft performance by allowing the smooth muscle of the artery to relax and allow normal blood flow [57, 58]. The use of papaverine was therefore introduced in order to aid in assuring an uninterrupted blood flow in the initial stages of the grafts implantation.

The results, in regards to in vivo experimentation, are still in their early stages yet stack up well as compared to the findings of both Malm [53] and Wipperman [54]. The luminal surface was largely populated by a cell population containing endothelial, or endothelial-like cells (which was confirmed via immunohistochemistry), a fibroblast population, along with some macrophages and giant cells, covered and infiltrated the adventitial surface. The occurrence of neo-vessel formation was found both, on the luminal (via immunohistochemistry staining) and adventitial (visible in the H&E staining and later confirmed in the immunohistochemistry) surfaces of the grafts. Cell infiltration and adhesion is largely limited to the surface and limits of the graft with the center of the BC graft wall which remaining largely unpopulated. Both authors reported similar findings though no neo-vessel formation was reported in their cases.

While coverage of the grafts adventitial surface was complete, the exact extension of surface coverage on the luminal surface could not be precisely determined. Also, the origin of the cells on the adventitial and luminal surfaces is undetermined. However, we believe these to be, in large part, cells that would have migrated from the anastomotic sites, at least in regards to the luminal surface, rather than circulating cells that adhered to the BC graft surface similarly to what was proposed by Malm and colleagues [53]. Finally, the giant cells present, consisted of a minimal population, with large vacuoles with what seemed to be a white material. We believe this white material to be BC that possibly still contained a small amount of endotoxin that would have triggered macrophage activation, the end result being giant cell formation. Their presence was largely negligible and absent from the luminal surface.

Conclusions

As mentioned, several methods have been proposed and patented for BC graft production and which all require dedicated bioreactors and production protocols. Our novel approach has allowed us to produce a dense, malleable and mechanically strong tubular BC prosthetic that meets most of the mechanical characteristic of native vasculature, most notably compliance. Both in vitro and in vivo, the BC grafts herein presented seem to constitute an important alternative as synthetic vascular grafts.

This work is still ongoing mostly in order to expand upon the sample size of the in vivo tests, as well as, prolonging those same tests into longer implantation times in order to gain a more significant perspective of the feasibility of a BC grafts as a long-term, off-the-shelf and cost-effective synthetic graft. This further work will demonstrate any potential limitations of the grafts, as is, and allow us to address possibilities such as nanocompositing the graft with other polymers, such as fibrin, or surface modifications, such as the incorporation of heparin, in order to extend implantation times.

References

[1] Chlupac J, Filova E, Bacakova L. Blood vessel replacement: 50 years of development and tissue engineering paradigms in vascular surgery. Physiol Res. 2009;58 Suppl 2:S119-39.

[2] Holmberg M, Hou X. Competitive protein adsorption of albumin and immunoglobulin G from human serum onto polymer surfaces. Langmuir. 2010;26:938-42.

[3] van Det RJ, Vriens BH, van der Palen J, Geelkerken RH. Dacron or ePTFE for femoro-popliteal above-knee bypass grafting: short- and long-term results of a multicentre randomised trial. European journal of vascular and endovascular surgery : the official journal of the European Society for Vascular Surgery. 2009;37:457-63.

[4] Tsai GJ, Su WH. J Food Protect. 1999;62:239.

[5] Schopka S, Schmid T, Schmid C, Lehle K. Current Strategies in Cardiovascular Biomaterial Functionalization. Materials. 2010;3:638-55.

[6] Ravi S, Chaikof EL. Biomaterials for vascular tissue engineering. Regenerative medicine. 2010;5:107-20.

[7] Stegemann JP, Kaszuba SN, Rowe SL. Review: advances in vascular tissue engineering using protein-based biomaterials. Tissue engineering. 2007;13:2601-13.

[8] Nemeno-Guanzon JG, Lee S, Berg JR, Jo YH, Yeo JE, Nam BM, et al. Trends in Tissue Engineering for Blood Vessels. Journal of Biomedicine and Biotechnology. 2012;2012:14.

[9] Kumar VA, Caves JM, Haller CA, Dai E, Li L, Grainger S, et al. Acellular Vascular Grafts Generated from Collagen and Elastin Analogues. Acta Biomater. 2013.

[10] Amarnath LP, Srinivas A, Ramamurthi A. In vitro hemocompatibility testing of UV-modified hyaluronan hydrogels. Biomaterials. 2006;27:1416-24.

[11] Jockenhoevel S, Zund G, Hoerstrup SP, Chalabi K, Sachweh JS, Demircan L, et al. Fibrin gel -- advantages of a new scaffold in cardiovascular tissue engineering. European journal of cardio-thoracic surgery : official journal of the European Association for Cardio-thoracic Surgery. 2001;19:424-30.

[12] de Valence S, Tille JC, Mugnai D, Mrowczynski W, Gurny R, Moller M, et al. Long term performance of polycaprolactone vascular grafts in a rat abdominal aorta replacement model. Biomaterials. 2012;33:38-47.

[13] Leitão A, Silva J, Dourado F, Gama M. Production and Characterization of a New Bacterial Cellulose/Poly(Vinyl Alcohol) Nanocomposite. Materials. 2013;6:1956-66.

[14] Klemm D, Schumann D, Udhardt U, Marsch S. Bacterial synthesized cellulose — artificial blood vessels for microsurgery. Progress in Polymer Science. 2001;26:1561-603.

[15] Svensson A, Nicklasson E, Harrah T, Panilaitis B, Kaplan DL, Brittberg M, et al. Bacterial cellulose as a potential scaffold for tissue engineering of cartilage. Biomaterials. 2005;26:419-31.

[16] Solway DR, Consalter M, Levinson DJ. Microbial cellulose wound dressing in the treatment of skin tears in the frail elderly. Wounds. 2010;22:17-9.

[17] Fontana JD, de Souza AM, Fontana CK, Torriani IL, Moreschi JC, Gallotti BJ, et al. Acetobacter cellulose pellicle as a temporary skin substitute. Appl Biochem Biotechnol. 1990;24-25:253-64.

[18] Andrade FK, Costa R, Domingues L, Soares R, Gama M. Improving bacterial cellulose for blood vessel replacement: Functionalization with a chimeric protein containing a cellulose-binding module and an adhesion peptide. Acta Biomater. 2010;6:4034-41.

[19] Leitão AF, Gupta S, Silva JP, Reviakine I, Gama M. Hemocompatibility study of a bacterial cellulose/polyvinyl alcohol nanocomposite. Colloids and Surfaces B: Biointerfaces. 2013;111:493-502.

[20] Bäckdahl H, Risberg B, Gatenholm P. Observations on bacterial cellulose tube formation for application as vascular graft. Materials Science and Engineering: C. 2011;31:14-21.

[21] Backdahl H, Helenius G, Bodin A, Nannmark U, Johansson BR, Risberg B, et al. Mechanical properties of bacterial cellulose and interactions with smooth muscle cells. Biomaterials. 2006;27:2141-9.

[22] Andrade F, Pertile R, Douradoa F. Bacterial cellulose: properties, production and applications. Cellulose: structure and properties, derivatives and industrial uses Nova Science Publishers, Inc. 2010:427-58.

[23] Bodin A, BÄCKDAHL H, Gatenholm P, Gustafsson L, Risberg B. Bacterial cellulose tubes. Google Patents; 2012.

[24] DICKERHOFF B, Farivar RS, RAGHAVAN ML, Kumar V. Vascular prosthetic assemblies. Google Patents; 2013.

[25] Gatenholm P, Backdahl H, Tzavaras TJ, Davalos RV, Sano MB. Three-dimensional bioprinting of biosynthetic cellulose (bc) implants and scaffolds for tissue engineering. Google Patents; 2011.

[26] Wan WK, Millon L. Poly(vinyl alcohol)-bacterial cellulose nanocomposite. Google Patents; 2005.

[27] Serafica G, Damien C, Wright F, Beam H. Implantable microbial cellulose materials for various medical applications. Google Patents; 2007.

[28] Zahedmanesh H, Mackle JN, Sellborn A, Drotz K, Bodin A, Gatenholm P, et al. Bacterial cellulose as a potential vascular graft: Mechanical characterization and constitutive model development. Journal of Biomedical Materials Research Part B: Applied Biomaterials. 2011;97B:105-13.

[29] Kowalska-Ludwicka K, Cala J, Grobelski B, Sygut D, Jesionek-Kupnicka D, Kolodziejczyk M, et al. Modified bacterial cellulose tubes for regeneration of damaged peripheral nerves. Archives of medical science : AMS. 2013;9:527-34.

[30] Kaźmierczak D, Kazimierczak J. Biosynthesis of modified bacterial cellulose in a tubular form. Fibres & Textiles in Eastern Europe. 2010;18:82.

[31] Putra A, Kakugo A, Furukawa H, Gong JP, Osada Y. Tubular bacterial cellulose gel with oriented fibrils on the curved surface. Polymer. 2008;49:1885-91.

[32] Diamantouros S, Hurtado-Aguilar L, Schmitz-Rode T, Mela P, Jockenhoevel S. Pulsatile Perfusion Bioreactor System for Durability Testing and Compliance Estimation of Tissue Engineered Vascular Grafts. Ann Biomed Eng. 2013;41:1979-89.

[33] Konig G, McAllister TN, Dusserre N, Garrido SA, Iyican C, Marini A, et al. Mechanical properties of completely autologous human tissue engineered blood vessels compared to human saphenous vein and mammary artery. Biomaterials. 2009;30:1542-50.

[34] L'Heureux N, Dusserre N, Konig G, Victor B, Keire P, Wight TN, et al. Human tissue-engineered blood vessels for adult arterial revascularization. Nature medicine. 2006;12:361-5.

[35] Syedain ZH, Meier LA, Bjork JW, Lee A, Tranquillo RT. Implantable arterial grafts from human fibroblasts and fibrin using a multi-graft pulsed flow-stretch bioreactor with noninvasive strength monitoring. Biomaterials. 2011;32:714-22.

[36] Shah S. Fabrication Of Small Diameter Vascular Graft Using Stacked Collagen Films. 2013.

[37] Isaka M, Nishibe T, Okuda Y, Saito M, Seno T, Yamashita K, et al. Experimental study on stability of a high-porosity expanded polytetrafluoroethylene graft in dogs. Annals of Thoracic and Cardiovascular Surgery. 2006;12:37.

[38] Zachrisson H, Lindenberger M, Hallman D, Ekman M, Neider D, Länne T. Diameter and compliance of the greater saphenous vein – effect of age and nitroglycerine. Clinical Physiology and Functional Imaging. 2011;31:300-6.

[39] Tai NR, Salacinski HJ, Edwards A, Hamilton G, Seifalian AM. Compliance properties of conduits used in vascular reconstruction. British Journal of Surgery. 2000;87:1516-24.

[40] Azevedo EP, Retarekar R, Raghavan ML, Kumar V. Mechanical properties of cellulose: chitosan blends for potential use as a coronary artery bypass graft. Journal of Biomaterials Science, Polymer Edition. 2012;24:239-52.

[41] Cunningham KS, Gotlieb AI. The role of shear stress in the pathogenesis of atherosclerosis. Laboratory investigation. 2005;85:9-23.

[42] Cecchi E, Giglioli C, Valente S, Lazzeri C, Gensini GF, Abbate R, et al. Role of hemodynamic shear stress in cardiovascular disease. Atherosclerosis. 2011;214:249-56.

[43] Resnick N, Yahav H, Shay-Salit A, Shushy M, Schubert S, Zilberman LCM, et al. Fluid shear stress and the vascular endothelium: for better and for worse. Progress in Biophysics and Molecular Biology. 2003;81:177-99.

[44] Silver AE, Vita JA. Shear Stress–Mediated Arterial Remodeling in Atherosclerosis: Too Much of a Good Thing? Circulation. 2006;113:2787-9.

[45] Milleret V, Hefti T, Hall H, Vogel V, Eberli D. Influence of the fiber diameter and surface roughness of electrospun vascular grafts on blood activation. Acta Biomater. 2012;8:4349-56.

[46] Shen F, Kastrup CJ, Liu Y, Ismagilov RF. Threshold Response of Initiation of Blood Coagulation by Tissue Factor in Patterned Microfluidic Capillaries Is Controlled by Shear Rate. Arteriosclerosis, Thrombosis, and Vascular Biology. 2008;28:2035-41.

[47] He W, Hu Z, Xu A, Liu R, Yin H, Wang J, et al. The Preparation and Performance of a New Polyurethane Vascular Prosthesis. Cell Biochem Biophys. 2013:1-12.

[48] Clasen C, Sultanova B, Wilhelms T, Heisig P, Kulicke WM. Effects of Different Drying Processes on the Material Properties of Bacterial Cellulose Membranes. Macromolecular Symposia. 2006;244:48-58.

[49] Sokolnicki AM, Fisher RJ, Harrah TP, Kaplan DL. Permeability of bacterial cellulose membranes. Journal of Membrane Science. 2006;272:15-27.

[50] Heumann D, Roger T. Initial responses to endotoxins and Gram-negative bacteria. Clinica Chimica Acta. 2002;323:59-72.

[51] Thubrikar MJ. Vascular mechanics and pathology: Springer; 2007.

[52] Andrade FK, Silva JP, Carvalho M, Castanheira EM, Soares R, Gama M. Studies on the hemocompatibility of bacterial cellulose. Journal of biomedical materials research Part A. 2011;98:554-66.

[53] Malm CJ, Risberg B, Bodin A, Bäckdahl H, Johansson BR, Gatenholm P, et al. Small calibre biosynthetic bacterial cellulose blood vessels: 13-months patency in a sheep model. Scandinavian Cardiovascular Journal. 2012;46:57-62.

[54] Wippermann J, Schumann D, Klemm D, Kosmehl H, Salehi-Gelani S, Wahlers T. Preliminary Results of Small Arterial Substitute Performed with a New Cylindrical Biomaterial Composed of Bacterial Cellulose. European Journal of Vascular and Endovascular Surgery. 2009;37:592-6.

[55] Thomas LV, Lekshmi V, Nair PD. Tissue engineered vascular grafts — Preclinical aspects. International Journal of Cardiology. 2013;167:1091-100.

[56] Takeuchi K, Sakamoto S, Nagayoshi Y, Nishizawa H, Matsubara J. Reactivity of the human internal thoracic artery to vasodilators in coronary artery bypass grafting. European journal of cardio-thoracic surgery : official journal of the European Association for Cardio-thoracic Surgery. 2004;26:956-9.

[57] Yavuz S, Celkan A, Goncu T, Turk T, Ozdemir IA. Effect of papaverine applications on blood flow of the internal mammary artery. Annals of thoracic and cardiovascular surgery : official journal of the Association of Thoracic and Cardiovascular Surgeons of Asia. 2001;7:84-8.

[58] Grondin CM, Lepage G, Castonguay YR, Meere C, Grondin P. Aortocoronary bypass graft. Initial blood flow through the graft, and early postoperative patency. Circulation. 1971;44:815-9.

Chapter 5

General Conclusions and Future Perspectives

.

This work consisted in the development of a viable vascular graft of bacterial cellulose (BC). Initially the worked focused on enhancing the production method described in the literature and implemented by a colleague in the course of a previous PhD. By feeding oxygen through an oxygen permeable silicone tubing and harnessing the way in which the bacteria produce bacterial cellulose the tubes were formed. However, they were found to be lacking in the mechanical properties that were required of a viable graft. As such, a nanocomposite based off of the bacterial cellulose hydrogel and containing poly(vinyl alcohol) (PVA) was devised, developed and characterized.

Before any further development the blood-material characterization was essential. If the material did not perform in regards to hemocompatibility and non-thrombogenicity there would be no reason to pursue it. There was a beneficial, side-effect of the addition on PVA; namely a slight improvement to the hemocompatibility and non-thrombogenicity of the material. Results showed that the BC/PVA nanocomposite outperformed the industry standard, ePTFE, in regards to blood/material interactions. Though the differences between the hemocompatibility parameters were comparable to those of BC; in all of them, there was a tendency for BC/PVA to also outperform BC.

Results showed that the addition of PVA did not, however, have the desired effect of improving the mechanical behavior of the BC hydrogel when the samples were dried completely. This was found to be due to changes that occurred on an organizational level of the fibrous network with noticeably large porous regions in dry BC/PVA contributing significantly to the mechanical behavior of the material. Observationally, the BC/PVA nanocomposite if never dried seemed to provide a mechanical resistance that was higher to that of BC but, this was never confirmed.

Through the successive developmental stages of the graft and various different configurations and production methods a novel and cost-effective method was discovered. This methodology allowed the consistent production of viable grafts with the mechanical and morphological characteristics that a vascular graft required with no need for additional manipulation and formulation. The cost-effective nature and logistically uncomplicated method of production also proved beneficial aspects. BC had already been shown to have potential *in vivo* and as such live animal testing

was performed that also showed viability with 1 month patency being shown. The presence of an endothelial cell population on the luminal surface also gave support to the notion that the grafts could become a viable option. This work ultimately led to the application for a provisionary patent.

Currently, studies are still ongoing and any future perspectives of the work, at the moment, will focus on continued *in vivo* studies and improvement so as to determine the long-term viability of the BC grafts. The intent is to attempt to achieve 3 month, 6 month and ultimately 1 year patency of the graft. Additionally, the vascular graft production method should also be optimized so as to automate and scale-up the production method. Most noticeably the use of laser cutting technology to perforate the BC hydrogels may be the ideal solution rather than a mechanical perforation, as is currently used. Also, the addition of bioactive molecules to the luminal surface of the graft are also a possible prospect. The addition of heparin, or other such chemicals may improve biocompatibility and allow long-term patency of the graft. Also, the possibility of a new nanocomposite, such as BC/fibrin, may prove a viable course of action. The mechanical behavior of BC would support the graft while fibrin would allow the material surface, at the least, to be populated with endothelial cells that would in turn, also, allow the grafts long-term performance.

Annex A

Provisionary Patent Application

Adapted from: Alexandre F. Leitão and Miguel Gama; *TUBULAR BACTERIAL CELLULOSE GRAFTS FOR VASCULAR APPLICATIONS AND METHOD OF PRODUCTION*; Provisionary Patent Number: 107904; Date of Priority: 23-09-2014

DESCRIPTION

"Tubular bacterial cellulose grafts for vascular applications and method of production"

Field of the Invention

The present invention relates to a method of production of graft for vascular application. More specifically consists in the production of a tubular, three-dimensional, bacterial cellulose structures for applications as a cardiovascular bypass grafts or other similar tubular structures.

Background of the invention

Data from the World Health Organization (WHO) suggests that the number of people that suffer from cardiovascular diseases (CVDs) will increase from 17.3, in 2008, to 23.3 million by 2030. In vascular surgery, surgical bypass is fundamental in the treatment of some diseases. Vascular grafts replace, bypass or maintain function of damaged, occluded or diseased blood vessels. The chosen conduit and its success depend on several factors such as availability, size, ease of handling and technical facility, thrombogenicity, resistance to infection and dilation, durability, long-term patency and price.

The most common, and generally considered ideal grafts, are autografts, i.e., vessels collected from the patient. There are generally two major downsides to the use of autografts. The first is the need for prior surgical interventions, before the actual bypass surgeries, in order to collect the autologous vessel. Along with this, the actual availability of these vessels may be limited, due to prior interventions. Secondly, these grafts are subject to the natural progression of the patient's disease which can lead to deterioration, over time, of the biological grafts [1] and so synthetic grafts have been used for potential application as cardiovascular grafts.

Polyethylene terephthalate (PET or Dacron) and expanded polytetrafluoroethylene (ePTFE) grafts are the gold standard, at the moment, for synthetic grafts in large and

medium diameter (>6 mm) vessels. However, these synthetic alternatives are not yet the ideal solution. While demonstrating acceptable results in larger diameter grafts, as internal diameter decreases so does its long-term patency [2, 3]. These grafts ultimately fail under 6mm in diameter, due to surface adsorption of proteins to the luminal and consequent activation of platelet activity resulting in clot formation and subsequent thrombosis [4, 5].

A large amount of work has therefore been aimed at finding alternative solutions to these materials through either natural or synthetic polymer materials [6-8]. The field is ever growing and the lack of a clear optimal polymer has led, and continues to lead, to many potential options. By either, further development and research into the already existing grafts (PET and ePTFE) or the creation of new non-degradable grafts of polyurethane, polyvinyl alcohol or bacterial cellulose (BC). Another option is researching and developing temporary grafts that ultimately allow for a tissue engineered solution, either by prior cell-seeding or allowing for native cell migration, attachment and ingrowth. Ultimately these tissue engineered grafts would end up producing a new vessel out of native tissue from a scaffold of collagen, fibrin, elastin, silk and polycaprolactone [9-12].

One promising solution for these problems is BC. This polymer is a highly pure linear polysaccharide, consisting of β (1→4)–linked D-glucose monomers. It is secreted by bacteria of the *Gluconacetobacter* genus. Once secreted, it forms a fibrous network hydrogel that has been extensively studied for biomedical applications due to its morphology, high purity, water-holding capacity, tensile strength, malleability and biocompatibility [13-15] and has been proposed for applications such as wound dressings [16], artificial skin[17] or blood vessels [18-20] and as a scaffold for tissue engineering [15, 21, 22]. The hemocompatibility of BC has been comprehensively studied in our group, with rather promising results (19).

Many methods have been proposed and patented [23-30] for the production of BC tubular grafts. Generally, the methods employed take advantage of the way the BC hydrogel is produced at air-medium interfaces [14, 31]. However, these production methods require dedicated bioreactors specifically designed for graft production. By using an oxygen permeable scaffold upon which BC is produced there are limits to the thickness and density of the BC structures because the oxygen rich environment produced by the likes of silicone tubing is limited to the immediate

vicinity of that tube. Additionally, the oxygen permeable scaffold must allow oxygen to permeate consistently and homogenously throughout its surface. Otherwise the BC on the material surface will not be produced in a homogenously. Also, some cases develop interconnected sheets or layers of BC in the wall of the graft. These sheets can potentially delaminate under arterial pressure resulting in pockets of pooled blood and pressure build-up which results in the graft ballooning and bursting. This heterogeneity in the BC structure translates to varying mechanical properties along and across a single BC tube. Meeting these conditions for heterogeneity, along with the logistic costs of producing and maintaining a series of graft producing bioreactors, oxygen to inflate the permeable scaffold, the oxygen permeable scaffold *per se* with appropriate characteristics and the inevitable optimization processes involved have yet to produce a viable model for large scale BC graft production.

As mentioned, BC has several properties that make it a good prospect as a biomaterial for biomedical applications and has shown potential as an *in vivo* vascular grafts [14, 18, 20, 23]. It is already widely produced commercially in membranes or sheets with varying thicknesses and scale depending on the producer and method adopted for production. However, these methods for graft production, as presented to date, have an inherent inability to assure an economically viable and reproducible approach to the graft production. The present invention is a novel approach to small caliber BC graft (<6mm) production that is both easily reproducible and provides a graft with adequate mechanical and biocompatible properties and, through *in vivo* experimentation, has already demonstrated promising patency.

General Description

The method for BC graft production, as described herein, is hinged on its simplicity and a few crucial steps, namely: perforation, simultaneous drying and shaping and freeze-drying (Figure A-1). By processing a single BC sheet this method can render multiple grafts while allowing fine control over the luminal diameter, thickness, and consequently density, of the graft wall.

Perforation of the graft by a sharp needle allows a precise control over the luminal diameter of the graft and directly affects the structure of the luminal surface of the graft (Figure A-1). There seems to be a consistent and dense (and apparently single layer, see Figure A-3E) of BC fibers over the entire luminal surface of the graft that is immediately followed by an open porous regions. The uniform layer that forms the luminal wall results from the perforation process used to create the luminal canal. As the needle penetrates the cellulose block it pushes BC fibers out of its way and to the sides, the end result is a dense inner wall of BC fibers. This luminal surface plays an important role in containing the blood in the lumen of the graft while serving as a semi-permeable barrier to plasma and potentially adhered cells.

Additionally, the surface created by this layer of BC fibers is quite smooth and, in regards to its profile, similar to that of a native artery (Figure A-2). Blood flow and shear stress have been shown to contribute to plaque formation due to non-uniform blood flow [41, 42]. Physiological levels of shear maintain the homeostatic functioning of vessels and so, ideally, grafts should aim for physiological levels of shear [43-47]. In this regard the topography of both ePTFE and Dacron are quite different from that of both BC and the artery (Figure A-2). The similarities between the surface roughness/topography of the BC grafts and that of the arterial wall should theoretically match and allow for an un-interrupted and consistent blood flow over the transition from artery to graft maintaining physiological levels which, in the end, is beneficial to graft performance.

The subsequent partial capillary drying, shaping and freeze-drying steps are largely responsible for the final structural and mechanical properties of the resulting grafts. The drying and shaping allows the BC block to be shaped into a cylindrical tube with 2mm in wall thickness. As a direct result the graft wall density is brought from $0.02g/cm^3$ to $0.09g/cm^3$, theoretically the density can range between 0.02-$0.15g/cm^3$. With the final freeze-drying step being required to eliminate the remaning water. This allows individual BC fibers to come into contact with each other and form H-bonds [48], while maintaining each individual fiber's spatial position. This step is essential in order to reduce swellability of the graft, which would otherwise cause the loss of the cylindrical shape, while retaining the malleability, flexibility, the degree of the water retaining capability of the BC hydrogel and, above all, the shape of the graft.

The contact and bonds created between fibers induced morphological changes in the BC hydrogel (Figure A-3). BC has been extensively characterized as presenting an open porous structure that is relatively homogenous throughout the hydrogel [14, 48, 49]. The grafts developed presents a dual structure, presenting dense sheets, formed by the collapse of fibers onto each other in the drying and with bonds formed during freeze-drying, (Figure A–3A and B) layered in between the characteristic open porous morphology of BC (Figure A–3D). These two distinct regions/structures complement each other structurally and functionally. The dense regions observed at a micro/sub-micro scale provide a slight increase in mechanical support while allowing the graft to maintain the shape and structural integrity essential to a functional vascular graft. Simultaneously, the open-porous regions allow for void space and pore interconnectivity that in turn allows the graft to preserve its flexibility while allowing cellular migration from the adjoining tissues to the graft.

A final step in graft preparation was the removal of bacterial lipopolysaccharide (LPS or endotoxin) from the grafts by SDS wash. A significant amount of endotoxin (2.65 ± 0.27EU/ml) remains on BC after alkaline wash, a standard procedure in purifying BC, which has been shown to induce a strong inflammatory response [50]. The inflammatory response triggers coagulation mechanics and could subsequently cause thrombosis. A 24 hour wash was enough to significantly reduce the overall concentration of LPS in BC by over 83%, and a subsequent succession of three washes completely removes any presence of LPS.

In terms of tensile strength untreated BC and the BC grafts show no statistically significant difference between each other; though there seems to be a slight increase in the tensile strength of the BC grafts due to the higher number of bonds in the denser regions (95.92 vs 91.47N). Since, the total number of BC fibers in a given cross-section is essentially identical the higher strength of the graft does not translate to significantly higher values. BC fibers are characteristically strong yet inelastic [13] as opposed to the elastin in a native vessel which, has lower tensile strength though capable of great deformation and shape memory. This is evident when comparing the tensile strength (95.92 vs 10.05N) and elasticity, or deformation, (41 vs 133%) of the graft compared to a porcine vessel.

Similar to what happens with the tensile strength of the graft, suture retention of the BC graft is influenced by the inelasticity of the BC fibers when compared to that of native vessels. The large number of fibers, some organized in the stronger dense regions, provide a solid anchor point for the suture. This translates to a suture retention strength that is noticeably higher than that of native vessels, which as mentioned, tend to deform rather than resist the tensile stress. This suture retention strength is both comparable to that of much stronger and rigid materials like ePTFE, which can also be seen when comparing the tensile strength and deformation, and also, greatly outperforms other polymers that are being proposed as grafts materials (see Table A-2).

Another important consequence, of the distribution and layered structure of the graft wall is the compliance behavior the graft. Intimal hyperplasia in both autologous saphenous vein and synthetic artery bypass grafts is a major reason for graft failure [40] and is closely associated with a mismatch in mechanical properties of the native vessel and the bypass graft. Diastolic and systolic pressure changes cause vessel walls to expand and contract. A mismatch in mechanical properties of native vessels and grafts adds direct stress to ingrown tissues. Specifically, at the point where the mechanical properties of the vessel wall changes. This can cause lesions to the cell layers which can expose underlying smooth muscle cells resulting in an abnormal migration and proliferation, along with the deposition of extracellular matrix, in the intimal layer (intimal hyperplasia). This leads to thickening of the vessel wall and causing a reduction in the lumen of the vessel, restricting blood flow which can eventually cause occlusion [51].

Therefore, mechanical compliance between the tissue and graft is paramount. The open porous regions of the graft, as mentioned, provide void spaces that allow for fiber movement inside the graft wall. The void spaces of the pores allow fiber movement in response to pressure changes on the grafts luminal surface. The graft wall seems to absorb the pressure change and does not translate outward to the surface of the material. Hence the difference in compliance values for the outer $(0.4 \times 10^{-2}$ %/mmHg) and inner (9.5×10^{-2} %/mmHg) measurements. Though the method used for measuring the diameter changes of the luminal surface is not extremely precise, when compared to the precision of the laser detector, we are comfortable in the assessment that inner (luminal) compliance is significantly

different from that of the outer (adventitial) compliance. While the BC grafts inner and outer surfaces comply differently, the end result is that the BC graft and native vessels present similar values of compliance on the blood-contacting surface. In this regard, the BC grafts greatly outperform the current synthetic materials available, such as ePTFE and PET, by a large margin (see Table A-3). As a final supporting note, in regards to the mechanical behavior of the BC graft, the ANSI/AAMI VP20-2001 standards outlines that arterial constructs are required to withstand normal arterial pressures and have a burst strength above 1680mmHg. We have measured burst pressure of the BC grafts to be above 1900mmHg (results not shown).

As a result of the findings presented in this work and our prior work with BC [18, 19, 52], along with all that presented in the literature, there was reason to believe that the graft could perform well *in vivo*. Previous *in vivo* studies have used rats, sheep and pigs as *in vivo* models for the study of the performance of BC grafts [14, 53, 54]. Due to the similar anatomy and physiology, domestic pigs were chosen as a model for this work. Despite drawbacks such as the lack of cooperation, without full general anesthesia, and a propensity for rapid growth, pigs constitute an optimal, analogous, model for pre-clinical protocol development and studies [55]. In order to comply with the set parameter of a small caliber vessel (<6mm) the femoral artery was chosen as the sight for implantation of the graft as a femoral artery bridge.

The use of the pig model proved invaluable in determining surgical procedure and complications that could otherwise remain undetermined. Namely, failure associated with vessel occlusion due to muscular and arterial spasm and contraction; as was the case in the first surgical procedure performed. Arterial contraction occurred during surgery and persisted after implantation which led to noticeably restricted blood flow before closing. The end result was an occluded vessel 15 days after surgery, though 24 hours after the procedure pulse was weak and the limb hypothermic. Papaverine is an antispasmodic drug commonly used in coronary artery bypass surgery [56] and, as a result of this initial experiment, was introduced as a procedural step to the implantation protocol.

The results, in regards to *in vivo* experimentation, are still in their early stages yet stack up well as compared to the findings of both Malm [53] and Wipperman [54]. The luminal surface was largely populated by endothelial, or endothelial-like cells (which was confirmed via immunohistochemistry). A fibroblast population, along

with some macrophages and giant cells, covered and infiltrated the adventitial surface with neo-vessel formation occurring inside these infiltrated regions. The third and larger structure was the center of the BC graft wall which remained largely unpopulated. Both authors reported similar findings though no neo-vessel formation was reported in their cases.

While coverage of the grafts adventitial surface was complete, the exact extension of surface coverage on the luminal surface could not be precisely determined. Also, the origin of the cells on the adventitial and luminal surfaces is undetermined. However, we believe these to be, in large part, cells that would have migrated from the anastomotic sites, at least in regards to the luminal surface, rather than circulating cells that adhered to the BC graft surface similarly to what was proposed by Malm and colleagues [53]. Finally, the giant cells present, consisted of a minimal population, with large vacuoles with what seemed to be a white material. We believe this white material to be BC that possibly still contained a small amount of endotoxin that would have triggered macrophage activation, the end result being giant cell formation. Their presence was largely negligible and absent from the luminal surface.

Method

In general, the process consists in Isolate a single bacterial cellulose block from a larger bacterial cellulose sheet with predetermined dimensions. The block is then perforated along the center line before a drying and shaping step until a desired wall thickness is achieved. The tubular structure is then freeze-dried (one or more times) in order to obtain the final tubular structure (Figure A-1).

The perforation of the bacterial cellulose block can be performed by mechanical and physical perforation. The initial perforation of the luminal channel can be created by mechanical perforation using a, periodically sharpened, metallic needle. Alternatively, the application of a laser, or other physical or chemical process, can be used to form an initial luminal channel; however, care should be taken in regards to the choice of gas for the laser since surface modification can incur from this process. The luminal diameter is determined by the application of a metallic needle

or rod, after or during perforation, that will widen the channel to a final desired diameter. The final luminal diameter can vary from 2mm to 10mm, ideally 4-5mm for small caliber grafts.

The drying process can be performed by mass transfer of water via capillary action, evaporation or compression that allows the controlled removal of water from the bacterial cellulose hydrogel. Mass transfer can be performed on blotting paper, or other such materials, at room temperature, same applies for compression. Evaporation should occur at temperatures ranging from 50-80°C in order to allow adequate control over final external diameter.

Shaping of the external surface should occur during, but is not limited to, the drying step. Shaping can be performed by mechanical application of an external force that results in a cylindrical shape. The external force can be applied by hands or any equipment suitable to deliver a consistent and controlled external force. If need be the external surface can be trimmed, sanded or shaved in order to produce an external surface that presents a smoother topography. Trimming or shaving should be performed after freeze-drying on the completely dried material, for operability. The best conditions for this depend on the graft.

Both the drying and shaping steps can be performed in order to control the final thickness of the wall of the tubular structure. Wall thickness is not limited to a predetermined thickness but should range between 1-4mm depending on luminal diameter ideally a 2mm thickness for a 4-8mm diameter graft. The total amount of bacterial cellulose used to form the final tubular structures dictates wall density and wall density dictates mechanical behavior of the final structure. A denser graft wall will translate to higher mechanical strength due to the total number of BC fibers in a same cross-section and can be adjusted accordingly (the ideal density should be $0.1g/cm^3$ but can range from 0.02 to $0.15g/cm^3$)

Surface modifications of the graft can be performed on the luminal and external surfaces in order to better accommodate for final desired application and the performance of the graft. The surface chemistry can be altered in order to improve biocompatibility and cell adhesion, by addition of RGD sequences or other cell signaling molecules, and/or reduce thrombogenicity, by addition of heparin for example. Surface modification can be performed chemically or physically through

methods such as covalent binding of the bioactive molecules or radicals and/or plasma-surface modifications.

The final lyophilization step is not limited to a freeze-drying process. The objective is the complete removal of water without altering the 3-dimensional shape of the graft and as such, any other methods, such as supercritical drying, can be performed.

As mentioned, mechanical properties of the tubular structure can be controlled by controlling wall density of the graft via inclusion of a larger amount of bacterial cellulose into the initial perforation step. Also, mechanical behavior of the graft can be controlled by controlling the number of freeze-drying cycles. The strength of the graft derives from the number of individual fibers in a cross-section and the amount of interaction between each fiber. Higher densities increase the number of fibers in a cross-section and cycle numbers increase the interaction levels both can be adjusted to improve mechanical behavior. We have found that the, aforementioned, ideal density for a 4mm graft is $0.1g/cm^3$ and a single freeze-drying cycle are sufficient.

Complete removal of water via lyophilization can be performed before the initial perforation. However, all following steps must be performed sequentially. This may be beneficial logistically since dry cellulose is easier to handle.

Detailed description

Material and Methods

Graft Fabrication

Bacterial cellulose was produced by *Gluconacetobacter xylinus* (ATCC 53582), or any other BC producing bacteria, in a modified Hestrin-Schramm medium, supplemented with 2% Corn Steep Liquor (Sigma Aldrich, Germany) and 0.6 % ethanol, at pH 5.0. The resulting BC membranes were then washed in 4% (w/v) NaOH. It should also be noted that any culture medium capable of supporting the production of BC can also be used. The membranes were then thoroughly washed with distilled water until pH was neutral. Finally, endotoxin removal was

accomplished by further washing in 5% SDS (w/v). The water and detergent solutions were changed after 24 hours over the course of 2 days.

Endotoxin removal was performed as follows: quadruplicate BC samples (1.5 x 2.5 x 4cm (height x width x length) were placed in 200 ml of distilled water (control) and 5% SDS (w/v). The water and detergent solutions were changed after every 24 hours over the course of 3 days. At each exchange, duplicate BC samples were taken and washed abundantly with distilled water and freeze-dried. The samples were subsequently cut into samples of the same weight 20 ± 4mg and rehydrated with 500µl of apyrogenic water. The concentration of endotoxin in each sample determined using the Pierce LAL Chromogenic Endotoxin Quantitation Kit and the standard protocol included (Thermo Scientific, Rockford, IL USA). Additionally, a non-washed BC graft was implanted in a single *in vivo* assay (as described ahead) and compared to the subsequent *in vivo* assays performed with the SDS washed BC grafts.

BC grafts were prepared by cutting large BC sheets (1.5x25x30cm) into 1.5 x 2.5 x 7cm (height x width x length) blocks with scissors. These were perforated along the center of the sample with a sharp 4mm (outer diameter) metallic needle and then dried by mass transfer of water from the hydrogel to blotting paper until a final wall thickness of roughly 2mm was achieved. The resulting tubular structures were then freeze-dried and stored at room temperature until needed (see Figure A-1). All grafts tested herein have a luminal caliber of 4mm and independently of the final length used in the varying assays were initially 7cm long. The BC grafts used for *in vivo* experimentation were rehydrated in sterile 0.9% (w/v) saline solution and autoclaved at 121oC for 20min 72 hours before surgery.

Surface Profilometry

BC grafts, created as previously described, were split open longitudinally and fixed with double-sided tape to glass slides. PFA, commercial ePTFE and Dacron grafts were also split longitudinally and affixed the same way (Dacron grafts were stretched as much as possible in order to remove the kinking inherent to the graft). The sample surface profiles were then measured 5 times along the same surface

(each measurement roughly 1mm apart) with a KLC TENCOR D-100 profilometer along 20mm (for Porcine Femoral Artery, ePTFE and PET) and 30mm for BC at set speed of 0.2mm/second and a resolution of 2000 points per mm. The results were then plotted on a 3D graph so to convey an idea of the 3 dimensional surface of the each sample. Roughness was calculated as the amplitude between maximum peak height and minimum valley depth.

Cryo-SEM Imaging

Cross sections of the BC grafts were imaged via Cryo-SEM on a JEOL JSM 6301F/ Oxford INCA Energy 350/ Gatan Alto 2500. The graft samples were prepared as described above and then cut into 1mm wide sections and placed upright in a metallic support. The samples were then rapidly cooled by plunging them into sub-cooled nitrogen (slush nitrogen) and transferred under vacuum to the cold stage of the preparation chamber. The samples were then fractured, sublimated for 180 seconds at -90°C, and coated with Au/Pd by sputtering for 40 seconds. The samples were finally transferred into the SEM chamber and imaged at -150°C. Pore size was estimated from the micrographs using Image J software.

Mechanical Tests

Tensile Strength Determination

BC grafts along with untreated BC (these are grafts that were not freeze-dried and as such did not finish the graft processing), ePTFE and porcine femoral artery (PFA) were tested for their tensile strength in quintuplicate (n=5) on a Shimadzu AG-X 50 kN at a traction speed of 5mm/min and a load cell of 1kN. Each sample tested was split open longitudinally and the materials thickness and width was measured with digital calipers and accounted for in the calculations of the strength parameters. Special care was taken in order to prevent sample slipping from the hydraulic grips by using both fine grain sandpaper and construction paper.

Suture Retention Assay

BC grafts with 6cm length (4mm internal diameter and 7mm external diameter) were fixed the top clamp of a Z2.5 Zwick/Roell (Zwick GmbH & Co. KG; Ulm; Germany). A 4-0 Prolene® suture (0.15mm diameter; Ethicon) was placed approximately 7mm from the edge of the prosthesis (measured with a digital micrometer) and looped around the bottom clamp before clamping. The assay was then carried out in quintuplicate, on both freeze-dried and non-freeze-dried bacterial cellulose prosthetics, at a set speed of 10mm/min and a 1N pre-load.

Compliance Characterization

Compliance characterization of BC grafts (n=5) was performed using the system and method described previously by Diamantouros and colleagues [32]. Briefly, the grafts were fixed into a chamber and initially exposed to a steady flow of purified water. A pulse (1Hz) was added by a linear magnetic actuator. The pressures were stabilized at 80-120mmHg. Variations in the outer diameter were measured by an optical micrometer sensor (LS-7030(M); Keyence Deutschland GmbH, Neu-Isenburg, Germany) placed perpendicularly to the graft. Pressures were recorded by pressure transducers (CODAN pvd Critical Care GmbH; Forstinning, Germany). The measurements were realized for 30 seconds once the pressures were stable. Variations in the outer diameter and pressures were recorded by a LabVIEW™ application (National Instruments; Texas, USA). The circumferential compliance was then calculated with the following equation:

$$C = \frac{(D_{Syst} - D_{Diast})\big/D_{Diast}}{P_{Syst} - P_{Diast}} \; x \; 100$$

Where C is compliance (%/mmHg), D is diameter (μm) and P is pressure (mmHg). "Syst" and "Diast" stand for the systolic and diastolic phase respectively.

A slight addition to the method presented by Diamantouros, consisting of the use of ultrasound imaging equipment (Vivid *I*, GE Healthcare; Freiburg, Germany), allowed for the acquisition of video of the changes in internal diameter in response to

pressure variation. The videos were then converted to still frames and the diameter of the lumen determined with Image J software on three points per image. Care was taken so that the measurements from each video would be performed at the same coordinates in each individual frame so as to account, as much as possible, for human error.

In vivo Experimentation and Histological Analysis

Surgical procedure

Four female domestic pigs (*Sus scrofa domesticus*) with weight ranging from 30-40kgs were restrained from food (24 hours) and water (6 hours) before each surgical procedure. All experiments were conducted according to the European Union Directive no.86/609/CEE for the use of animals in research and approved by the board for the ethical treatment of animals of the Faculty of Medicine of the University of Porto (ORBEA, FMUP, Oporto, Portugal). All procedures were performed under general anesthesia, with endotracheal intubation and spontaneous ventilation. A pre-anesthesia intramuscular injection of 32mg/ml azaperone (Stressnil®, Esteve Veterinaria) at a dose of 4 mg/kg reconstituted with 1mg/ml midazolam (Dormicum®, Roche) at a dose of 0.15–0.2ml/kg was administered. Venous access was obtained through an IV line placed in the marginal ear vein. Anesthesia was induced with 3μg/kg fentanyl (Fentanest®, Janssen-Cilag), and sodium thiopental (12.5mg/kg IV initially and then to effect Tiopental 0.5 B Braun®, B. Braun). After orotracheal intubation, the 7- to 7.5-mm tube was connected to the anesthetic equipment (Ohmeda, Boc Health Care), and anesthesia was maintained with a mixture of isoflurane (1.5% to 2.5%; Isoflo®, Esteve Veterinaria) in 100% oxygen and fentanyl at constant-rate infusion of 30-50μg/kg/h. Afterwards an epidural analgesia protocol was implemented with application of 1mg/kg morphine (Morfina 1% Braun®, B. Braunl). To address infection prophylaxis, all animals received intramuscular injection of 1g ceftriaxone (Rocephin®, Roche) before surgery. End-tidal CO_2, oxygen saturation, electrocardiography and temperature were monitored continuously (Cygnus 1000C Vet® Monitor, Servive Portugal). Pigs were placed in supine position and shaved,

and electrocardiographic electrodes were attached to the chest for continuous evaluation of cardiac electrical function. Normal saline (2 to 4mL/kg hourly) was infused through the venous cannula in the auricular vein during surgery, to maintain adequate preload stability.

Open surgery was then performed with isolation of the common femoral artery, the *profunda femoris* artery and the superficial artery. The BC grafts were implanted in the left hind limb in a femoro-femoral artery bridge. Papaverine was administered via wash to the artery to avoid arterial spasm. The animals were heparinized systemically with an intravenous bolus injection of 200units/kg of heparin (Heparina Sódica B.Braun®, B.Braun), five minutes before clamping of the target arteries. BC grafts were then sutured with continuous 6-0 monofilament polypropylene sutures (Prolene®, Ethicon). The femoral artery from the right hind limb was sham-operated with all the surgical procedures being equally performed, excluding the implantation of the graft.

After the surgery, the pigs were transported back to their quarters, only when arterial oxygen tension stabilized above 95%. Pigs were monitored until their body temperature normalized (with digital thermometers) and they were able to ambulate. They then were observed at least 2 or 3 times daily for locomotor activity, respiratory changes, body temperature, and food and water intake. Analgesia was maintained during the first 24h after surgery by using meloxicam (0.5mg/kg IM; Metacam, Boehringer Ingelheim). Acetylsalicylic acid (150mg/animal *per os* daily; Ácido Acetilsalicílico ratiopharm 100mg, Ratiopharm) was given once daily until euthanasia, to prevent platelet aggregation.

After the designated times, the animals were sacrificed by IV KCl injection after sedation with azaperone reconstituted with midazolam administered IM prior to induction with sodium thiopental (12.5mg/kg IV initially and then to effect) and the grafts and sham-operated arteries were harvested and histologically evaluated for signs of chronic inflammation, infection, foreign body responses, clot formation, cell ingrowth, and diameter via electron microscopy.

Histology

Tissues were preserved in formalin for a minimum of 4 days and were embedded in paraffin in an automated tissue processor (Microm STP 120). Tissues were then transferred to embedding workstation to obtain paraffin blocks. From these, sections (2μm) were cut on a rotary microtome (Leica RM 2035) and stained with Hematoxylin and Eosin (H&E) for light microscopic examination. Observations and photographs were made using an Olympus BX51 microscope with an Olympus camera attached

Immunohistochemistry

Immunostaining of endothelial cells was performed using the primary antibody – Mouse Anti Pig CD31 (AbD Serotec; Oxford, England). This is a mouse monoclonal antibody designed to detect porcine CD31. The slides were immersed in 10mM sodium citrate (pH 6.0) buffer. Antigen visualization was done with the Novocastra Novolink Polymer Detection System (Leica Microsystems GmbH, Wetzlar, Germany) and involved the following steps: Sections were incubated with H_2O_2 (3%) for 10 min to eliminate endogenous peroxidase activity followed by a 5 min incubation with a protein blocking agent. Sections were subsequently incubated overnight at 4 ^{o}C with the primary antibody diluted at 1:100 with BSA (5%), and on the following day, washed in TBS-buffered saline solution before incubation for 30 min with the secondary antibody system using diaminobenzidine (DAB) as a chromogen.

Statistical Data Analysis

All data and statistical analysis was performed using both GraphPad Prism and Origin Pro 9 software. Statistical significances were determined via One-way and Two-Way ANOVA tests after verifying the Normal distribution ($p < 0.05$) of the data.

Results

Graft Fabrication

The novel methodology presented herein for production of the BC graft is schematically outlined in Figure A-1. The BC grafts were produced with needles that were purposely built, regularly sharpened and exchanged in order to assure consistent perforation. Special care was taken during perforation in order assure a smooth luminal channel. An unsharpened needle resulted in tears during the perforation with the appearance of "flaps" that could occlude or restrict flow through the graft. Also, while all grafts produced and presented in this work were 4mm in diameter we found that by using different diameter needles allows the production of grafts with different diameters.

The drying and shaping was performed with the needle in place with special care to avoid changes to the luminal diameter of the graft and an irregular topography of the external surface. Also, the grafts were found to dry quickly during the freeze-drying process (a maximum of 2 days is required for complete drying) and the least irregular grafts were obtained the quicker this process was performed.

Surface Profilometry

The surface profiles we present here were obtained by 5 consecutive measurements that were 1 mm spaced (side-by-side) and plotted together in a three-dimensional topological graph so as to convey an idea of the topography of the materials (see
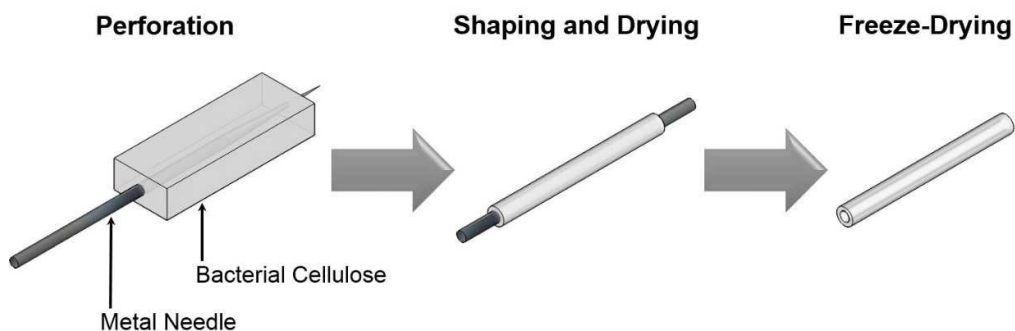

Figure A-1 - Schematic representation BC vascular graft formation process. From left to right: the BC perforated with a sharp metallic needle, dried by capillary action and shaped into a cylinder and finally freeze-dried.

Figure A-2). Our results show that the surface roughness of BC is in the same range of that of porcine femoral artery, ranging roughly 300nm in both cases from highest peaks to lowest valley, with no statistically significant difference between them ($p > 0.05$). On the other hand, both ePTFE and, to a greater extent, PET show a much greater surface roughness with a distance of approximately 600 and 1600nm between peaks and valleys respectively.

Cryo-SEM Imaging

Several BC grafts samples, and several different regions of each graft, were observed via Cryo-SEM so as to maintain the hydrated three-dimensional structure of the grafts; the images presented here are representative of those observations (Figure A-3). The fibril distribution inside of our grafts showed markedly different structures throughout the graft wall that are well distributed throughout. In lower magnifications dense sheets of BC fibers intersecting each other are visible and
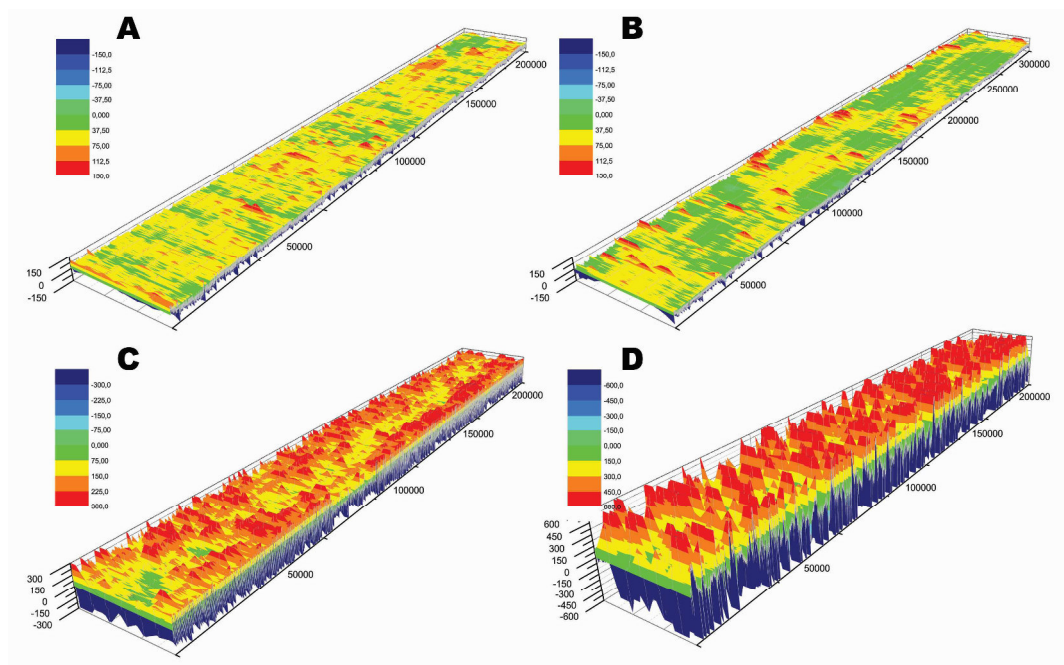

Figure A-2 - Surface profiles of Porcine Femoral Artery (A), BC graft (B), ePTFE graft (C) and a PET graft (D). The plots were obtained from 5 separate linear measurements (2000 points/mm) over 2 cm (3cm for BC), spaced 1mm apart and plotted in a 3D graph.

appear in wave-like patterns, parallel to the luminal surface of the graft (Figure A-
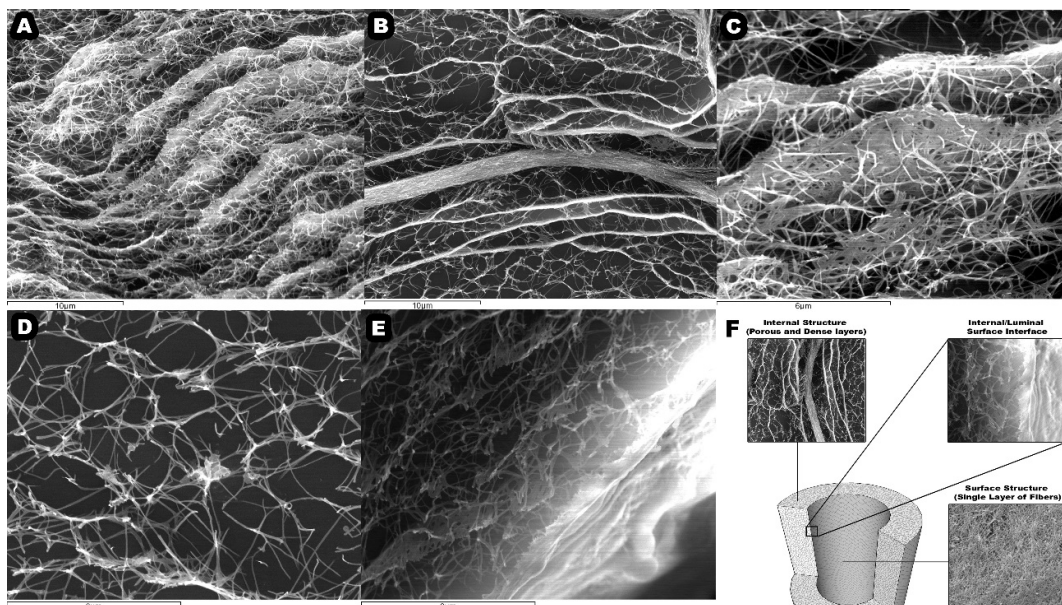
Figure A - 3 - Cryo-SEM images of a portion of the cross-section of the graft wall. (A) and (B) 4000x magnification with noticeable dense regions layered between open-pore structures; (C) 10000x magnification of the dense BC regions; (D) 10000x magnification of the open-pore structures and (E) 10000x magnification of the edge of the luminal surface of the graft. (F) is a schematic representation of the interface between the luminal surface and inner wall structure.

3A, B and C). Dense sheets are surrounded by low density open porous regions (Figure A-3D) with pore sizes ranging from 1 to 5 µm in diameter. Additionally, there seems to be a consistent and dense single layer of BC fibers over the entire luminal surface of the graft that is immediately followed by open porous regions (Figure A-3E).

Endotoxin Removal Study

Endotoxin (Lipopolysaccharide; LPS) concentration on non-washed and SDS washed BC was determined with the Pierce LAL Chromogenic Endotoxin Quantitation Kit. Total LPS concentration on non-washed BC over the course of the study was 2.65 ± 0.27EU/ml (Endotoxin Units/ml) and dropped to 0.43 ± 0.15, 0.06 ± 0.04 and 0.003 ± 0.02EU/ml over the following 3 days (Figure A-4). Total LPS concentration was shown to be significantly different between washed and non-washed BC ($p<0.05$). Results also show a significant difference between a single and
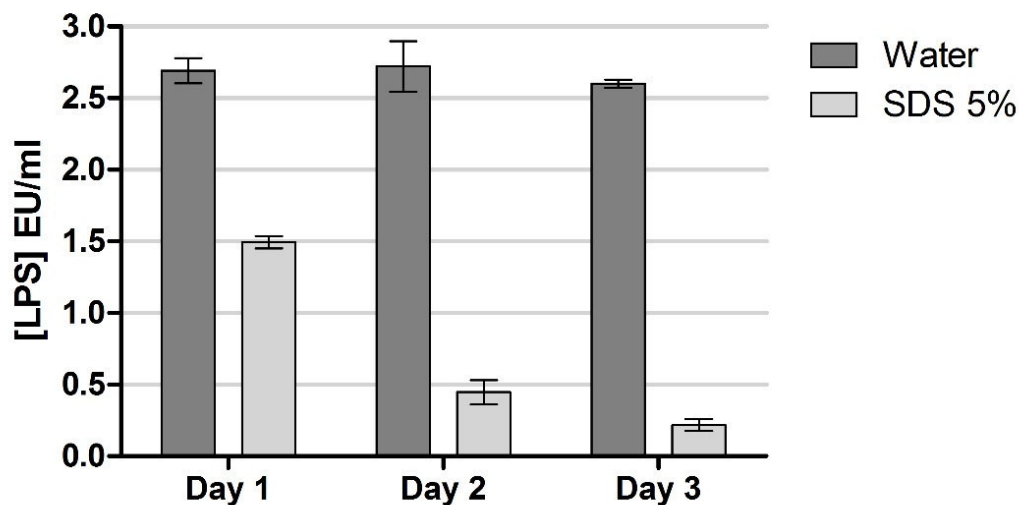
Figure A-4 - Endotoxin (LPS) concentration in EU/ml (Endotoxin Units/ml) as determined over 3, 24 hour, washes in 5% SDS and water (negative control).

twice washed ($p<0.05$) and no significant difference between the second and third washes.

Mechanical Tests

Tensile Strength Determination

Mechanical testing demonstrated marked differences between porcine femoral artery (PFA), ePTFE and BC (both as a graft and untreated) - see Table A-1. The BC graft and untreated BC show no statistically significant difference between them ($p>0.05$) in regards to any of the parameters though. However, the BC graft did show higher values for maximum tensile strength (Max Force), maximum stress and strain. PFA, while mechanically weak as compared to the other materials in regards to strength, was by far the most elastic, deforming 133% before rupture. Also noteworthy, ePTFE was shown to be most rigid of the tested materials, with the highest values in all the parameters. The BC grafts thus better resembles the biological vessels than ePTFE, in the sense that it presents higher elasticity, translated in a Young modulus in the same order of magnitude as PFA´s.

Table A-1 - Mechanical test results for Porcine Femoral Artery (PFA), ePTFE the BC Graft and unprocessed BC (n=5). Values marked with an asterisk (*) are not statistically different from each other in their respective columns (p>0.05). Data is presented as mean ± standard deviation.

Material	Young's Modulus (N/mm^2)	Max Force (N)	Max Stress (N/mm^2)	Max Strain (%)
PFA	2.58 ± 0.95	10.05 ± 3.39	1.15 ± 0.39*	133.46 ± 11.25
ePTFE	125.40 ± 24.33	198.54 ± 13.33	23.57 ± 1.00	40.62 ± 9.92*
BC Graft	10.56 ± 1.53*	95.92 ± 5.62*	2.75 ± 0.38*	41.08 ± 8.65*
BC	10.70 ± 2.23*	91.47 ± 16.33*	2.10 ± 0.26*	34.5 ± 4.27*

Suture Retention Strength

Results show that untreated BC and our BC grafts demonstrate suture retention strength of 3.94 ± 0.38 and 4.20 ± 0.99 N respectively, with no statistically significant difference between them (p>0.05). The results demonstrate a superior performance of the BC grafts, as compared to most materials, presenting a suture retention strength comparable to that of ePTFE.

Table A-2 Suture Retention strength (N) of several autologous and synthetic grafts for Tissue Engineered Blood Vessels (TEBV), Internal Mammary Artery (IMA), Polytetrafluoroethylene (ePTFE), Fibrin and Fibrin/polylactic acid (PLA), Human Saphenous Vein (HSV), Collagen and Bacterial Cellulose (BC). Suture retention strength for the BC graft and untreated BC are not statistically different (p>0.05; n=4)

Graft Material	Retention Strength (N)	SD	References
IMA	1.35	± 0.49	29
HSV	2.60		30
TEBV	1.49	± 0.49	29
Fibrin	0.19	± 0.05	31
Fibrin/PLA	1.32	± 0.58	31
Collagen	0.82-2.87	± 0.12-0.09	32
ePTFE	4.70	± 0.50	33
BC graft	4.20	± 0.99	--
BC	3.94	± 0.38	--

Compliance Characterization Assay

We measured the compliance for our BC grafts externally via laser detector and estimated compliance internally by sonography imaging. Results show a significant difference between the compliance of the BC graft in regards to the internal and external measurements (see Table A-3). Externally compliance was measured as

being 0.4×10^{-2} %/mmHg while internally graft compliance was determined to be 9.5×10^{-2} %/mmHg. While the external compliance falls far from the results for the most of the other materials found in the literature internally compliance seems to be much better matching, in most regards, the compliance values found for autografts.

Table A-3 - Compliance (presented as value x10-2 %/mmHg) with standard deviation (SD) as collected from the literature for Internal Mammary Artery (IMA), Human Saphenous Vein (HSV), Human Iliac Artery (HIA), Tissue Engineered Blood Vessel (TEBV), Polyurethane (PU), Polyethylene terephthalate (PET), expanded Polytetrafluoroethylene (ePTFE), Bacterial Cellulose/Chitosan blend (BC/Chi) and measurements for the compliance of the BC grafts as measured externally and internally (n=5).

Graft Material	Compliance (%/mmHg; x10^{-2})	SD	References
IMA	11.5	± 3.9	29
HSV	3.7-12.8	± 1.3-1.9	34
HIA	8	± 5.9	35
TEBV	1.5-3.4	± 0.3	29; 30
PU	8.1	± 0.4	35
PET	1.8	± 1.2	35
ePTFE	1.2-1.6	± 0.3	35; 36
BC/Chi	5.9	± 2.7	36
BC graft External	0.4	± 0.1	--
BC graft Internal	9.5	± 2.8	--

In vivo Experimentation and Histological Analysis

As a preliminary *in vivo* assay 4 surgical procedures have been performed to date, with implantation of the BC graft in a femoral-femoral artery bridge on the left hind limb of female domestic pigs (see Figure A-5A). The right femoral artery was also isolated in a sham-operated procedure and served as a control for the implanted graft. No significant changes to the arterial wall of the control vessel were detected.

During the first surgical intervention severe arterial spasm and contraction was noted during, and after, the procedure. There was noticeably reduced pulse after graft implantation and the limb was slightly cold to the touch 24 hours post-operatively both situations attributed to arterial contraction. All further procedures were performed with papaverine administration, via topical wash to the artery. The following three procedures resulted in 1 month patency that were all confirmed via

Doppler ultrasound imaging (see Figure A-5B) being terminated at that point for explantation of the BC graft and subsequent histological analysis.

Histological analysis and Immunohistochemistry were performed on the grafts harvested after the experiments were terminated. The BC grafts that were recovered one month after surgical intervention were intact and well integrated into the surrounding tissue with no significant fibrosis or macroscopic evidence of inflammation. Later histological analysis showed a distinct, three-layered, structure with cellular adhesion and infiltration on both the luminal and adventitial surfaces of the graft and an unpopulated and larger BC central region. The cells detected on the luminal surface were believed initially, and later confirmed via immunohistochemistry, to be endothelial or progenitor endothelial cells that are believed to have migrated from the adjoining femoral artery (Figure A-5C). Figure A-5E and F are representative of the cellular infiltration and population found on the adventitial surface of all the recovered grafts with special note to the presence of neo-vessels inside the BC graft itself (see Figure A-5D). The cell populations in these regions were determined to be composed mostly of fibroblasts, macrophages and some giant cells.
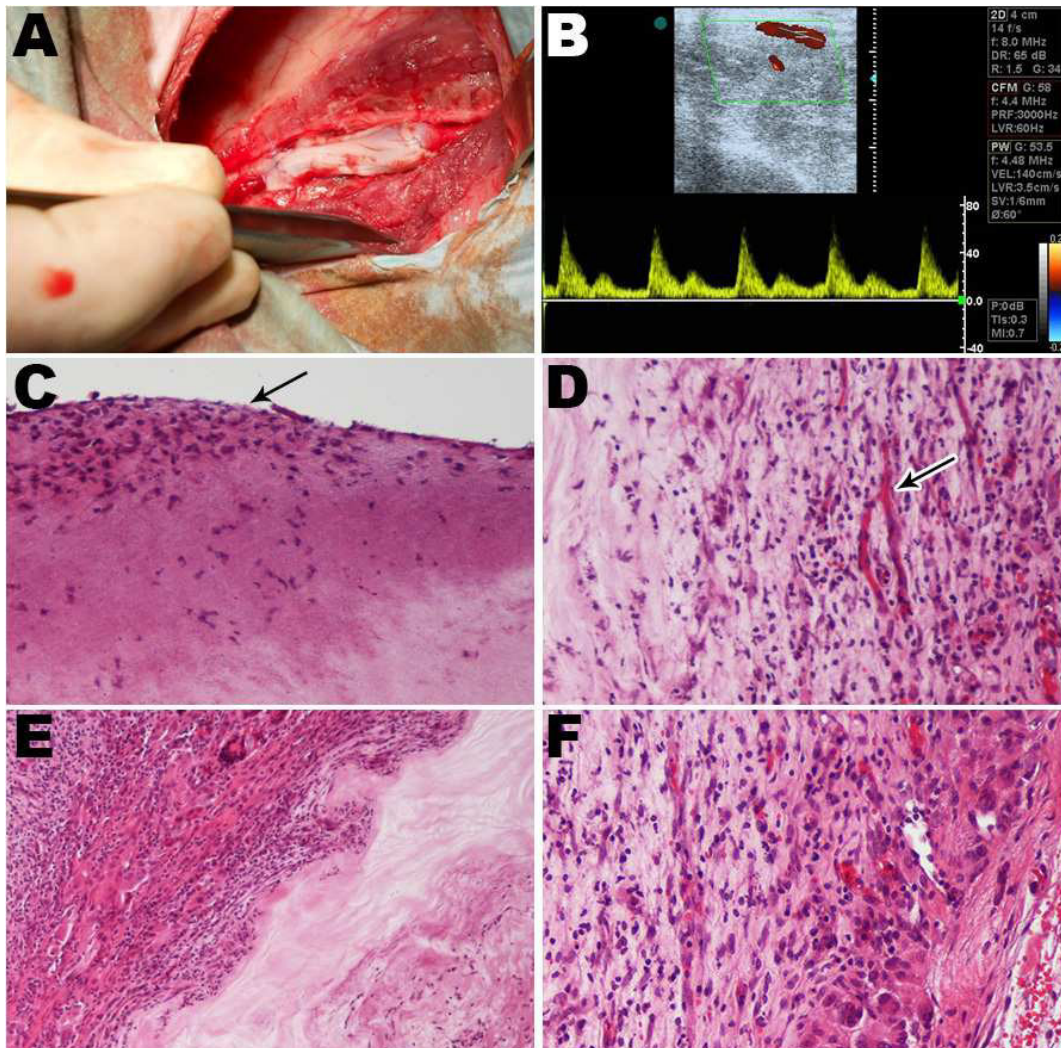
Figure A-5 Representative photographs and Haematoxylin and Eosin histopathological microscopy images of in vivo tests. (A) Femoral-femoral artery BC graft placement, (B) Doppler Sonography screenshot showing blood flow through the BC graft after one month of implantation, (C) 100x magnification of the luminal surface of the graft with cell adhesion on the surface of the graft along and some cell infiltration, (D) 200x External surface of BC graft showing formation of neo-vessels (arrow), (E) External surface of the BC grafts showing a smooth transition from surrounding tissues into the BC graft with cell infiltration, (F) 200x magnification of a cell population in a transitional region from adventitia into the BC grafts.

Bibliography

[1] Chlupac J, Filova E, Bacakova L. Blood vessel replacement: 50 years of development and tissue engineering paradigms in vascular surgery. Physiol Res. 2009;58 Suppl 2:S119-39.

[2] Holmberg M, Hou X. Competitive protein adsorption of albumin and immunoglobulin G from human serum onto polymer surfaces. Langmuir. 2010;26:938-42.

[3] van Det RJ, Vriens BH, van der Palen J, Geelkerken RH. Dacron or ePTFE for femoro-popliteal above-knee bypass grafting: short- and long-term results of a multicentre randomised trial. European journal of vascular and endovascular surgery : the official journal of the European Society for Vascular Surgery. 2009;37:457-63.

[4] Tsai GJ, Su WH. J Food Protect. 1999;62:239.

[5] Schopka S, Schmid T, Schmid C, Lehle K. Current Strategies in Cardiovascular Biomaterial Functionalization. Materials. 2010;3:638-55.

[6] Ravi S, Chaikof EL. Biomaterials for vascular tissue engineering. Regenerative medicine. 2010;5:107-20.

[7] Stegemann JP, Kaszuba SN, Rowe SL. Review: advances in vascular tissue engineering using protein-based biomaterials. Tissue engineering. 2007;13:2601-13.

[8] Nemeno-Guanzon JG, Lee S, Berg JR, Jo YH, Yeo JE, Nam BM, et al. Trends in Tissue Engineering for Blood Vessels. Journal of Biomedicine and Biotechnology. 2012;2012:14.

[9] Leitão A, Silva J, Dourado F, Gama M. Production and Characterization of a New Bacterial Cellulose/Poly(Vinyl Alcohol) Nanocomposite. Materials. 2013;6:1956-66.

[10] Klemm D, Schumann D, Udhardt U, Marsch S. Bacterial synthesized cellulose — artificial blood vessels for microsurgery. Progress in Polymer Science. 2001;26:1561-603.

[11] Svensson A, Nicklasson E, Harrah T, Panilaitis B, Kaplan DL, Brittberg M, et al. Bacterial cellulose as a potential scaffold for tissue engineering of cartilage. Biomaterials. 2005;26:419-31.

[12] Solway DR, Consalter M, Levinson DJ. Microbial cellulose wound dressing in the treatment of skin tears in the frail elderly. Wounds. 2010;22:17-9.

[13] Fontana JD, de Souza AM, Fontana CK, Torriani IL, Moreschi JC, Gallotti BJ, et al. Acetobacter cellulose pellicle as a temporary skin substitute. Appl Biochem Biotechnol. 1990;24-25:253-64.

[14] Andrade FK, Costa R, Domingues L, Soares R, Gama M. Improving bacterial cellulose for blood vessel replacement: Functionalization with a chimeric protein containing a cellulose-binding module and an adhesion peptide. Acta Biomater. 2010;6:4034-41.

[15] Leitão AF, Gupta S, Silva JP, Reviakine I, Gama M. Hemocompatibility study of a bacterial cellulose/polyvinyl alcohol nanocomposite. Colloids and Surfaces B: Biointerfaces. 2013;111:493-502.

[16] Bäckdahl H, Risberg B, Gatenholm P. Observations on bacterial cellulose tube formation for application as vascular graft. Materials Science and Engineering: C. 2011;31:14-21.

[17] Backdahl H, Helenius G, Bodin A, Nannmark U, Johansson BR, Risberg B, et al. Mechanical properties of bacterial cellulose and interactions with smooth muscle cells. Biomaterials. 2006;27:2141-9.

[18] Andrade F, Pertile R, Douradoa F. Bacterial cellulose: properties, production and applications. Cellulose: structure and properties, derivatives and industrial uses Nova Science Publishers, Inc. 2010:427-58.

[19] Bodin A, BÄCKDAHL H, Gatenholm P, Gustafsson L, Risberg B. Bacterial cellulose tubes. Google Patents; 2012.

[20] DICKERHOFF B, Farivar RS, RAGHAVAN ML, Kumar V. Vascular prosthetic assemblies. Google Patents; 2013.

[21] Gatenholm P, Backdahl H, Tzavaras TJ, Davalos RV, Sano MB. Three-dimensional bioprinting of biosynthetic cellulose (bc) implants and scaffolds for tissue engineering. Google Patents; 2011.

[22] Wan WK, Millon L. Poly(vinyl alcohol)-bacterial cellulose nanocomposite. Google Patents; 2005.

[23] Serafica G, Damien C, Wright F, Beam H. Implantable microbial cellulose materials for various medical applications. Google Patents; 2007.

[24] Zahedmanesh H, Mackle JN, Sellborn A, Drotz K, Bodin A, Gatenholm P, et al. Bacterial cellulose as a potential vascular graft: Mechanical characterization and constitutive model development. Journal of Biomedical Materials Research Part B: Applied Biomaterials. 2011;97B:105-13.

[25] Kowalska-Ludwicka K, Cala J, Grobelski B, Sygut D, Jesionek-Kupnicka D, Kolodziejczyk M, et al. Modified bacterial cellulose tubes for regeneration of damaged peripheral nerves. Archives of medical science : AMS. 2013;9:527-34.

[26] Kaźmierczak D, Kazimierczak J. Biosynthesis of modified bacterial cellulose in a tubular form. Fibres & Textiles in Eastern Europe. 2010;18:82.

[27] Putra A, Kakugo A, Furukawa H, Gong JP, Osada Y. Tubular bacterial cellulose gel with oriented fibrils on the curved surface. Polymer. 2008;49:1885-91.

[28] Diamantouros S, Hurtado-Aguilar L, Schmitz-Rode T, Mela P, Jockenhoevel S. Pulsatile Perfusion Bioreactor System for Durability Testing and Compliance Estimation of Tissue Engineered Vascular Grafts. Ann Biomed Eng. 2013;41:1979-89.

[29] Konig G, McAllister TN, Dusserre N, Garrido SA, Iyican C, Marini A, et al. Mechanical properties of completely autologous human tissue engineered blood vessels compared to human saphenous vein and mammary artery. Biomaterials. 2009;30:1542-50.

[30] L'Heureux N, Dusserre N, Konig G, Victor B, Keire P, Wight TN, et al. Human tissue-engineered blood vessels for adult arterial revascularization. Nature medicine. 2006;12:361-5.

[31] Syedain ZH, Meier LA, Bjork JW, Lee A, Tranquillo RT. Implantable arterial grafts from human fibroblasts and fibrin using a multi-graft pulsed flow-stretch bioreactor with noninvasive strength monitoring. Biomaterials. 2011;32:714-22.

[32] Shah S. Fabrication Of Small Diameter Vascular Graft Using Stacked Collagen Films. 2013.

[33] Isaka M, Nishibe T, Okuda Y, Saito M, Seno T, Yamashita K, et al. Experimental study on stability of a high-porosity expanded polytetrafluoroethylene graft in dogs. Annals of Thoracic and Cardiovascular Surgery. 2006;12:37.

[34] Zachrisson H, Lindenberger M, Hallman D, Ekman M, Neider D, Länne T. Diameter and compliance of the greater saphenous vein – effect of age and nitroglycerine. Clinical Physiology and Functional Imaging. 2011;31:300-6.

[35] Tai NR, Salacinski HJ, Edwards A, Hamilton G, Seifalian AM. Compliance properties of conduits used in vascular reconstruction. British Journal of Surgery. 2000;87:1516-24.

[36] Azevedo EP, Retarekar R, Raghavan ML, Kumar V. Mechanical properties of cellulose: chitosan blends for potential use as a coronary artery bypass graft. Journal of Biomaterials Science, Polymer Edition. 2012;24:239-52.

[37] Heumann D, Roger T. Initial responses to endotoxins and Gram-negative bacteria. Clinica Chimica Acta. 2002;323:59-72.

[38] Clasen C, Sultanova B, Wilhelms T, Heisig P, Kulicke WM. Effects of Different Drying Processes on the Material Properties of Bacterial Cellulose Membranes. Macromolecular Symposia. 2006;244:48-58.

[39] Sokolnicki AM, Fisher RJ, Harrah TP, Kaplan DL. Permeability of bacterial cellulose membranes. Journal of Membrane Science. 2006;272:15-27.

[40] Thubrikar MJ. Vascular mechanics and pathology: Springer; 2007.

[41] Cunningham KS, Gotlieb AI. The role of shear stress in the pathogenesis of atherosclerosis. Laboratory investigation. 2005;85:9-23.

[42] Cecchi E, Giglioli C, Valente S, Lazzeri C, Gensini GF, Abbate R, et al. Role of hemodynamic shear stress in cardiovascular disease. Atherosclerosis. 2011;214:249-56.

[43] Resnick N, Yahav H, Shay-Salit A, Shushy M, Schubert S, Zilberman LCM, et al. Fluid shear stress and the vascular endothelium: for better and for worse. Progress in Biophysics and Molecular Biology. 2003;81:177-99.

[44] Silver AE, Vita JA. Shear Stress–Mediated Arterial Remodeling in Atherosclerosis: Too Much of a Good Thing? Circulation. 2006;113:2787-9.

[45] Milleret V, Hefti T, Hall H, Vogel V, Eberli D. Influence of the fiber diameter and surface roughness of electrospun vascular grafts on blood activation. Acta Biomater. 2012;8:4349-56.

[46] Shen F, Kastrup CJ, Liu Y, Ismagilov RF. Threshold Response of Initiation of Blood Coagulation by Tissue Factor in Patterned Microfluidic Capillaries Is

Controlled by Shear Rate. Arteriosclerosis, Thrombosis, and Vascular Biology. 2008;28:2035-41.

[47] He W, Hu Z, Xu A, Liu R, Yin H, Wang J, et al. The Preparation and Performance of a New Polyurethane Vascular Prosthesis. Cell Biochem Biophys. 2013:1-12.

Braga, 08 of August of 2014.

CLAIMS

1. Method for production of tubular bacterial cellulose grafts for use in vascular applications comprising the following steps:

- isolate a single bacterial cellulose block from a larger bacterial cellulose sheet with predetermined dimensions;

- perform 2 to 4 24 hour washes of the bacterial cellulose blocks in SDS at a concentration of 2-5% (w/v) followed by 5 washes a day over 3 days in water;

- perforate the bacterial cellulose block along the center line with a needle or a laser or physical or chemical process in a manner to get a luminal channel;

- maintain the needle inside the block or insert one after the laser or physical or chemical process of perforation;

- perform a drying process by mass transfer of water via capillary action, or evaporation or compression for the removal of water from the bacterial cellulose;

- shape the external surface by mechanical application of an external force in manner to result in a cylindrical shape;

- remove the needle;

- perform a freeze-drying process;

2. Method, according to previous claim, wherein the drying process and the shaping are optionally made simultaneously.

3. Method, according to previous claims, wherein optionally the surface is trimmed, or sanded or shaved in order to produce an external surface with a smoother topography.

4. Method, according to claim 1, wherein preferably is used a sharpened and metallic needle to perforate the bacterial cellulose block.

5. Method, according to previous claim, wherein the luminal channel produced by the needle has a diameter between 2mm and 10mm, preferably 4-5mm.

6. Method, according to claim 1, wherein the mass transfer or compression is performed on blotting paper at room temperature.

7. Method, according to claim 1, wherein the evaporation occur at temperatures ranging from 50-80ºC.

8. Method, according to claim 1, wherein the external force of the shaping consists in a mechanical force applied uniformly over the surface.

9. Tubular bacterial cellulose grafts for use in vascular applications, according to claims 1 to 8 wherein the graft has a wall density ranging from 0.02 to 0.15g/cm^3 and a wall thickness ranging from 1 to 4mm.

10. Tubular bacterial cellulose graft, according to previous claim, wherein the preferable wall density is 0.1g/cm^3 to 0.09g/cm^3.

11. Tubular bacterial cellulose graft, according to previous claim, wherein the preferable wall thickness is 2 mm.

12. Tubular bacterial cellulose graft, according to claims 9 to 11, wherein can have a surface altered by addition of RGD sequences or other cell signaling molecules, and/or any other bioactive molecules such as, heparin .

Braga, 08 of August of 2014.